เกณฑ์วิธีที่เหมาะสมในการถ่ายภาพรังสีทรวงอกโดยใช้เอกซเรย์ระบบดิจิทัลโทโมซินทีซีส

นายศราวุธ ทองคุ้ม

วิทยานิพนธ์นี้เป็นส่วนหนึ่งของการศึกษาตามหลักสูตรปริญญาวิทยาศาสตรมหาบัณฑิต
สาขาวิชาฉายาเวชศาสตร์ ภาควิชารังสีวิทยา
คณะแพทยศาสตร์ จุฬาลงกรณ์มหาวิทยาลัย
ปีการศึกษา 2560

THE DETERMINATION OF OPTIMAL PROTOCOL FOR DIGITAL CHEST TOMOSYNTHESIS

Mr. Sarawut Tongkum

A Thesis Submitted in Partial Fulfillment of the Requirements
for the Degree of Master of Science Program in Medical Imaging
Department of Radiology
Faculty of Medicine
Chulalongkorn University
Academic Year 2017

Thesis Title	THE DETERMINATION OF OPTIMAL PROTOCOL FOR DIGITAL CHEST TOMOSYNTHESIS
By	Mr. Sarawut Tongkum
Field of Study	Medical Imaging
Thesis Advisor	Kitiwat Khamwan, Ph.D.

Accepted by the Faculty of Medicine, Chulalongkorn University in Partial Fulfillment of the Requirements for the Master's Degree

.....Dean of the Faculty of Medicine
(Professor Suttipong Wacharasindhu, M.D.)

THESIS COMMITTEE

.....Chairman
(Associate Professor Anchali Krisanachinda, Ph.D.)

.....Thesis Advisor
(Kitiwat Khamwan, Ph.D.)

.....Examiner
(Yothin Rakvongthai, Ph.D.)

.....Examiner
(Associate Professor Kosuke Matsubara, Ph.D.)

.....External Examiner
(Professor Franco Milano, Ph.D.)

ศราวุธ ทองคุ้ม : เกณฑ์วิธีที่เหมาะสมในการถ่ายภาพรังสีทรวงอกโดยใช้เอกซเรย์ระบบดิจิทัลโทโมซินทีซีส (THE DETERMINATION OF OPTIMAL PROTOCOL FOR DIGITAL CHEST TOMOSYNTHESIS) อ.ที่ปรึกษาวิทยานิพนธ์หลัก: อ. ดร. กิติวัฒน์ คำวัน, 119 หน้า.

ในปัจจุบันเครื่องเอกซเรย์ระบบดิจิทัลโทโมซินทีซีสถูกนำมาใช้ในการประเมินรอยโรคในการถ่ายเอกซเรย์ทรวงอกมากขึ้น เนื่องจากสามารถแสดงภาพได้หลายภาพโดยที่ไม่เกิดการซ้อนทับกันของอวัยวะภายในร่างกาย อย่างไรก็ตามปริมาณรังสีที่ได้รับจากการตรวจด้วยวิธีนี้จะสูงกว่าการถ่ายเอกซเรย์ทรวงอกแบบปกติ งานวิจัยนี้มีวัตถุประสงค์เพื่อต้องการหาเกณฑ์วิธีที่เหมาะสมสำหรับการถ่ายภาพรังสีทรวงอกโดยใช้เอกซเรย์ระบบดิจิทัลโทโมซินทีซีส เพื่อลดปริมาณรังสีที่ผู้ป่วยได้รับโดยที่คุณภาพของภาพเพียงพอต่อการวินิจฉัยโรค โดยทำการทดสอบในหุ่นจำลองทรวงอก ความหนา 23 เซนติเมตร ซึ่งภายในบรรจุรอยโรคจำลองที่มีขนาดเส้นผ่านศูนย์กลาง 3, 5, 8, 10 และ 12 มิลลิเมตร ตามลำดับ ทำการทดสอบพารามิเตอร์ต่างๆ โดยใช้ค่าความต่างศักย์ที่ 100, 110 และ 120 เควีพี ค่าอัตราส่วนโดสที่ 1:5, 1:8 และ 1:10 และการศึกษาจะมีการใส่ตัวกรองรังสีที่ทำจากทองแดงที่ความหนา 0.1, 0.2 และ 0.3 มิลลิเมตร และแบบไม่ใส่ตัวกรองรังสี ถ่ายภาพเอกซเรย์หุ่นจำลองด้วยเครื่องเอกซเรย์ระบบดิจิทัลโทโมซินทีซีส ยี่ห้อยีอี รุ่น Definium 8000 ทุกพารามิเตอร์ใช้ระบบควบคุมปริมาณรังสีแบบอัตโนมัติ โดยจะทำการสแกน 3 ครั้ง ในแต่ละพารามิเตอร์ เพื่อหาค่าเฉลี่ยของปริมาณรังสีที่ผ่านผิว โดยใช้การวัดปริมาณรังสีด้วยชุดวัดรังสีแบบแก้ว โดยติดที่ระดับกึ่งกลางทรวงอกของหุ่นจำลอง บันทึกผลค่าผลคูณปริมาณรังสีกับพื้นที่จากจอมอนิเตอร์ และประเมินคุณภาพของภาพในเชิงปริมาณโดยการหาค่าสัญญาณของภาพต่อสัญญาณรบกวน ประเมินคุณภาพของภาพในเชิงคุณภาพด้วยรังสีแพทย์ 2 ท่าน ที่มีประสบการณ์ในการอ่านผลเอกซเรย์ระบบดิจิทัลโทโมซินทีซีสใกล้เคียงกัน

ผลการศึกษาพบว่าค่าปริมาณรังสีเฉลี่ยที่ผ่านผิวจากพารามิเตอร์ตั้งต้นของบริษัทที่ค่าความต่างศักย์ 120 เควีพี อัตราส่วนโดส 1:10 และไม่ใช้ตัวกรองรังสี มีค่าเท่ากับ 1.68±0.15 มิลลิเกรย์ ค่าปริมาณรังสีเฉลี่ยที่ผ่านผิวที่ได้จากพารามิเตอร์ที่เหมาะสมมีค่าเท่ากับ 0.47±0.02 มิลลิเกรย์ โดยใช้ความต่างศักย์ 110 เควีพี อัตราส่วนโดส 1:5 โดยใช้ตัวกรองรังสีความหนา 0.3 มิลลิเมตร ค่าปริมาณรังสียังผลจากค่าพารามิเตอร์ของบริษัทและจากพารามิเตอร์ที่เหมาะสมมีค่าเท่ากับ 313.98±0.72 ไมโครซีเวิร์ต และ 100.55±0.28 ไมโครซีเวิร์ต ตามลำดับ โดยคุณภาพของภาพที่ได้ซึ่งประเมินโดยรังสีแพทย์มีความแตกต่างกันเพียงเล็กน้อย และเมื่อนำค่าพารามิเตอร์ที่เหมาะสมที่ได้จากการทดสอบในหุ่นจำลองไปใช้กับผู้ป่วยจำนวน 30 ราย ที่มีความหนาของทรวงอกใกล้เคียงกับหุ่นจำลอง โดยมีความหนาเฉลี่ยเท่ากับ 22.51±1.70 เซนติเมตร ที่หน่วยรังสีวินิจฉัย โรงพยาบาลจุฬาภรณ์ พบว่าค่าปริมาณรังสียังผลที่ผู้ป่วยได้รับมีค่าเท่ากับ 98.87±0.08 ไมโครซีเวิร์ต งานวิจัยนี้สรุปได้ว่าการใช้พารามิเตอร์ที่เหมาะสมจากงานวิจัยนี้สามารถช่วยลดปริมาณรังสีให้แก่ผู้ป่วยได้มากกว่า 3 เท่า โดยที่ยังคงคุณภาพของภาพเพื่อการวินิจฉัยโรค

ภาควิชา รังสีวิทยา ลายมือชื่อนิสิต .....

สาขาวิชา ฉายาเวชศาสตร์ ลายมือชื่อ อ.ที่ปรึกษาหลัก .....

ปีการศึกษา 2560

5974045730 : MAJOR MEDICAL IMAGING
KEYWORDS: DIGITAL RADIOGRAPHY, DIGITAL CHEST TOMOSYNTHESIS, RADIATION DOSE, IMAGE QUALITY

SARAWUT TONGKUM: THE DETERMINATION OF OPTIMAL PROTOCOL FOR DIGITAL CHEST TOMOSYNTHESIS. ADVISOR: KITIWAT KHAMWAN, Ph.D., 119 pp.

Recently, digital chest tomosynthesis (DTS) is introduced as alternative technique in digital chest radiography for evaluating pulmonary disease and enhancing the internal structures in different slices. However, the radiation dose is higher compared to general chest radiography. The present study was to determine the optimal protocol for DTS in order to reduce the radiation dose to patients while maintaining the image quality. The multipurpose chest phantom N1 "LUNGMAN'' was scanned by digital radiographic systems model Definium 8000.Such phantom was inserted with simulated nodules with size diameter of 3, 5, 8, 10, 12 mm, and the data were acquired using chest VolumeRAD protocol with AEC technique. Parameters were varied in tube voltage (100, 110, 120 kVp) copper filter (0.0, 0.1, 0.2, 0.3 mm) and dose ratio (1:5, 1:8, 1:10) for evaluating the optimal protocol. All of protocols were performed three times. The entrance surface dose (ESD) was measured using glass dosimeter attached at the mid-chest level of the phantom. The effective dose (ED) was calculated using the recorded DAP value. The signal-to-noise ratio (SNR) was measured for qualitative image quality evaluation. The image criteria and nodule detection capability were scored by two experienced radiologists.

The results indicated that the average±SD of ESD obtained from vendor's default protocol at 120 kVp, dose ratio 1:10 and no copper filter was 1.68±0.15 mGy. The optimal parameter for DTS was obtained at 110 kVp, dose ratio 1:5, and copper filter at 0.3 mm with the ESD of 0.47±0.02 mGy. The effective doses for the default protocol and optimal protocol were 313.98±0.72 µSv and 100.55±0.28 µSv, respectively. There were slightly different of the image criteria and nodule detection between optimal and default protocols using visual assessment by two radiologists. In the clinical study, the average patient's thickness of 22.51±1.70 cm (range 19.30-25.80 cm) was obtained. The average±SD effective dose of 98.87±0.08 µSv was obtained after applied the optimal protocol in 30 patients. The dose ratio and tube voltage were in slightly correlation with the radiation dose since the AEC technique was applied. A copper filter has a potential to reduce radiation dose to the patients. In conclusion, the optimal protocol can reduce radiation dose substantially while preserving the image quality compared to the vendor default protocol.

Department: Radiology Student's Signature .....
Field of Study: Medical Imaging Advisor's Signature .....
Academic Year: 2017

ACKNOWLEDGEMENTS

I would like to thankfulness and deepest appreciation to my advisor Mr. Kitiwat Khamwan, Ph.D., Department of Radiology, Faculty of Medicine, Chulalongkorn University, for his invaluable, helpful, comments, suggestion, constructive direction, motivation and polishing of the thesis writing to improve English expression. Also, I would like to express my deeply thankfulness to my co-advisors Mr.Yothin Rakvongthai, Ph.D., and Miss Petcharleeya Suwanpradit, M.Sc., Department of Radiology, Faculty of Medicine, Chulalongkorn University, for their encouragement, kind guidance, sharing useful experience, constructive direction, support in equipment in this research.

I would like to greatly grateful to Associate Professor Anchali Krisanachinda, Ph.D., Department of Radiology, Faculty of Medicine, Chulalongkorn University, Chairman of thesis defense for her kind suggestion, invaluable advice, and constructive comments. Deeply thanks Professor Franco Milano, Ph.D., University of Florence, Italy, and Associate Professor Kosuke Matsubara, Ph.D., Kanazawa University, Japan, the external examiners of thesis defense for their invaluable suggestion and constructive comments in this research.

I would like to deeply thank Associate Professor Sivalee Suriyapee, M.Eng., and Mr. Sornjarod Oonsiri, M.Sc., Division of Radiation Oncology, Department of Radiology, Faculty of Medicine, Chulalongkorn University, for their invaluable guidance and for great support and contribution the radiation dose measurement in this research.

I would like extremely grateful for all teachers, lecturers, and staffs at Master of Science Program in Medical Imaging, Faculty of Medicine, Chulalongkorn University, for teaching, suggestion, and supports.

I would like extremely grateful all radiological technologists at Diagnostic Radiology Department, Chulabhorn Hospital for their kind helpfull, contributing and providing the digital radiography system in this research.

Finally, I must express my very profound gratitude to my parents for providing me with unfailing support and continuous encouragement throughout my years of study and through the process of researching and writing this thesis. This accomplishment would not have been possible without them.

CONTENTS

Page

Page

Page

Page

LIST OF FIGURES

LIST OF TABLES

LIST OF ABBREVIATIONS

AAPM	American Association of Physicist in Medicine
ALARA	As low as reasonably achievable
AEC	Automatic exposure control
BSF	Backscatter factor
CR	Computed radiography
CT	Computed tomography
CXR	Chest radiography
DE	Dual-energy subtraction
DR	Digital radiography
DQE	Detective quantum efficientcy
DRL	Diagnostic reference levels
DTS	Digital tomosynthesis
ESAK	Entrance surface air kerma
ESD	Entrance surface dose
FPDs	Digital x-ray flat panel detectors
HU	Hounsfield unit
IAEA	International Atomic Energy Agency
ICRP	International Commission of Radiological Protection
KCARE	King's Center for the Assessment of Radiological Equipment
MTF	Modulation transfer function
NPS	Noise power spectrum
PA	Posterior anterior
PACS	Picture archiving and communications system
QA	Quality assurance
RIS	Radiology information system
ROI	Region of interest
RPL	Radiophotoluminescent glass dosimeter
SD	Standard deviation
SNR	Signal-to-noise ratio
TLD	Thermoluminescent dosimeter

CHAPTER I
INTRODUCTION

1.1 Background and Rationale

World Health Organization (WHO) has reported that global cancers are leading cause of death worldwide, accounting for 8.8 million deaths in 2015. The most five common causes of cancer death are the cancers of lung (1.69 million deaths), liver (788,000 deaths), colorectal (774,000 deaths), stomach (754,000 deaths) and breast (571,000 deaths). This indicated that the death rate of CA lung is higher than other cancers [1].

The early detection would increase the chances of survival rate. Although the advantage of technology in field of radiology to indicate the abnormality of chest radiography has several techniques, the first diagnostic tools for observing the abnormality of chest is still the digital chest radiography.

Digital chest radiography is the most commonly used screening tool for pulmonary disease. The advantages are a short examination time, easy and low cost. Other advantages of digital radiography include higher patient throughput, increase dose efficiency, and the greater dynamic range of digital detectors with possible reduction of radiation exposure to the patient as illustrated in Figure 1.1. However, pulmonary lesion can be missing by conventional chest radiography because it shows the three-dimensional chest anatomy and pulmonary lesions on a two-dimensional image, resulting into overlapping of internal organs. Digital chest radiography shows high specificity according to confidence level for early detection of lung carcinoma, but its sensitivity is quite low.

Computed tomography (CT) is another imaging modality that shows high sensitivity for nodule detection. Consequently, it becomes a gold standard for the detection of pulmonary abnormalities and pulmonary nodules. However, this modality gives higher radiation dose and higher cost compared to general radiography [2].

Recently, the evolution in advances acquisition technique using x-ray flat panel detector namely digital chest tomosynthesis or “DTS” has increasingly interested for tomographic reconstruction and its clinical applications. As the outstanding benefits of DTS, therefore, it has been recommended by several authors as an alternative investigation beside both chest radiography and CT image. Furthermore, the greater diagnostic performance of DTS for detecting pulmonary nodules has been reported. For the radiologists, although DTS studies spend time to read more than routine digital

chest radiography due to multiple images scrolling, the overall interpretation time is lower than CT because of the lower number of images to be evaluated.

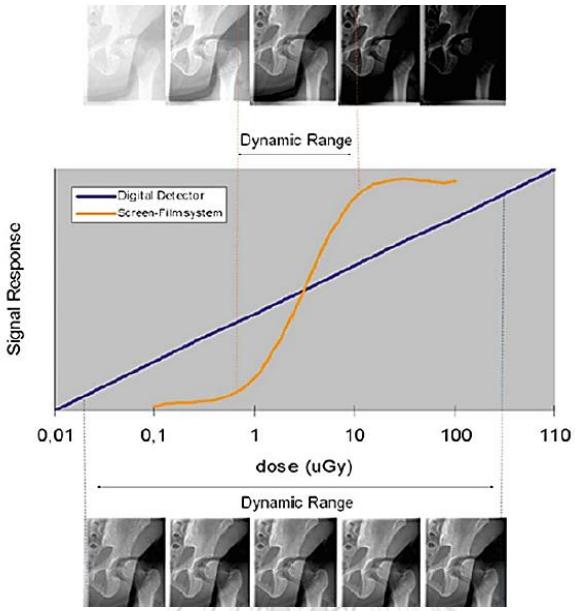

Figure 1.1 The dynamic range of screen film and digital [3].

DTS is increasingly accepted as an effective method for improving pulmonary abnormalities and nodule detections; however, the radiation dose is still substantially higher compared to digital radiography. According to previous studies, the radiation dose obtained from DTS was higher than digital chest radiography approximately 3 times [4].

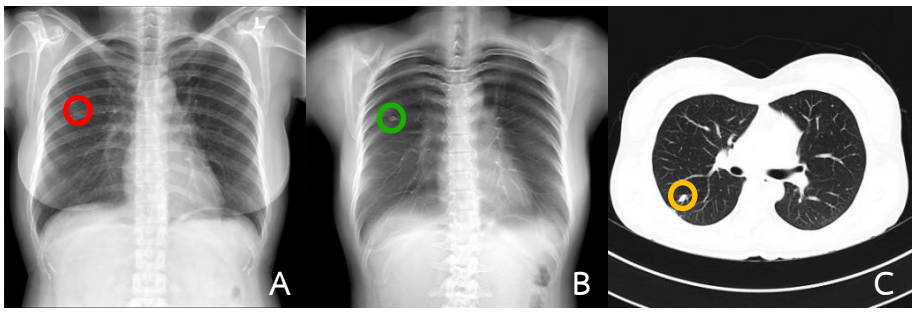

Figure 1.2 The images of lung nodule in difference modality (A) digital radiography (B) digital tomosynthesis and (C) computed tomography.

Therefore, it is of great interest to determine the optimization parameters in DTS for reducing the radiation dose to the patient following the “As low as reasonably achievable (ALARA) principle as well as balancing the image quality for

interpretation. Furthermore, the optimal protocol developed from this study will provide a great contribution of the knowledge in diagnostic clinical dosimetry.

1.2 Research objectives

1.2.1 To determine the optimal protocol of digital chest tomosynthesis in phantom study.

1.2.2 To apply the optimal protocol of digital chest tomosynthesis to patients at Chulabhorn hospital.

1.3 Definitions

Absorbed dose: The energy imparted to matter per unit mass of the irradiated matter (J/kg). The unit of absorbed dose is gray (Gy).

Back scatter factor (BSF): The ratio of a radiation quantity measured by dosimeter at the phantom/material surface exposed directly from the radiation source and the radiation quantity measured at the same position without the matter.

Entrance surface dose (ESD): The absorbed dose in air at the center point of the x-ray beam at the surface of patient or phantom including back scatter factor.

Detective quantum efficiency (DQE): The efficiency of the x-ray detector converts x-ray energy into the image signal.

Optimization: The balancing between the approximate image quality of the clinical image of the patient and the proper radiation dose.

CHAPTER II
REVIEW OF RELATED LITERATURES

2.1 Theory

2.1.1 Principles of Digital Radiography

Wilhelm Roentgen, German professor of experimental physics, discovered x-rays in 1895 while working on emissions from electric current in vacuum. He noticed a glow from a barium platinocyanide coated screen kept across the room whenever the current was passed between the two electrodes in a charged cathode tube. Over the years, many significant refinements were made in the techniques and the equipment. Presently, radiological facilities are found in even the smallest hospital and emergency units involved in health care [5].

The first digital imaging system was introduced in 1980. For general radiography, x-ray images were first recorded digitally with cassette-based storage-phosphor image plates, which were also introduced in 1980. The evolution of digital x-ray image receptor is described as below [6].

1980	Computed radiography (CR), storage phosphors
1987	Amorphous selenium-based image plates
1990	Charge-coupled device (CCD) slot-scan direct radiography (DR)
1994	Selenium drum DR
1995	Amorphous silicon-cesium iodide flat-panel detector Selenium-based flat-panel detector
1997	Gadolinium-based (scintillator) flat-panel detector
2001	Gadolinium-based (scintillator) portable flat-panel detector
2001	Dynamic flat-panel detector fluoroscopy–digital subtraction angiography (DSA)
2006	Digital tomosynthesis
2009	Wireless DR (flat-panel detector)

Digital systems are traditionally split into two broadly defined categories computed radiography and digital radiography as in Figure 2.1. Digital imaging comprises four separate steps: generation, processing, archiving, and presentation of the image.

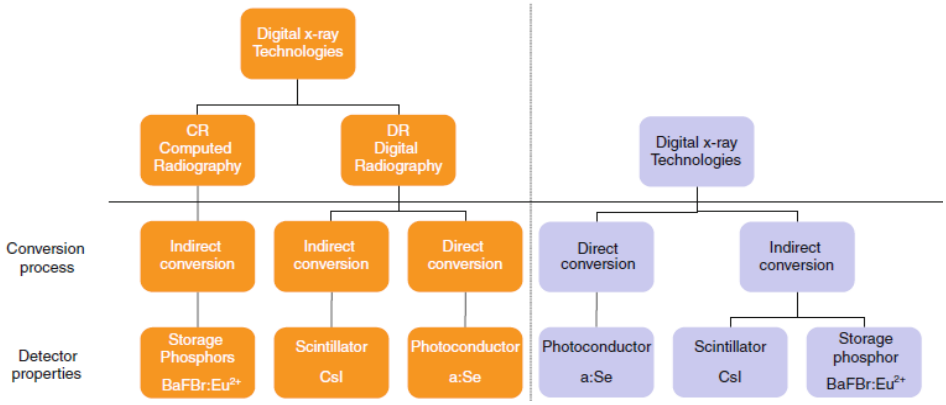

Figure 2.1 Digital radiography technologies.

The digital detector is exposed to x-rays generated by x-ray tube. The energy absorbed by detector must be transformed into electrical charges, which are then recorded, digitized, and quantified into a gray scale that represents the amount of x-ray energy deposited at each digitization locus in the resultant digital image. After sampling, post processing software is needed for organizing the raw data into clinical images.

Digital images have a number of potential advantages over film because the images are collected and stored electronically in such a manner that image acquisition, signal processing, storage and display. In particular, post-processing options, especially contrast enhancement can improve visualization. Also, digital images are stored in a computer, the ability of the computer to perform routine pre-programmed tasks with a high degree of accuracy means that computer-aided detection and diagnosis may become a useful aide to the radiologist.

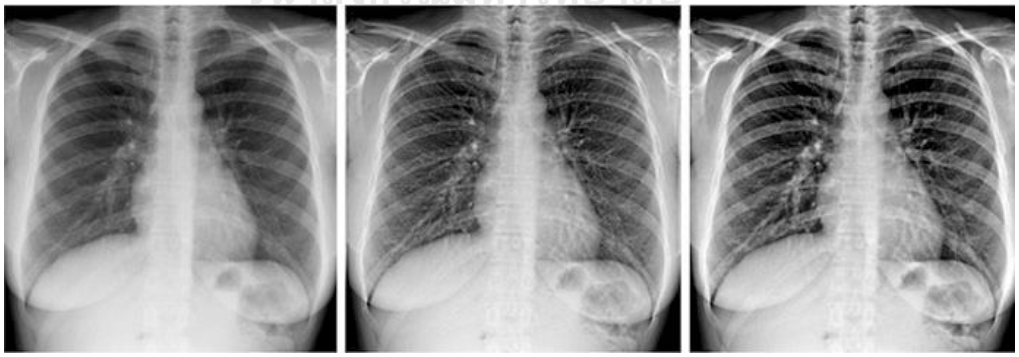

Figure 2.2 The results of image processing using contrast enhancement [7].

After final image generation, images are sent to a digitized storage archive. A digital header file containing patient demographic information is linked to each image. Digital images can be manipulated during viewing with functions like panning, zooming, inverting the gray scale, measuring distance and angle, and windowing. Image distribution over local area networks is possible. Digital images

and associated reports can be linked to the hospital information system (HIS) and radiology information system (RIS) and storing the images on a Picture Archiving and Communications System (PACS). Images can also be reported off site using teleradiology.

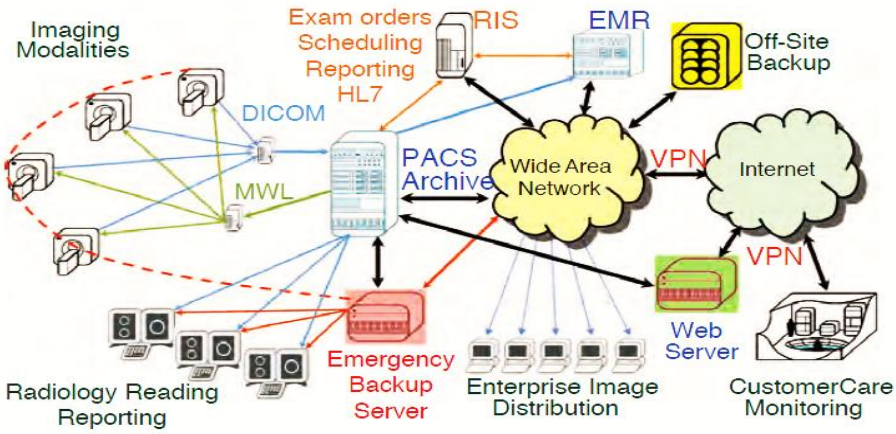

Figure 2.3 Picture Archiving and Communications System (PACS) [8].

2.1.2 Digital Radiography (DR)

2.1.2.1 Direct Conversion

Direct conversion requires a photoconductor that converts x-ray photons into electrical charges by setting electrons free. Typical photoconductor materials include amorphous selenium, lead iodide, lead oxide, thallium bromide, and gadolinium compounds. The most commonly used element is selenium. All of these elements have a high intrinsic spatial resolution.

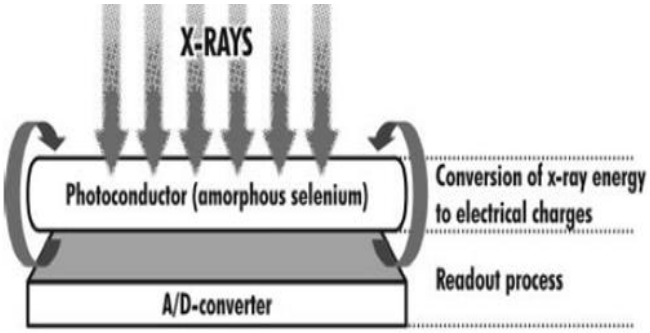

Figure 2.4 DR system based on selenium drum detector [9].

A rotating selenium-dotted drum with a positive electrical surface charge is exposed to x-rays. The charge pattern of the drum surface is proportional to the incident x-ray. The charge pattern is then converted into a digital image by analog-to-digital converter.

Selenium-based direct conversion DR systems are equipped with either a selenium drum or a flat-panel detector. Several clinical studies have confirmed that selenium drum detectors provide good image quality that is superior to that provided by screen-film or CR systems.

A newer generation of direct conversion DR systems makes use of selenium-based flat-panel detectors. These detectors make use of a layer of selenium with a corresponding underlying array of thin-film transistors (TFTs). The principle of converting x-rays into electrical charges is similar to that with the selenium drum, except that the charge pattern is recorded by the TFT array, which accumulates and stores the energy of the electrons.

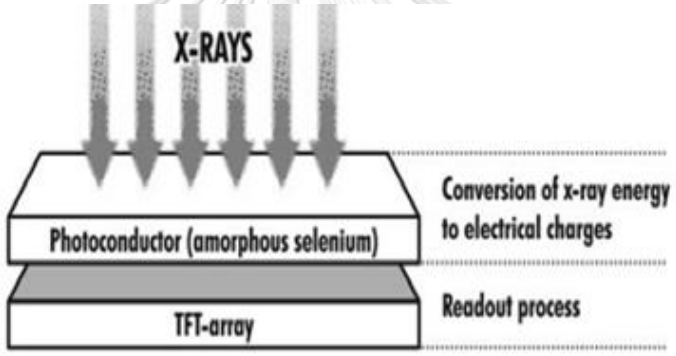

Figure 2.5 DR system based on thin-film transistors (TFTs) [9].

2.1.2.2 Indirect Conversion

Indirect conversion DR systems are “sandwich” constructions consisting of a scintillator layer, an amorphous silicon photodiode circuitry layer and a TFT array. When x-ray photons reach the scintillator, visible light proportional to the incident energy is emitted and then recorded by an array of photodiodes and converted to electrical charges. These charges are then read out by a TFT array similar to that of direct conversion DR systems.

Indirect conversion flat-panel detectors can provide superior image quality. Studies comparing indirect conversion flat-panel detectors with conventional screen-film combinations storage-phosphor image plates or other digital detectors have verified that flat-panel detectors offer the best image quality and low-contrast performance of all digital detectors.

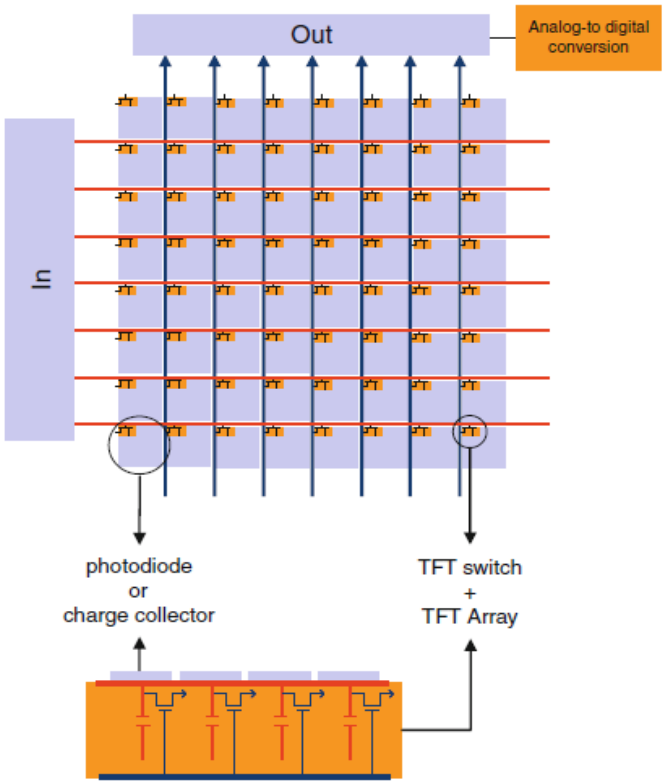

Figure 2.6 TFT thin-film transistor [6].

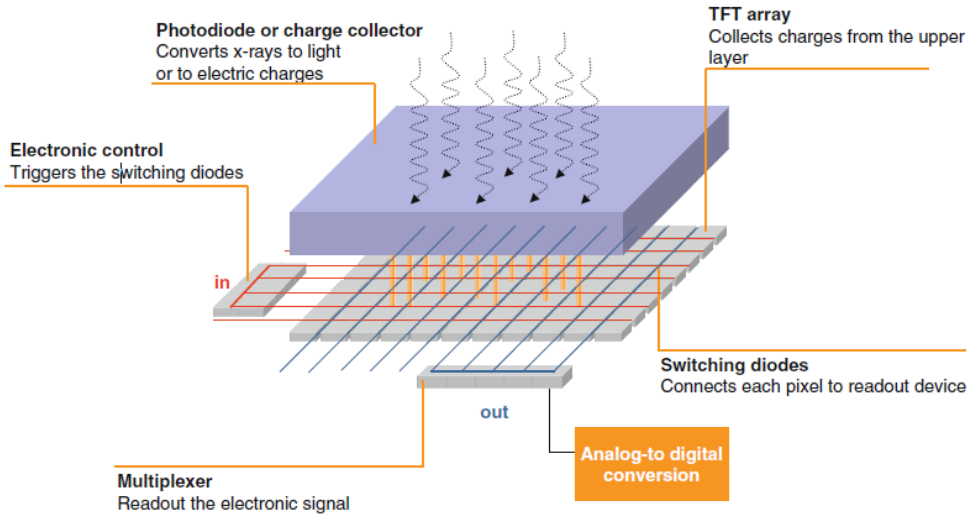

Figure 2.7 Flat-panel structures [6].

2.1.3 Image Processing

One of the best advantages of digital radiography (DR) is the ability to use image processing. Image processing is used to improve image quality by reducing noise, removing technical artifacts, and optimizing contrast for viewing. Spatial resolution cannot be influenced by the processing software because it is dependent on the technical variables of the detector (e.g., pixel size).

2.1.4 Advances in digital radiography

2.1.4.1 Dual-energy subtraction

Dual Energy (DE) imaging is an imaging technique in which a low kVp image and a high kVp image are acquired in rapid succession. The acquired images are processed to create a soft-tissue image and a bone image, which are provided in addition to the standard (high kVp for chest DE and low kVp for abdomen) image. Dual Energy has significant potential for improving the conspicuity of chest pathology by removing the bone structures and for improving specificity by providing calcification information in the bone image.

2.1.4.2 Computer-aided diagnosis (CAD)

Computer-aided diagnosis (CAD) programs have the goal to aid the radiologist in detecting or differentiating various disease entities in the chest. Usually the system suggests a lesion or abnormal region that then has to be verified by the radiologist.

2.1.5 Digital tomosynthesis (DTS)

DTS is a new medical imaging technique in digital radiography (DR) based on the linear tomography concept. The default configuration for a chest tomosynthesis examination includes the acquisition of 60 projection images distributed evenly over an angular range of 30° centered around the standard orthogonal posteroanterior (PA) direction as same as routine chest x-ray. The x-ray output is constant for all projection images and is determined by the resulting exposure of a scout view image. This scout view is a conventional PA projection acquired prior to the tomosynthesis projection image acquisition with automatic exposure control at a source-to-image distance (SID) of 180 cm. The tube load used for the scout view is multiplied by a user-adjustable dose ratio and distributed evenly between the 60 tomosynthesis projection images. Possible tube load settings for the projection images. During the acquisition of the projection images, the x-ray tube performs a continuous vertical motion. The projection images are used to reconstruct an arbitrary number of coronal section images [4].

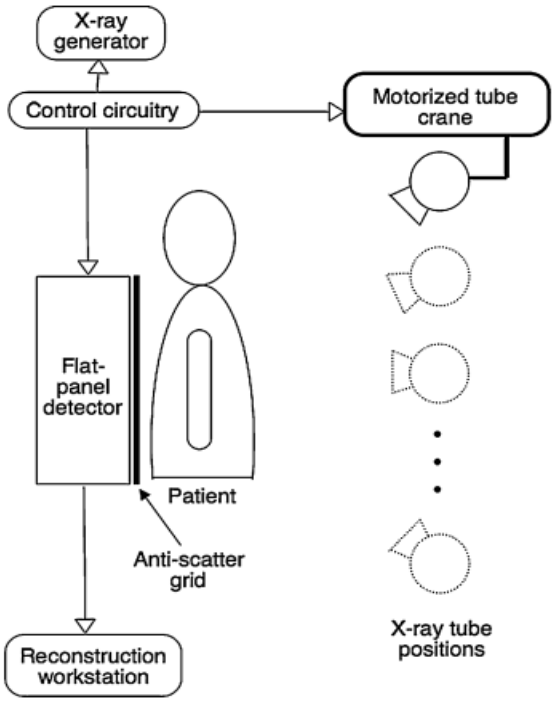

Figure 2.8 Basic components of a chest tomosynthesis device [10].

Image acquisition of digital chest tomosynthesis

The acquisition consists of two main parts:

1. Scout – a standard, single energy acquisition used to determine the exposure settings and patient positioning.

2. Sweep – the system takes multiple, low-dose exposures as the tube travels through the arc. The system then creates the "slices" to visualize the anatomy at various depths. Additional sweeps should only be made if the patient moved during the sweep and the slices are not of acceptable quality.

2.1.5.1 Tomosynthesis reconstruction methods

Tomosynthesis algorithms can be divided into three categories: 1) backprojection algorithms, 2) filtered backprojection (FBP) algorithms, and 3) iterative algorithms. The step in the reconstruction procedure is to perform a simple shift and add computation, equivalent to simple FBP, to generate conventional tomosynthesis images plane is enhanced while that in other planes is blurred. The basis for filtered back-projection (FBP) is the backprojection of data acquired in projections acquired over all angles. Iterative algorithm, unlike the one-step operation in backprojection and FBP algorithms. During iterative reconstruction, a 3D object model is repeatedly updated until the model converges to the solution that optimizes

an objective function. The objective function defines the criteria of the reconstruction solution. The objective function in the maximum likelihood (ML) algorithm is the likelihood function, which is the probability of getting the measured projections in a given object model. The solution of the ML algorithm is an object model that maximizes the probability of getting the measured projections [11].

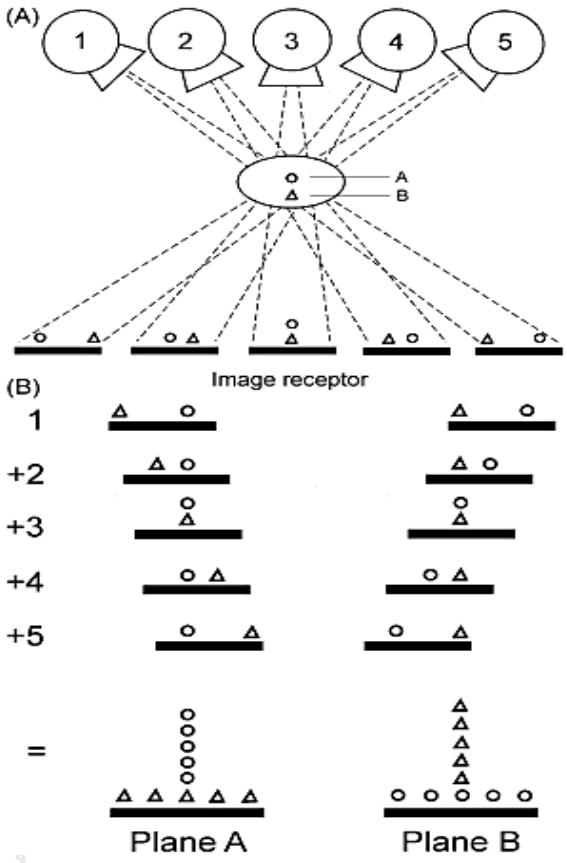

Figure 2.9 The shift and add method [10].

2.1.6 Principles of Patient Dose Measurement

The principal quantities to be measured for use in general radiography are the incident air kerma, the entrance surface air kerma and the air kerma–area product. For phantoms, the incident air kerma is measured but for patient exposures it is determined using recorded exposure parameters. Additionally for patients, the entrance surface air kerma may be determined from measurements with TLDs and the air kerma–area product can be measured using a KAP meter. (IAEA, TECHNICAL REPORT SERIES NO.457)

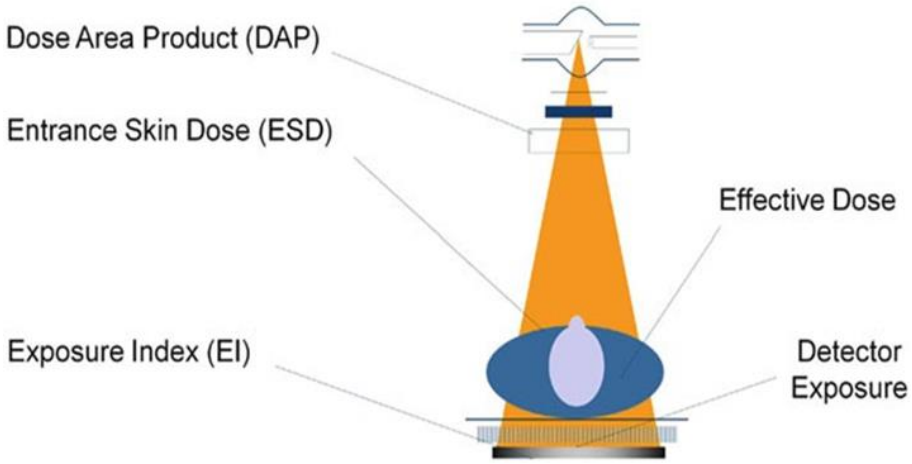

Figure 2.10 Patient dosimetry measurements [12].

There is a very large amount of attenuation as a diagnostic x-ray beam passes through the body. Thus the exit dose will be typically between 0.1% and 1% of the entrance dose depending on the thickness of the body part being exposed and its composition. The doses to different organs within the beam will be very dependent on their depth and radiation dose to a critical organ may be substantially different for AP and PA projections.

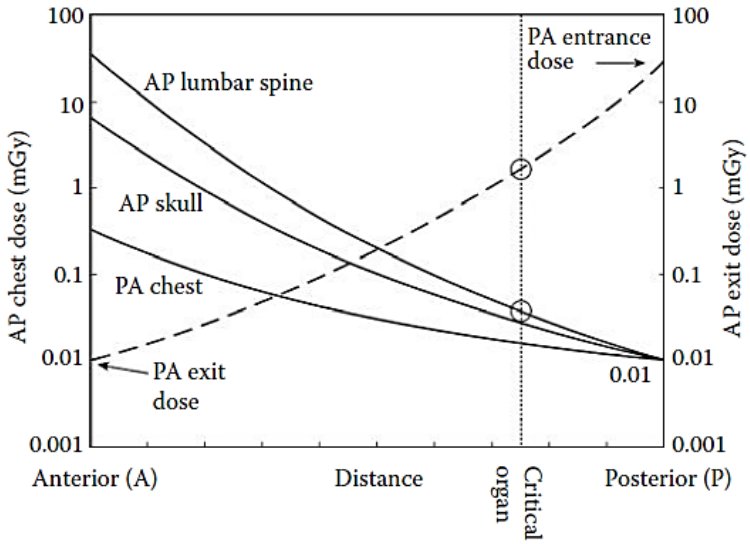

Figure 2.11 Attenuation of x-ray passing through the body [13].

2.1.7 Entrance Surface Dose

ESD or entrance surface dose (ESD) is the most common of the patient dose measures. ESD represents the skin patient dose at the center of the incident x-ray beam**,** and is measured in mGy. It is the sum of the dose directly from the incident x-ray beam and scattered x-rays into that area from surrounding and underlying tissue. ESD can define as the absorbed dose to air at the center of the beam, including backscattered radiation. The patient ESD during standard radiographic examination can be measured directly by placed dosimeter on the patient's skin or, in an alternative way, can be estimated by a calculation using the exposure factors (kV and mAs) coupled with measurements of x-ray tube output. Due to the difficulty to obtain dosimeter measures in practical situations involving patients ESD estimation is often used as a procedure [12].

2.1.7.1 Indirect measurement

The indirect assessment of the entrance surface air kerma consists of the following steps:

1. Measure the beam HVL and the x-ray tube output.
2. Establish the incident air kerma for exposure parameters recorded during patient examination.
3. Establish the entrance surface air kerma from the incident air kerma and an appropriate backscatter factor.

2.1.7.2 Direct measurement

The entrance surface air kerma is directly measured using sachets of dosimeter to the patient's skin.

2.1.8 Radio-photoluminescence Glass Dosimeter (RPLGD)

Glass dosimeter is commonly used passive dosimeters. The dosimeters are made of silver activated phosphate glass, which form stable luminescent centers when exposed to ionizing radiation. When these radiated dosimeters are exposed to pulsed UV laser, the luminescent centers emit orange luminescence. The luminescent amount is proportional to the absorbed dose.

The glass dosimeter GD-352M with tin filter in the capsule is used for lower the energy dependence effect. The can be used for measuring the dose from low energy photons as in diagnostic radiology. In the process of dose readout, based on the dose values, the dose ranges are divided into two categories, low dose range (10 μGy – 10 Gy) and high dose range (1 Gy - 500 Gy).The readout system can

automatically distinguish the dose range according to different readout magazine used by the users.

Table 2.1 The characteristics of RPLGD [14].

Type	SC-1	GD-450	Dose Ace
Effective atomic number	12.04	12.04	12.04
The dose linearity range	10 μGy - 10 Gy	10 μGy - 10 Gy	10 μGy - 10 Gy 1 Gy - 500 Gy
Energy dependency (20 keV / ^{137}Cs)	1.2 (with energy compensator filter)	1.2 (with energy compensator filter)	3.4 (w/o energy compensator filter) 0.8 (with energy compensator filter)
Fading effect	< 5 % / yr	< 5 % / yr	< 5 % / yr
Repeatable readout	yes	yes	yes
Angular dependency	± 8% (0 ~ 80 degree)	± 3% (0 ~ 80 degree)	0 (0 ~ 80 degree)

2.1.8.1 Characteristics of RPLGD for clinical applications

1. Repeatable readout: the luminescence signal does not disappear after readout; therefore, repeated readout for a single exposure is possible for RPLGD.

2. Small difference in individual sensitivity: the readout variation between different PRLGDs with the same exposure is small. RPLGD is manufactured with melted glass; therefore, its individual sensitivity is small as compared to that of either TLD or OSLD.

3. No correction factor needed: the luminescence single can be converted to the exposure dose directly without the need of correction factors. The exposure dose can be determined with the help of readout from reference PRLGD built-in to the readout system.

4. Small energy dependence: the energy dependence existed in glass, if there is no energy compensator filter with it. However, energy dependence can be reduced with energy compensator filter.

5. Small fading effect: the stability of color centers in RPLGD is high. Hence the effects of environment conditions such as humidity and temperature have very little impact to color centers, hence low fading effects for RPLGD.

6. Better reproducibility: by using pulse ultra-violet laser as excited source, the accuracy of repeated readout can be maintained. Therefore, RPLGD has a very good reproducibility.

7. Wide measurable dose range: the dose linearity range for RPLGD is 0 – 500 Gy. This range covers the dose range used in the medical field. RPLGD can therefore be applied for dose verification in radiotherapy as well as in diagnostic radiology.

8. Feasibility of personal dose monitor tools: the characteristics, physical and chemical, of RPLGD are equal to or better than that of TLD and OSLD because of its luminescence material and readout technique. RPLGD can be used as dose monitor for radiation field worker.

2.1.9 The factors affecting image quality

2.1.9.1 Pixel Size, Matrix, and Detector Size

Digital images consist of picture elements or pixels. The two-dimensional collection of pixels in the image is called the matrix, which is usually expressed as length (in pixels) by width (in pixels). Maximum achievable spatial resolution is defined by pixel size and spacing. The smaller the pixel size, the higher the maximum achievable spatial resolution. The overall detector size determines if the detector is suitable for all clinical applications [9].

2.1.9.2 Spatial Resolution

Spatial resolution refers to the minimum resolvable separation between high-contrast objects. In digital detectors, spatial resolution is defined and limited by the minimum pixel size. Increasing the radiation applied to the detector will not improve the maximum spatial resolution. On the other hand, scatter of x-ray quanta and light photons within the detector influences spatial resolution. The intrinsic spatial resolution for selenium based direct conversion detectors is higher than that for indirect conversion detectors. Structured scintillators offer advantages over unstructured scintillators.

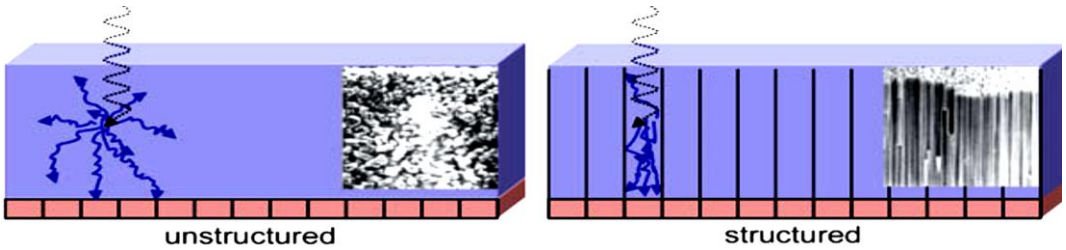

Figure 2.12 Structure of scintillators [6].

2.1.9.3 Contrast

Contrast (radiographic contrast) is proportional to the magnitude of the signal difference between the structure of interest and its surroundings in the displayed image, which is expressed in terms of the optical density difference between two adjacent areas on the SF film or as the relative brightness difference between the corresponding areas in a digital image displayed on a monitor.

For both screen film and digital imaging, radiographic contrast is influenced by subject contrast and receptor sensitivity. However, in digital imaging, contrast in the displayed image can also be altered by the adjustment of display parameters independent of the acquisition parameters. Subject contrast is proportional to the relative difference in x-ray exposure on the exit side of the patient and is the result of the attenuating properties of the tissues under study. Attenuation is strongly dependent on the x-ray energy spectrum and is determined by the target material, kilovoltage, and total beam filtration. Subject contrast is further reduced by the presence of scatter [15].

2.1.9.4 Noise

Image noise is typically measured by illuminating the receptor with uniform x-ray fluence, then measuring the variance in selected regions of the resulting image. A more informative measure of noise can be obtained by estimating the noise power spectrum (NPS), which characterizes the spatial frequency dependence of the noise. Knowledge of the frequency response of noise in an imaging system is important because there are a number of additional noise sources in digital radiography, such as aliasing and electronic noise.

2.1.9.5 Modulation Transfer Function (MTF)

Modulation transfer function (MTF) is the capacity of the detector to transfer the modulation of the input signal at a given spatial frequency to its output. At radiography, objects having different sizes and opacity are displayed with different gray-scale values in an image. MTF has to do with the display of contrast and object size. More specifically, MTF is responsible for converting contrast values of different-sized objects (object contrast) into contrast intensity levels in the image (image contrast). MTF is a useful measure of true or effective resolution, since it accounts for the amount of blur and contrast over a range of spatial frequencies.

2.1.9.6 Dynamic Range

Digital detectors have a wider and linear dynamic range, which, in clinical practice, virtually eliminates the risk of a failed exposure. Another positive effect of a wide dynamic range is that differences between specific tissue absorptions (e.g., bone vs soft tissue) can be displayed in one image without the need for additional images. On the other hand, because detector function improves as radiation exposure increases, special care has to be taken not to overexpose the patient by applying more radiation than is needed for a diagnostically sufficient image.

2.1.9.7 Detective Quantum Efficiency

Detective quantum efficiency (DQE) is one of the fundamental physical variables related to image quality in radiography and refers to the efficiency of a detector in converting incident x-ray energy into an image signal. DQE is calculated by comparing the signal-to-noise ratio at the detector output with that at the detector input. DQE is dependent on radiation exposure, spatial frequency, MTF, and detector material. High DQE values indicate that less radiation is needed to achieve identical image quality; increasing the DQE and leaving radiation exposure constant will improve image quality [9].

2.1.10 Factors affecting radiation dose

2.1.10.1 Exposure Parameters

Exposure parameters influence and determine the quantity and quality of the x-ray beam. The four main exposure parameters are tube potential (kV), tube intensity (mA), exposure time (s) and source to image distance (SID). Exposure time and tube intensity could be a unique exposure factor: milliampere second (mA-s). To obtain a radiographic image the tube potential and exposure time are the most important factors to take into account. Adjustment actions of beam quality could be

altered by the radiographer aiming a particular radiological study and patient characteristics.

The modifications of exposure factors such as the penetrating power of the beam (by adjusting tube potential—kV) and the beam quantity (by adjusting the tube current—mA) are actions that provide influence in image quality and dose. By changing exposure parameters a more penetrating primary beam could be obtained increasing tube potential (kV) and thus the quality of x-rays produced. This action provides a better penetration of the x-ray beam in tissues leading to reduced scatter radiation and thus lower absorbed dose to the patient. Patient dose will generally be lower at high tube potentials and a compromise must be sought in order to use the highest tube potential (kV) possible.

This action leads to reduction of dose to the patient at the lowest possible level, without reducing the image contrast to an unacceptable level. Lowering exposure time may also improve image quality affecting positively both entrance skin dose (ESD) and effective dose. As an alternative keeping the same mA s by increasing the mA and reducing exposure time (s) is an option. This also may yield image quality improvements by reduction of motion blurring due to shorter exposure time [3].

2.1.10.2 Source to Image–Detector Distance

Source to image distance (SID) is a determinant factor concerning beam intensity that achieves the detector. Radiation intensity achieving the detector follows the inverse square law principle. According to this principle, radiation intensity decrease is inversely related to the square of the distance from the source. Thus if you double the distance you reduce the dose by a factor of four. By choosing a correct SID an improvement of spatial resolution (sharpness) and lower dose to the patient will be achieved. This means that SID will affect detector exposure and image quality.

2.1.10.3 Beam Filtration

Beam filtration can contribute for an ESD reduction to the patient. Additional filtrations exceeding 4 mm Al allow a significant reduction of nearly 50% of doses. Chest radiographs obtained in a DR system with copper (Cu) filtration were of similar image quality as radiographs obtained without copper filtration and a patient dose reduction of 31% was estimated with Monte Carlo calculations.

Experimental studies using phantoms confirm that ESD could be significantly reduced in a CR system when using beam filtering. When using additional filtration at 125 kV in a chest PA projection performed at 180 cm, the ESD decreases when increasing the Cu filtration. A reduction of 52% (ESD_{DAP}) is found at 125 kV when increasing beam filtration from 0 mm Cu to 0.3 mm Cu.

Table 2.2 Technique groups and filtration (chest PA projection) [3].

Tube potential	Filtration	mA s	DFD (cm)	FSD (cm)	DAP (μGy * m^2)	ESD_{DAP} (mGy)
125 kV	0 mm Cu	3.26	180	155	12	0.19
	0.1 mm Cu	3.76	180	155	8.7	0.14
	0.2 mm Cu	4.24	180	155	7.3	0.12
	0.3 mm Cu	4.77	180	155	6.3	0.10

DFD displaced frame distance, *FSD* focus-to-skin distance, *DAP* dose-area product, *ESD* entrance skin dose, *mA s* milliampere second

The observed mAs increase while the additional filtration increases is due to the lower energy photons that are attenuated with the filter thickness augmentation. In consequence an increase of the x-ray tube output is necessary to maintain the necessary exit beam photon flux.

This indicates a similar exposure at the CR detector at different filtrations, and that a proper exposure at the detector produces an accurate image with the expected exposure at the detector. In this case it is important to remind that at different beam filtration exposure at the detector is quite similar, but patient ESD could be reduced by 52% (ESD_{DAP}) at 125 kV when increasing beam filtration from 0 mm Cu to 0.3 mm Cu. No substantial differences are found in exposure index when using additional filtration, but a marked reduction in patient exposure is achievable.

2.1.10.4 Collimation and Field Size

Collimation restricts the useful x-ray beam to the part of the body being examined. Adjustable light locating collimators are the most frequently used and they restrict beam size protecting adjacent tissue from unnecessary exposure. Collimation also reduces scatter radiation and thus improves image contrast resolution. Field size is probably one of the most important factors, which causes exposure variation in tissue dose. It is essential that all examinations should be carried out considering the need of keeping the field size to the minimum possible area. Field size collimation has an effect in image quality and dose. It is related to dose area product (DAP) measure [3].

2.1.10.5 Thickness

Tissue thickness, body habitus and tissue composition result in differences in x-ray beam attenuation. This is the basis on which digital and all radiologic imaging creates radiographs. For example, muscle tissue is denser than fat tissue, and requires an increase in technique so that the beam can adequately penetrate the muscle tissue. Grids typically are not used when anatomy is less than 10 cm thick, so radiographers must carefully consider whether to use grids based on the patient's actual size and tissue composition.

2.1.10.6 Anti-scatter Grid

Anti-scatter grids are generally used when particular body areas are exposed (e.g., lumbar spine). Areas with high absorption producing a high level of scattered radiation that leads to image quality deterioration with respect to signal-to-noise ratio and contrast require the use of anti-scatter grid. The grid is placed inside the Bucky between the patient and the detector. Grid design allows a high percentage of primary radiation to pass to the detector while absorbing a high percentage of scattered radiation. DR systems represent area detectors that are vulnerable to scatter effects. For that reason general practice is that anti-scatter grids are used in applications similar to those in conventional radiography (e.g., upright chest radiography, radiographs of the spine, pelvis, and limbs) [3].

2.1.10.7 Automatic Exposure Control

The Automatic Exposure Control terminates an x-ray exposure to produce optimum quality images. AEC compensates for changes in patient thickness, opacity, and different technique factors of mA, kVp, and SID. Proper patient positioning is very important. In extreme cases of misalignment, some radiation bypasses the patient and ends the exposure prematurely, causing underexposed images. Conversely, positioning the heaviest patient area over the detector sensing area may cause overexposed image areas. AEC helps to produce uniform quality images regardless of patient thickness or opacity. This system feature, AEC, automatically selects the mAs and exposure time.

2.1.11 Diagnostic reference levels (DRLs) and ALARA

Diagnostic reference levels (DRL) are defined as dose levels for typical examinations for groups of standard-sized patients or standard phantoms for broadly defined types of equipment. They are specified as entrance surface air kerma (ESAK, measured in air without backscatter) or as entrance surface dose (ESD, measured in specified material with backscatter).

The concept of DRL was introduced by the International Commission of Radiological Protection (ICRP) in the 1990s. DRL are typically set at the third quartile (75% value) of the dose distribution, derived from a suitable patient dose survey. The DRL specified are not to be exceeded with routine practice. The reference levels are periodically reviewed and, if necessary and possible, modified on the basis of knowledge of current practice.

DRL for radiographic examinations in adults for different countries are given. Specific values have also been set for pediatrics examinations in different age groups. The DRL are advisory. That is, they do not distinguish between acceptable and unacceptable practice. It should be noted that the reference levels derived from these

surveys represent the “state of practice” and not the “state of the art,” and should be considered as such. However, because digital systems have this greater freedom in setting the dose level without “overexposing,” adherence to reference levels is even more important to avoid dose levels to the patient that do not contribute to the clinical purpose of medical imaging task.

The radiation dose to patients should be as low as reasonably achievable (ALARA) while still providing image quality adequate to enable an accurate diagnosis. ALARA does not necessarily mean the lowest radiation dose, nor, when implemented, does it result in the least desirable radiographic image. The minimal dose to reliably answer a specific diagnostic question in a prospective manner seems to be impossible, given the vast variety of patient-related and disease-related conditions and the workflow for radiographic examinations.

2.1.12 Visual grading analysis (VGA)

Visual grading is to let the observer grade the visibility of important structures, for example the structures from the European quality criteria, using a multistep scale. In this way, the observer is given more freedom to state his opinion about the image quality. VGA is either performed in an absolute manner, where the observer states his opinion about the visibility of a certain structure on an absolute scale (typically consisting of four to five scale steps ranging from “very bad” to “very good”), or in a relative manner, where the observer compares an image with a reference image and gives a statement of the relative visibility of the structure (typically consisting of five scale steps ranging from “much worse” to “much better”)

2.2 Review of related literatures

Sarvana G, et al. [16] studied the role of digital tomosynthesis and dual energy subtraction digital radiography in detecting pulmonary nodules year 2015. The authors suggested that DTS can be used as a problem-solving tool for findings pulmonary lesion on chest radiograph. In addition, it can be used as an alternative to MDCT for tracking changes in nodules over time and as a potential low dose, low cost modality in lung cancer screening programs. Compared to DR, DTS showed increased sensitivity in detection of pulmonary nodules in all size categories with a significant improvement in overall diagnostic accuracy ($p1<0.003$, $p2 = 0.001$).

In detecting calcification in pulmonary nodules, chest dual energy and DTS showed increased sensitivities as compared to chest radiograph in both observers. They found that there was no statistically significant difference between chest dual energy and DTS either ($p1 = 0.590$, $p2 = 0.614$). Chest dual energy has been shown to be superior to chest radiograph in detecting calcification many studies except in the

multi-centric international study. The small number and small proportion 20% approximately of calcified nodules might have accounted for the lack of statistical significance. Thus, the DTS showed a distinct advantage over chest radiograph and chest dual energy in detecting pulmonary nodules of all sizes with a modest increase in radiation dose. Early detection of nodules can provide a significant therapeutic window. The detection of additional nodules on DTS can change the possible differential diagnosis.

In conclusion, DTS performs significantly better than DES-DR and DR at the cost of moderate increase in radiation dose. DTS compensates special resolution of DR for detecting pulmonary nodules by decreasing the summation, and clinically utilized.

Table 2.3 Comparison of performance in detection of pulmonary nodules [16].

	Observer 1		
	DR	DES-DR	DTS
Sensitivity	24.54%	27.27%	60%
Specificity	65.22%	84.78%	84.78%
Positive Predictive	62.79%	81.08%	90.41%
Negative Predictive	26.55%	32.77%	46.99%
	Observer 2		
	DR	DES-DR	DTS
Sensitivity	26.36%	28.18%	61.82%
Specificity	70.73%	80.49%	85.37%
Positive Predictive	70.73%	79.49%	90.89%
Negative Predictive	26.36%	26.46%	45.45%

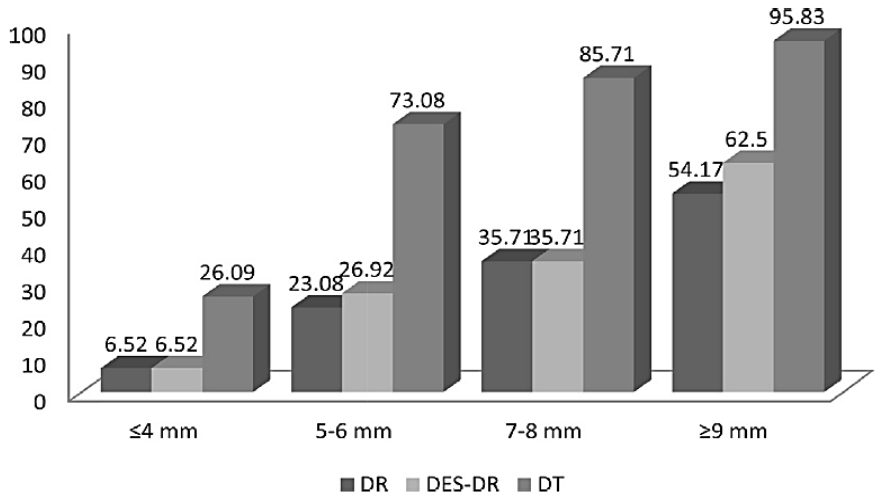

Figure 2.13 Sensitivities for detection of nodules [16].

Table 2.4 Comparison of performance in detection of calcification in pulmonary nodules [16].

	Observer 1		
	DR	DES-DR	DTS
Sensitivity	25%	36%	48%
Specificity	97.7%	99.24%	98.47%
Positive Predictive	72.72%	90%	85.71%
Negative Predictive	88.28%	89.04%	90.84%
	Observer 2		
	DR	DES-DR	DTS
Sensitivity	32%	36%	52%
Specificity	99.21%	99.24%	99.21%
Positive Predictive	88.89%	90%	92.86%
Negative Predictive	88.03%	88.65%	91.24%

Quaia E, et al. [17] studied the diagnostic impact of digital tomosynthesis in oncologic patients with suspected pulmonary lesions on chest radiography. They found that the advantage of DTS is the resolution of doubtful findings directly in the x-ray unit without moving the patient to CT and with comparable effective dose to chest radiograph and lower radiation dose than CT. The preliminary assessment of the chest radiograph by a radiologist does not introduce a time delay because DTS can be scheduled immediately after chest radiograph, e.g. the same day or few days after chest radiograph, since the examination time is comparable to chest radiograph. DTS had a dramatic effect on the CT utilization even in oncologic patients, since DTS resolved doubtful chest radiograph findings for 123/237 (52 %) patients, reducing the need for CT to only 48 % (114/237) of patients. According to these results, DTS could be proposed as a problem-solving technique to confirm or exclude potential thoracic lesions based on chest radiograph in oncologic patients and avoid CT examination in about 50% of patients with a consequent optimization of CT resources as shown in previous studies.

Chest radiograph examination is routine for management and follow-up of many oncologic patients. According to this study, chest radiograph with DTS could replace chest radiograph alone in the follow-up of oncologic patients since it provides a higher diagnostic accuracy and confidence with only a slightly higher radiation dose. Low radiation-dose chest CT represents an alternative imaging modality for lung cancer screening, while the real advantage of DTS over low-dose CT is the immediate verification of doubtful findings directly in the x-ray unit in patients with pseudolesions without moving the patient to CT and with comparable effective dose to chest radiograph and low-radiation-dose CT.

However, low-dose CT represents an accurate imaging modality to detect ground-glass opacities which may not be detected by DTS. In fact, these results were proven only in solid nodules, pulmonary opacities or pleural plaques since we did not observe any ground-glass nodules, as DTS may have some limitations in the detection of sub-solid nodules.

Table 2.5 Diagnostic performance and confidence [17].

	CXR					95 %CIs	DTS				95 % CIs	*P*
Sensitivity (%)	15 (16/103)					9.15–24	92 (95/103)				85.27–96.59	0.0001
Specificity (%)	9 (13/134)					5.27–16.02	91 (122/134)				84.88–95.29	0.0001
Positive likelihood ratio	–[a]						10.3 (95/91)				5.99–17.72	
Negative likelihood ratio	–[a]						0.09 (8/91)				0.04–0.17	
PPV (%)	12 (16/137)					6.82–18.27	88 (95/107)				81.23–94.07	0.0001
NPV (%)	13 (13/100)					7.11–21.2	93 (122/130)				88.23–97.31	0.0001
Accuracy (%)	12 (29/237)					8.35–17.09	92 (217/237)				87.26–94.76	0.0001
Diagnostic confidence												
	Number	TP	TN	FP	FN		Number	TP	TN	FP	FN	
Score 1	10	–	10	–	–		111	–	111	–	–	
Score 2	3	–	3	–	–		11	–	11	–	–	
Score 3	208	–	–	121	87		20	–	–	12	8	
Score 4	2	2	–	0	–		6	6	–	0	–	
Score 5	14	14	–	0	–		89	89	–	0	–	
AUC (95 % CI)	0.619 (0.554–0.681)						0.997 (0.978–1)					0.0001

CXR chest radiography, *DTS* digital tomosynthesis, *TP* true positive, *TN* true negative, *PPV* positive predictive value, *NPV* negative predictive value, *AUC* area under the receiver-operating characteristic curve, *CI* confidence interval

[a] As a result of a value of sensitivity and specificity less than 50 %, positive and negative likelihood ratios were not calculated

In conclusion, DTS improved diagnostic accuracy and confidence in comparison to CXR alone in oncologic patients with suspected pulmonary lesions on CXR with only a slight, though significant, increase in radiation dose.

Hwang HS, et al. [18] investigated digital tomosynthesis of the chest: comparison of patient exposure dose and image quality between standard default setting and low dose setting. They sought to optimize the low dose setting for DT by varying the DTS parameters. Based on their previous studies, 0.3 mm copper filter was firstly added. Image quality of chest radiograph was found with an estimated 30% dose reduction after the addition of 0.3 mm copper filter with flat-panel CsI/a-Si technology. By adding a copper filter with DT, the ESD was decreased by 38% in comparison to the standard setting. This was comparable with previous study. When dose ratio was changed from 1:10 to 1:5 with the use of a Cu filter, the ESD was reduced by 37-50%. However, the ESD in 1:5 was not one half of the ESD in 1:10. This was why that exposure time of equipment was adjusted to several steps (ex. 25 ms, 40 ms, 64 ms). As kVp is decreased, ESD is decreased.

Table 2.6 Effective dose and entrance surface dose [18].

Setting	Tube Voltage	Dose Ratio	0.3 mm Copper Filter	ESD (mGy)	ED (μSv)
1*	120 kVp	1 : 10	(-)	0.98	140
2	120 kVp	1 : 10	(+)	0.60	129
3	120 kVp	1 : 5	(+)	0.38	82
4	100 kVp	1 : 10	(-)	1.25	151
5	100 kVp	1 : 10	(+)	0.58	115
6	100 kVp	1 : 5	(+)	0.31	62
7	80 kVp	1 : 10	(-)	1.27	125
8	80 kVp	1 : 10	(+)	0.73	118
9	80 kVp	1 : 5	(+)	0.37	63

Note.— *Standard default setting. ESD = entrance surface dose, ED = effective dose, DT = digital tomosynthesis

They found little correlation between kVp and ESD. Accordingly, the selected low dose DTS parameters were 100 kVp, a dose ratio 1:5, and with the use of an additional copper filter. The estimated effective dose was 62 μSv using the low dose setting, which showed a 56.7% decrease compared with the standard setting. This result was about 2-3 times that of standard routine chest radiograph and was comparable with the dose of standard 2-view chest radiograph. Evaluated image quality was not significantly different between the low dose and standard settings, with the exception of images of micro nodules in the thick area. Using the standard setting, the detection sensitivities for micronodules and subcentimeter nodules were 55-95% and 88-95%, respectively. Using the low dose setting, detection sensitivities were similar to those of standard setting, with the exception of micronodules in the thick area (63% vs. 44% for standard and low dose setting). The reason for this might be a decrease in signal and an increase in noise due to the attenuation of vertebral bodies using the low dose setting.

CHAPTER III
RESEARCH METHODOLOGY

3.1 Research design

This is an observational cross-sectional descriptive study.

3.2 Research design model

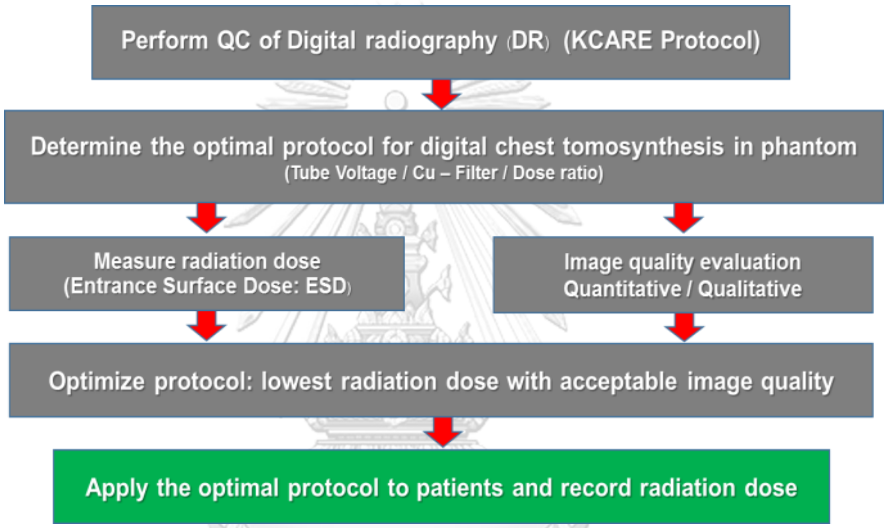

3.3 Conceptual framework

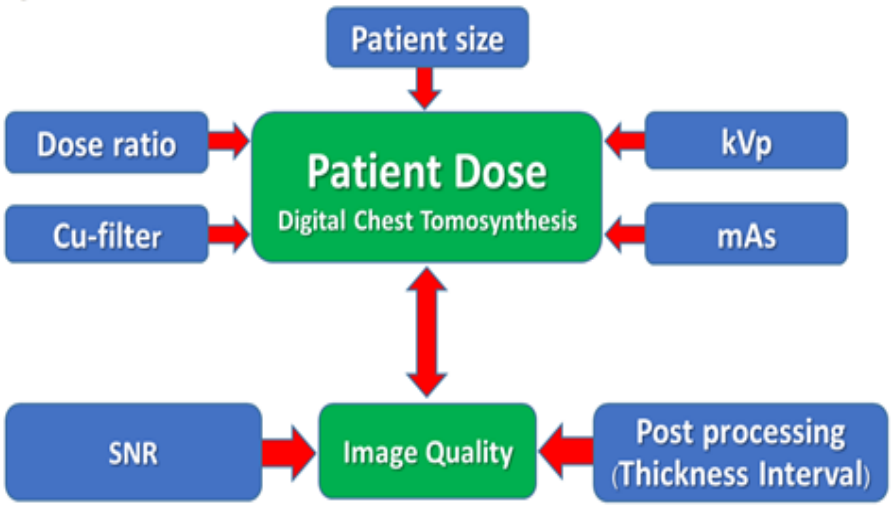

3.4 Research questions

3.4.1 What are the optimal parameters for chest tomosynthesis in phantom study?

3.4.2 What is the patient radiation dose after applying optimized protocol?

3.5 Keywords

Digital radiography, Digital chest tomosynthesis, Image quality, Radiation dose

3.6 Materials

3.6.1 Digital radiography system

Digital radiography system manufactured GE Healthcare, model Definium 8000 with VolumeRAD Technology at Department of Diagnostic Radiology, Chulabhorn Hospital, Bangkok, and was used in this study.

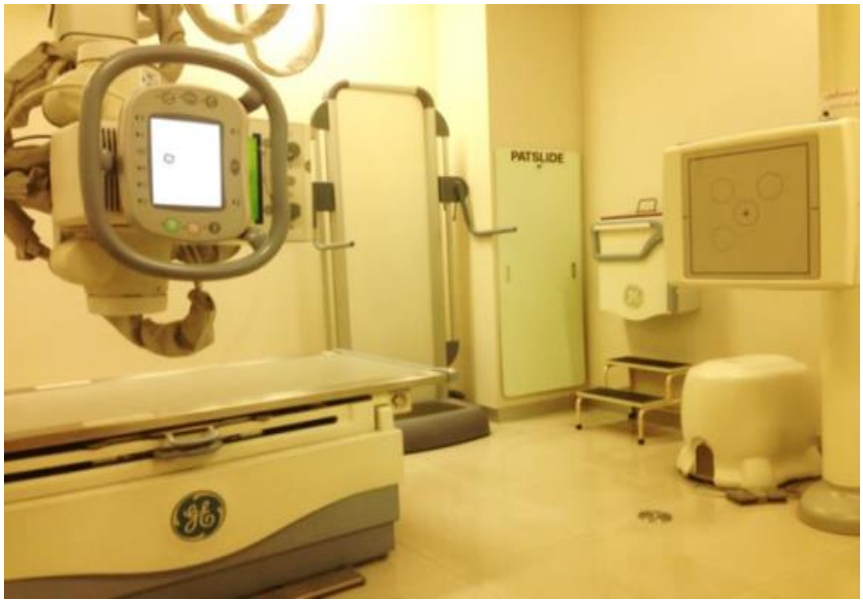

Figure 3.1 DR system model Definium 8000 with VolumeRAD Technology.

Table 3.1 Specifications of Definium 8000 (GE Healthcare).

Definium 8000	Specifications
X-ray tube	x-ray tube heat capacity: 350 KHU
	Total heat capacity of tube: 1500 KHU
	Focal point of x-ray tube: 0.6 mm (small) and 1.25 mm (large)
	Anode heat cooling rate: 75 KHU/min
	Cooling rate of tube housing: 60 KHU/min
High -voltage generator	~150 kV, minimum increment: 1 kV
	Allowable deviation: < ±3% ± 2 kVp
Collimator	Automatic and manual x-ray beam collimation.
	Operator selectable added filters: 0.1 mm, 0.2 mm or 0.3 mm copper
Digital Detector	GE x-ray digital detector is based on amorphous silicon technology.
	Detector Size 41 × 41cm
Power supply conditions	Voltage: Three-phase; AC; 380, 400, 420, 440, 460, 480V±10%
	Frequency: 50/60Hz ±1Hz
	Power impedance: < 0.9

3.6.2 Multipurpose chest phantom

Chest phantom manufacturer Kyoto Kagaku Co. Ltd. model N1 LUNGMAN (male chest torso) is designed and constructed commercially to simulate standard human (170cm/70kg). The phantom provides life-like radiographs very close to actual clinical images. The phantom bones and vessels show life-like contrast gradations on the image along with tube voltages.

Figure 3.2 Multipurpose Chest phantoms N1 LUNGMAN.

Specifications of Multipurpose chest phantom N1 LUNGMAN

Main body:

Synthetic bones are embedded.

Internal parts: (separates into four parts)

1. Mediastinum: heart, trachea
2. Pulmonary vessels (right and left)
3. Abdomen (diaphragm) block: no internal structure
4. five artificial nodules:
    - Hounsfield number: approximately +100
    - five sizes for each type: diameters 3, 5, 8, 10, 12 mm.

Material:

- Soft tissue: polyurethane (gravity 1.06) synthetic
- Bones: epoxy resin

Phantom size:

43 x 40 x 48H cm, chest girth 94 cm, weight: approx. 18 kg

Packing size:

59 x 52 x 30 cm, 25 kg

3.6.3 RPL glass dosimeter

Radiophotoluminescent (RPL) glass dosimeter as illustrated in Figure 3.3 is a true accumulation type solid state dosimeter, which is based on radiophotoluminescent phenomenon of silver activated phosphate glass exposed to ionizing radiation.

Figure 3.3 Glass dosimeter element model GD-352M (AGC TECHNO GLASS CO., LTD).

Table 3.2 Specifications of glass dosimeter element.

Specifications of glass dosimeter element	
Mode	GD-352M (with ID and tin filter)
Glass element dimensions	Diameter 1.5×12 mm
Measuring	Photon (gamma ray & x-ray)
Dose range	10 µGy to 10 Gy [to 500 Gy by option]

3.6.4 Glass dosimeter reader (FGD-1000)

Instrument unit used to make an UV excitation to glass elements, read-out RPL quantity from glass elements and indicate the read-out dose value. The reader is automatically calibrated by using the internal calibration glass which is traced with standard glass.

Figure 3.4 Glass dosimeter reader (FGD-1000).

Table 3.3 Specifications of reader (FGD-1000).

Display value range	1 µGy to 10 Gy [to 500 Gy by option]
Reproducibility	Coefficient of variation - 5 % or less (at 100 µGy) - 2 % or less (at 1 mGy)
Continuous reading	20 glass elements
Read-out time	6 seconds or less / element
Printer	Page printer (Option)
Power supply	100, 115, 220 & 240 AC (50/60Hz)
Power consumption	Max. 200 W

3.6.4.1 Automatic calibration using the internal calibration

By standard calibration, the dose value of the internal calibration glass is used to determine the reader correction factor (unit in nanocoulombs, nC) for daily use. When starting read-out, and when exchanging a read-out magazine, the internal calibration is executed automatically. At this time, the type of the calibration mode and the read-out magazine is detected automatically and the calibration is executed on suitable conditions.

3.6.5 Laboratory oven (Carbolite Gero)

Laboratory ovens as illustrated in Figure 3.5, use thermal convection in order to deliver heat to the glass dosimeter element, which allows them to maintain uniform temperatures. The details of annealing, pre-heating, and build up procedures using laboratory oven are described as below.

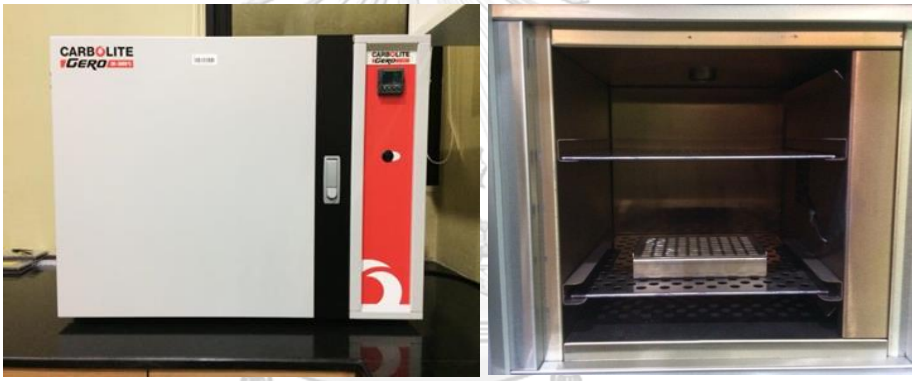

Figure 3.5 Laboratory oven used for annealing and pre heating of glass dosimeter.

Annealing (Program 3: 400 °C for 60 min): Controlled thermal treatment which erases the radiophotoluminescent which the glass element has memorized, and is returned to the state before radiation irradiation and which is performed for accumulating.

Preheating (Program 1: 70 °C for 30 min): Heat treatment for acceleration of build up.

Build up: The phenomenon which the amount of fluorescence of the radiophotoluminescent in the glass element with which radiation was irradiated increases and stabilizes with progress of time.

3.6.6 Patients

The patients who underwent digital chest tomosynthesis at Diagnostic Radiology Department, Chulabhorn Hospital were included in the study.

Inclusion criteria

The patients who were requested for chest x-ray by digital chest tomosynthesis technique. The inclusion criteria consist of:

- Age > 35 year-olds.
- Chest thickness in between 15 and 25 cm.
- Checkup (high risk) smoker, family history of cancer, pulmonary nodules follow-up.

Exclusion criteria

Emergency case and unstable patients were excluded from this study.

3.7 Methods

3.7.1 Perform quality control of digital radiography system

The quality control of digital radiography system was performed following the AAPM report No.74 (2002): quality control in diagnostic radiology [19]. The quality control program consists of the test of performance of electromechanical components, image quality and radiation dose. The example of the x-ray tube output and HVL measurement is illustrated as in Figure 3.6.

Figure 3.6 Quality control of digital radiography system.

3.7.2 Perform quality control of digital image receptor

The quality control of digital image receptor was performed following the KCARE protocol for the QC of direct digital radiography system [20]. The tests were intended to test image quality and artifacts.

Figure 3.7 Quality control of digital image receptor.

3.7.3 Phantom study

3.7.3.1 Simulated nodules in phantom study

The five sizes of simulated nodule (Hounsfield unit: approx. +100) with the inner diameter of 3, 5, 8, 10, 12 mm were attached in the lung field of lung man phantom as illustrated in Figure 3.10 at the position as followings:

- Nodule size 3 mm 2/3 in peripheral of right middle lobe (red color).
- Nodule size 5 mm 1/3 in peripheral of left upper lobe (blue color).
- Nodule size 8 mm in right lower lobe (green color).
- Nodule size 10 mm in peripheral of left lower lobe (pink color).
- Nodule size 12 mm in right upper lobe (yellow color).

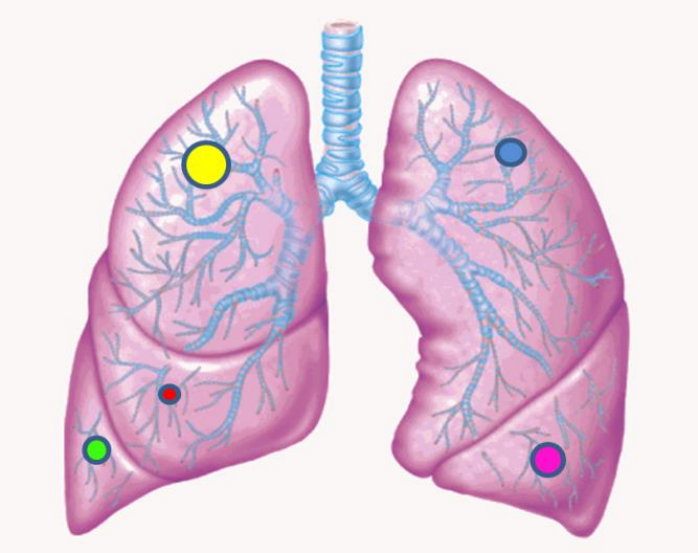

Figure 3.8 The location of simulated nodules.

Figure 3.9 Five simulated nodules inserted in N1 LUNGMAN phantom.

3.7.3.2 Parameter setting in phantom study

The anthropomorphic phantom was then scanned by digital radiographic systems model Definium 8000 manufactured by GE Healthcare. We scanned a phantom using chest VolumeRAD acquisition protocol and adjusted parameters by varying tube voltage of 100, 110, 120 kVp, copper filter thickness of 0.0, 0.1, 0.2, 0.3 mm and dose ratio of 1:5, 1:8, 1:10 for evaluating the optimal protocol in phantom study.

3.7.3.3 Performed quality control before DTS examination

The Quality Assurance Process (QAP) consists of a series of tests that should be performed before scanned phantom to quantify image quality according to vendor recommendation. There are two types of phantoms used in the QAP process. The first phantom is the flat-field phantom and the second is IQST phantom.

1. The flat-field phantom is used to check the following factors:
    - Brightness non uniformity global
    - Brightness non uniformity local
    - Signal-to-noise ratio (SNR) non uniformity
    - Artifacts number of bad pixels

Figure 3.10 Insert flat field phantom into the collimator rail.

2. The composite phantom (or IQST phantom) is used to check MTF (Modulation Transfer Function).

3. Follow the instructions of QAP process.

Figure 3.11 Insert the composite phantom into the grid holder.

4. Check the result of QAP test.

IMAGE QUALITY TEST RESULTS Sat Aug 19 15:51:24 ICT 2017

TEST	MEASUREMENT	LSL	USL	STATUS
OVERALL RESULT				PASS
No. Of Bad Pixels	0.00	-	30	PASS
Global Brightness Non Uniformity	2.56	-	10	PASS
Local Brightness Non Uniformity	0.90	-	5	PASS
SNR Non Uniformity	23.99	-	60	PASS
Spatial MTF at 0.5 lp/mm	83.56	65	-	PASS
Spatial MTF at 1.0 lp/mm	61.41	48	-	PASS
Spatial MTF at 1.5 lp/mm	41.19	31	-	PASS
Spatial MTF at 2.0 lp/mm	26.18	21	-	PASS
Spatial MTF at 2.5 lp/mm	16.73	15	-	PASS

Figure 3.12 The result of QAP test.

3.7.3.4 Optimize the radiation dose and image quality in phantom

Set up phantom for examination

1. Setup position the LUNGMAN phantom at the center of x-ray beam.

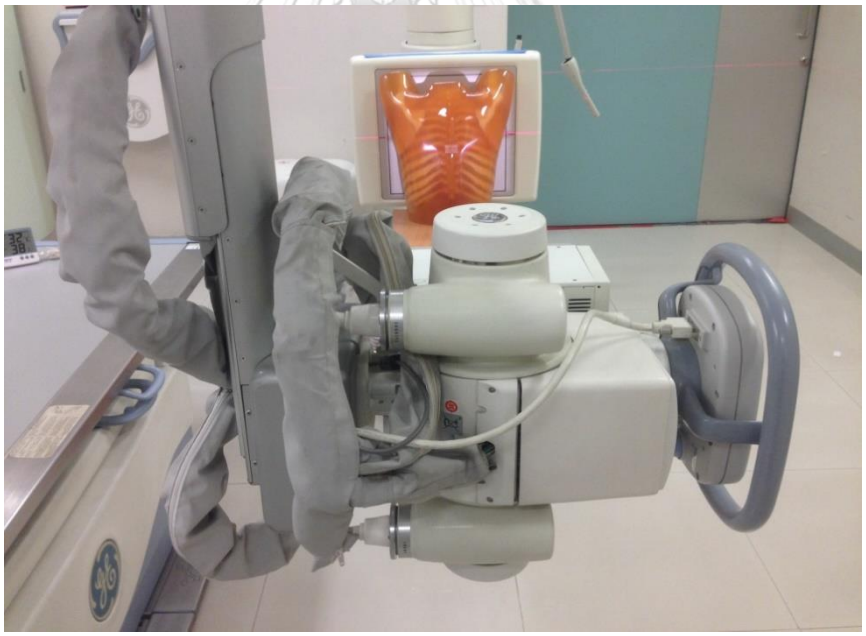

Figure 3.13 Positioning the LUNGMAN phantom.

2. Select chest tomosynthesis protocol and adjusted parameters by varying tube voltage of 100,110,120 kVp, copper filter of 0.0, 0.1, 0.2, 0.3 mm and dose ratio of 1:5, 1:8, 1:10 for evaluating the optimal protocol.

3. Perform the DTS using the acquisition process as follows:

Scout – a standard, single energy acquisition used to determine the exposure settings and patient positioning.

Sweep – the system takes multiple, low-dose exposures as the tube travels through the arc. The system then creates the "slices" to visualize the anatomy at various depths. Additional sweeps should only be made if the patient moved during the sweep and the slices are not of acceptable quality.

4. Expose the phantom. Totally, 36 protocols including default protocol were performed; each protocol was scanned 3 times.

5. Record total DAP from monitor for effective dose evaluation in phantom (Total DAP: the entrance dose estimate multiplied by the field of view area at the corresponding distance from receptor after exposure is taken).

3.7.3.5 Radiation dose measurement in phantom

3.7.3.5.1 Measure entrance surface dose (ESD)

The glass dosimeter was used to measure the entrance surface dose (ESD) from DTS in each protocol. Three glass dosimeters (Type GD-352M, AGC Techno Glass Co., Ltd, Japan) were attached at the surface of LUNGMAN phantom and measured the ESD at the center of x-ray beam in order to represent maximum intensity of x-ray beam (T7 level approximately). The details of glass dosimeter reading process are described in APPENDIX G.

Figure 3.14 Setting of glass dosimeter for measuring ESD in phantom.

3.7.3.5.2 Effective dose evaluation

The dose-area-product (DAP, dGy.cm^2) was then recorded from displayed monitor. A conversion factor according to Svalkvist A, et al [21] was applied to determine the effective doses from VolumeRAD in chest tomosynthesis examination from the total registered DAP. The effective dose to a standard patient (170 cm / 70 kg) can be calculated by equation as followings:

$$\textbf{ED (mSv) = Total DAP (Gy.cm}^2\textbf{) × conversion factor (mSv Gy}^{-1}\textbf{ cm}^{-2}\textbf{)}$$

Table 3.4 The conversion factor between DAP and effective dose for DTS at different tube voltages [21].

Tube voltage	Conversion factor (mSv Gy^{-1} cm^{-2})
100 kV	0.257
110 kV	0.277
120 kV	0.285
130 kV	0.295
140 kV	0.304
150 kV	0.311

3.7.3.6 Evaluate the image quality in phantom

3.7.3.6.1 Quantitative image quality analysis

The quantitative image quality was evaluated by determining signal-to-noise ratio (SNR) using SYNAPSE PACS software at PACS workstation. The region of interest (ROI) was manually drawn at the simulated nodule size of 12 mm. The average pixel intensity and the standard deviation (SD) were recorded in order to evaluate the SNR in each protocol. The SNR is determined using the equation as followings:

$$\textbf{SNR} = \frac{\textit{The mean pixel value of ROI in nodule}}{\textit{The standard deviation of ROI in nodule}}$$

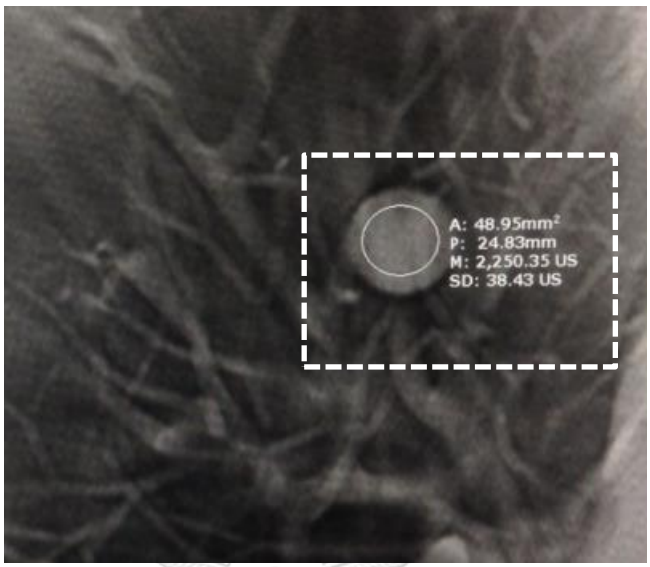

Figure 3.15 The ROI measured at nodule size 12 mm.

3.7.3.6.2 Qualitative image quality analysis

Image criteria score

The image quality criteria were evaluated independently by two radiologists who have similar experienced for DTS interpretation (SV and SS). Currently, there is no protocol particularly for DTS interpretation criteria; as a result, we used the European guidelines on quality criteria of chest radiography instead for DTS diagnostic radiographic images [22].

Figure 3.16 PACS workstation using for image quality interpretation.

Table 3.5 Image criteria score of digital chest tomosynthesis.

Image criteria **Item Image Criteria Score**	**Not fulfilled (0)**	**Partly fulfilled (0.5)**	**Fulfilled (1)**
1. Visually sharp reproduction of the vascular pattern in the whole lung, particularly the peripheral vessels.			
2. Visually sharp reproduction of the trachea and proximal bronchi.			
3. Visually sharp reproduction of the borders of the heart and aorta.			
4. Visually sharp reproduction of the diaphragm and lateral costophrenic angles.			
5. Visualization of the retrocardiac lung and the mediastinum.			
6. Visualization of the spine through the heart shadow.			
*Criteria Score > 3 (Acceptable image quality)			

*Rating image score: 0, 0.5 and 1
Where 0 = not fulfilled, 0.5 = partly fulfilled, 1 = fulfilled

Nodule detection capability

Nodule detection was also evaluated by two radiologists independently who have similar experience in chest DTS interpretation according to Fleischer Society Guideline, and MacMahon H et al [23, 24]. They were blinded to the DTS scanning parameter techniques, and the images were analyzed in randomized order by each reader. Nodule detection capability was graded on a PACS workstation using a five-point rating scale as in Table 3.6. The acceptable score for nodule detection capability must be equal or greater than 3.

Table 3.6 The five scale of image quality for artificial nodule detections.

Score	Image quality	Criteria
1	Poor	- Visualize 12 mm. in diameter with sharp edge - Partly visualize 10 mm in diameter
2	Fair	- Visualize 10 mm. in diameter with sharp edge - Partly visualize 8 mm in diameter
3	Good (Acceptable)	- Visualize 8 mm. in diameter with sharp edge - Partly visualize 5 mm in diameter
4	Very good	- Visualize 5 mm in diameter with sharp edge - Partly visualize 3 mm in diameter
5	Excellence	- Visualize all simulated nodules with sharp edge

Optimization protocol consideration

The optimal protocol for DTS in this work was selected by considering the highest image quality score and lung nodule detection interpreted by two radiologists as the priority. Then the lowest possible radiation dose was considered accordingly.

3.7.4 Clinical study

The appropriate protocol obtained from phantom study was applied with 30 patients who underwent digital chest tomosynthesis at Chulabhorn Hospital. The patient's information was recorded following the case record form, such as the chest thickness, exposure parameters and the total DAP value from monitor.

To evaluate the patient effective dose after applying the optimal protocol, the conversion factor [21] was multiplied by the recorded DAP value following the equation in as 3.7.3.5.2.

3.8 Sample size determination

3.8.1 Target population

The patients who underwent chest x-ray using digital chest tomosynthesis technique at Department of Diagnostic Radiology, Chulabhorn Hospital were collected.

Inclusion criteria

- The patients who were requested for chest x-ray by digital chest tomosynthesis technique.
- Age > 35 year-olds.
- Chest thickness in between 15 and 25 cm.
- Checkup (high risk) smoker, family history of cancer, pulmonary nodules follow-up.

Exclusion criteria

- Emergency case or unstable patients.

3.8.2 The sample population

The sample population in each group is independent and was determined by formula as follows:

$$N = \frac{(Z_{\alpha/2})^2 \cdot \sigma^2}{d^2}$$

Where N = Sample size
$Z_{\alpha/2}$ = 95% confidence interval (1.96)
σ^2 = Variance of data (0.25)
d = Acceptable error (0.1)

Solve equation $N = \frac{(1.96)^2 \cdot (0.25)^2}{(0.1)^2} = 24.01$

Therefore: 30 patients were collected.

3.9 Statistical analysis

3.9.1 Descriptive statistics: mean, standard deviation (SD), minimum and maximum of radiation dose, score of image criteria and nodule detection were determined.

3.9.2 Weighted Kappa (k) representing the inter-observer reliability was analyzed using software SPSS version 22.

3.10 Outcome measurements

3.10.1 The optimal protocol for digital chest tomosynthesis at Chulabhorn Hospital.

3.10.2 The entrance surface dose calculated from glass dosimeter.

3.10.3 The effective dose calculated from total DAP value.

3.10.4 The image quality scored by two observers based on

3.10.4.1 Quantitative: Signal-to-noise ratio (SNR)

3.10.4.2 Qualitative: Image scoring

3.11 Measurement variables

Independent variables:

- Acquisition protocol, exposure parameter

Dependent variables:

- Radiation dose, image scoring, signal-to-noise ratio.

3.12 Data presentation format

The table and graph were presented in terms of the number of maximum, minimum, mean and standard deviation of radiation dose, image criteria score and nodule detection.

3.13 Expected benefits

- To obtain the optimize protocol for digital chest tomosynthesis according to ALARA principle as well as maintaining good image quality.
- To apply optimal protocol of digital chest tomosysthesis for follow-up lung nodule patients.

3.14 Ethical consideration

As this study were investigated in both of phantom and patient, the research proposal has been submitted and already approved by Institutional Review Board (IRB) of the Faculty of Medicine, Chulalongkorn University, Bangkok, Thailand.

CHAPTER IV
RESULTS

4.1 Quality control of digital radiography system

The quality control of digital radiography system was performed following the AAPM report No.74. The results were within acceptable range of the AAPM protocol. The details of quality control and the performance tests are shown in Appendix A.

4.2 Quality control of digital image receptor

The quality control of digital image receptor was performed following the KCARE protocol [20]. The results were within acceptable range of the KCARE protocol. The details of quality control are shown with the summarized reports of digital image receptor in Appendix B.

4.3 Phantom study

The anthropomorphic phantom was scanned by digital radiographic system model Definium 8000 manufactured by GE Healthcare at Chulabhorn Hospital. We scanned and adjusted parameters by varying tube voltage of 100, 110, 120 kVp, copper filter of 0.0, 0.1, 0.2, 0.3 mm, and dose ratio at 1:5, 1:8, 1:10 for evaluating the optimal protocol. In this study, the AEC technique was applied in all protocols. Totally, 36 protocols were performed. Each protocol was scanned 3 times in order to determine the average the radiation dose. The default parameter setting at 120 kVp, 0.0 mm copper filter and dose ratio of 1:10 was done in order to compare the radiation dose and image quality with other protocols before considering the optimal parameter. The artificial nodules were used for assessment of image quality. The signal-to-noise ratio (SNR) was measured in order to determine image quality in terms of quantitative analysis. The image criteria and nodule detection capability were assessed independently by two radiologists who have similar experience in DTS interpretation.

4.3.1 Radiation dose

Table 4.1 Parameters of 36 DTS protocols performed in phantom study.

No.	Dose Ratio	kV	Cu filter	mA	Speed	AEC	Ion chamber	Focal spot	Grid	SID
1	1:5	100	0	320	400	on	R-L	Large	in	180
2			0.1	320	400	on	R-L	Large	in	180
3			0.2	320	400	on	R-L	Large	in	180
4			0.3	320	400	on	R-L	Large	in	180
5		110	0	320	400	on	R-L	Large	in	180
6			0.1	320	400	on	R-L	Large	in	180
7			0.2	320	400	on	R-L	Large	in	180
8			0.3	320	400	on	R-L	Large	in	180
9		120	0	320	400	on	R-L	Large	in	180
10			0.1	320	400	on	R-L	Large	in	180
11			0.2	320	400	on	R-L	Large	in	180
12			0.3	320	400	on	R-L	Large	in	180
13	1:8	100	0	320	400	on	R-L	Large	in	180
14			0.1	320	400	on	R-L	Large	in	180
15			0.2	320	400	on	R-L	Large	in	180
16			0.3	320	400	on	R-L	Large	in	180
17		110	0	320	400	on	R-L	Large	in	180
18			0.1	320	400	on	R-L	Large	in	180
19			0.2	320	400	on	R-L	Large	in	180
20			0.3	320	400	on	R-L	Large	in	180
21		120	0	320	400	on	R-L	Large	in	180
22			0.1	320	400	on	R-L	Large	in	180
23			0.2	320	400	on	R-L	Large	in	180
24			0.3	320	400	on	R-L	Large	in	180
25	1:10	100	0	320	400	on	R-L	Large	in	180
26			0.1	320	400	on	R-L	Large	in	180
27			0.2	320	400	on	R-L	Large	in	180
28			0.3	320	400	on	R-L	Large	in	180
29		110	0	320	400	on	R-L	Large	in	180
30			0.1	320	400	on	R-L	Large	in	180
31			0.2	320	400	on	R-L	Large	in	180
32			0.3	320	400	on	R-L	Large	in	180
33*		120	0	320	400	on	R-L	Large	in	180
34			0.1	320	400	on	R-L	Large	in	180
35			0.2	320	400	on	R-L	Large	in	180
36			0.3	320	400	on	R-L	Large	in	180

*****Default parameter *(120 kVp, dose ratio 1:10 and no adding copper filter)*

Table 4.2 The results of entrance surface dose: ESD (mGy) in phantom study.

No	Dose Ratio	kVp	Cu	Glass dosimeter (GD-352M)			Average	CF	ESD (mGy)
				1	2	3			
1	1:5	100	0	1.00	0.91	0.90	0.934	1.141	1.07 ± 0.06
2			0.1	0.63	0.60	0.60	0.608	1.141	0.69 ± 0.02
3			0.2	0.47	0.45	0.43	0.448	1.141	0.51 ± 0.02
4			0.3	0.37	0.36	0.36	0.360	1.141	0.41 ± 0.01
5		110	0	1.20	1.15	1.16	1.169	1.076	1.26 ± 0.03
6			0.1	0.77	0.75	0.74	0.753	1.076	0.81 ± 0.01
7			0.2	0.58	0.56	0.54	0.559	1.076	0.60 ± 0.02
8			0.3	0.46	0.42	0.43	0.436	1.076	0.47 ± 0.02
9		120	0	1.40	1.29	1.42	1.371	1.077	1.48 ± 0.07
10			0.1	0.93	0.85	0.83	0.872	1.077	0.94 ± 0.05
11			0.2	0.70	0.76	0.78	0.748	1.077	0.81 ± 0.04
12			0.3	0.57	0.74	0.69	0.666	1.077	0.72 ± 0.08
13	1:8	100	0	0.98	1.17	1.15	1.100	1.141	1.25 ± 0.10
14			0.1	0.78	0.85	0.70	0.774	1.141	0.88 ± 0.08
15			0.2	0.57	0.64	0.68	0.631	1.141	0.72 ± 0.05
16			0.3	0.54	0.64	0.63	0.603	1.141	0.69 ± 0.05
17		110	0	1.22	1.35	1.27	1.278	1.076	1.38 ± 0.06
18			0.1	0.77	0.71	0.76	0.745	1.076	0.80 ± 0.03
19			0.2	0.73	0.67	0.65	0.683	1.076	0.73 ± 0.04
20			0.3	0.58	0.66	0.70	0.646	1.076	0.70 ± 0.06
21		120	0	1.37	1.45	1.35	1.390	1.077	1.50 ± 0.05
22			0.1	0.97	1.03	1.13	1.040	1.077	1.12 ± 0.08
23			0.2	0.70	0.68	0.66	0.681	1.077	0.73 ± 0.02
24			0.3	0.57	0.59	0.58	0.578	1.077	0.62 ± 0.01
25	1:10	100	0	1.44	1.37	1.43	1.413	1.141	1.61 ± 0.04
26			0.1	0.92	0.93	0.84	0.897	1.141	1.02 ± 0.05
27			0.2	0.84	0.78	0.79	0.802	1.141	0.92 ± 0.03
28			0.3	0.66	0.63	0.66	0.652	1.141	0.74 ± 0.02
29		110	0	1.49	1.62	1.45	1.519	1.076	1.63 ± 0.09
30			0.1	0.93	1.18	0.94	1.015	1.076	1.09 ± 0.14
31			0.2	0.88	0.80	0.82	0.836	1.076	0.90 ± 0.04
32			0.3	0.68	0.82	0.81	0.771	1.076	0.83 ± 0.08
33		120	0	1.41	1.71	1.57	1.560	1.077	1.68 ± 0.15
34			0.1	0.93	0.90	0.94	0.923	1.077	0.99 ± 0.02
35			0.2	0.85	0.93	0.98	0.921	1.077	0.99 ± 0.07
36			0.3	0.71	0.82	0.73	0.753	1.077	0.81 ± 0.06

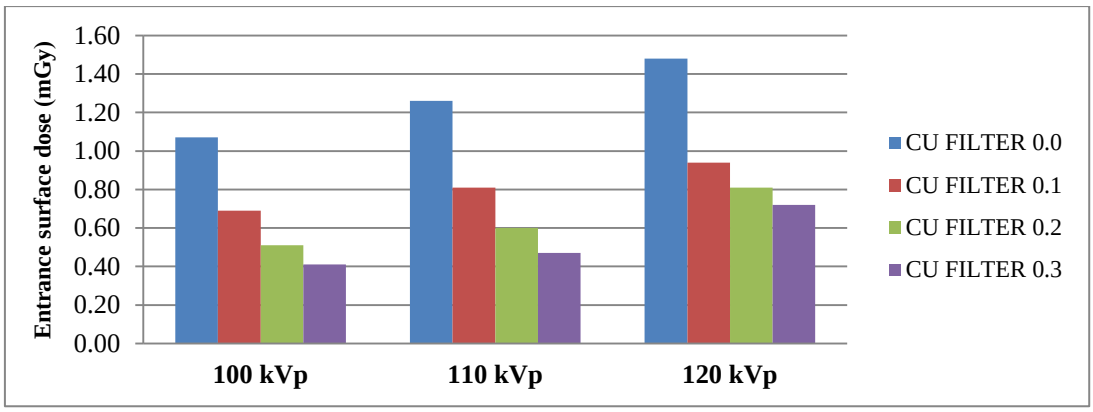

Figure 4.1 Relation between cu-filter, kVp, and ESD (mGy) at dose ratio 1:5.

Table 4.3 The results of entrance surface dose (mGy) at dose ratio 1:5 using various kVp and copper filter.

Dose ratio 1:5	Cu-filter 0.0 mm	Cu-filter 0.1 mm	Cu-filter 0.2 mm	Cu-filter 0.3 mm
100 kVp	1.07±0.06	0.69±0.02	0.51±0.02	0.41±0.01
110 kVp	1.26±0.03	0.81±0.01	0.60±0.02	0.47±0.02
120 kVp	1.48±0.07	0.94±0.05	0.81±0.04	0.72±0.08

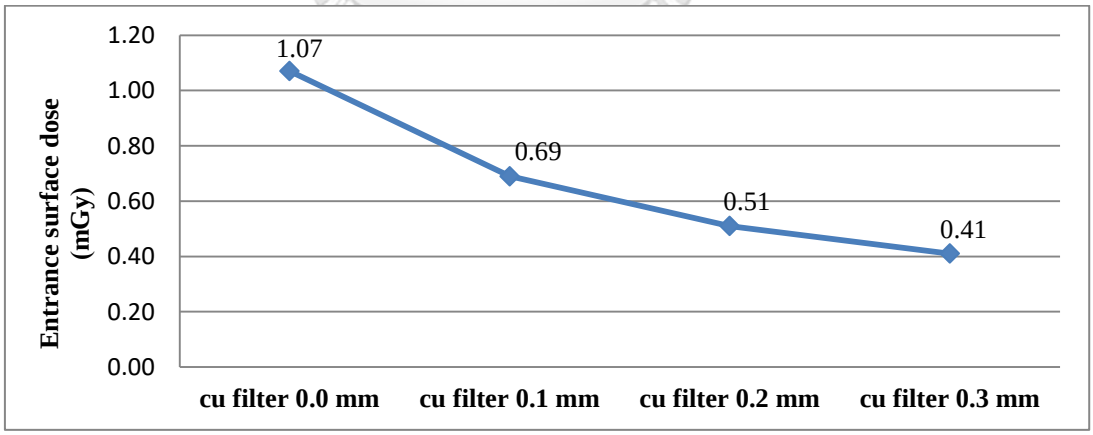

Figure 4.2 The results of ESD (mGy) using various copper filter thickness at 100 kVp.

The lowest ESD was found at parameter of 100 kVp, dose ratio 1:5 and additional copper filter 0.3 mm with the ESD of 0.41±0.01 mGy, which similar to the previous study reported by Hwang HS et al [18]. Using a copper filter has a potential to use for reducing the radiation dose to the patients.

Table 4.4 The results of effective dose: ED (µSv) in phantom study.

No	Dose Ratio	kVp	Cu	Total DAP dGy.cm^2			CF	ED (µSv)	S.D.
				DTS 1	DTS 2	DTS 3			
1	1:5	100	0	7.95	8.01	8.00	0.257	205.26	0.83
2			0.1	4.93	4.96	4.95	0.257	127.13	0.39
3			0.2	3.56	3.58	3.57	0.257	91.75	0.26
4			0.3	2.88	2.90	2.90	0.257	74.36	0.30
5		110	0	9.38	9.41	9.40	0.277	260.29	0.42
6			0.1	6.03	6.08	6.05	0.277	167.68	0.70
7			0.2	4.45	4.48	4.47	0.277	123.73	0.42
8			0.3	3.62	3.64	3.63	0.277	100.55	0.28
9		120	0	11.01	11.05	11.02	0.285	314.26	0.59
10			0.1	7.29	7.32	7.30	0.285	208.15	0.44
11			0.2	5.47	5.50	5.48	0.285	156.28	0.44
12			0.3	4.51	4.52	4.50	0.285	128.54	0.28
13	1:8	100	0	7.95	7.99	7.99	0.257	205.00	0.59
14			0.1	6.14	6.15	6.14	0.257	157.88	0.15
15			0.2	4.40	4.41	4.42	0.257	113.34	0.26
16			0.3	4.30	4.32	4.32	0.257	110.85	0.30
17		110	0	9.39	9.42	9.42	0.277	260.66	0.48
18			0.1	6.04	6.06	6.05	0.277	167.59	0.28
19			0.2	4.45	4.46	4.46	0.277	123.45	0.16
20			0.3	4.50	4.51	4.51	0.277	124.83	0.16
21		120	0	11.03	11.05	11.03	0.285	314.55	0.33
22			0.1	7.29	7.30	7.32	0.285	208.15	0.44
23			0.2	5.49	5.50	5.50	0.285	156.66	0.16
24			0.3	4.51	4.52	4.51	0.285	128.63	0.16
25	1:10	100	0	9.94	9.95	9.94	0.257	255.54	0.15
26			0.1	7.48	7.53	7.50	0.257	192.84	0.65
27			0.2	5.36	5.39	5.39	0.257	138.27	0.45
28			0.3	5.24	5.26	5.26	0.257	135.01	0.30
29		110	0	11.79	11.81	11.79	0.277	326.77	0.32
30			0.1	7.55	7.57	7.55	0.277	209.32	0.32
31			0.2	5.56	5.60	5.56	0.277	154.38	0.64
32			0.3	5.50	5.52	5.51	0.277	152.63	0.28
33		120	0	10.99	11.04	11.02	0.285	313.98	0.72
34			0.1	7.29	7.32	7.28	0.285	207.96	0.59
35			0.2	6.85	6.89	6.87	0.285	195.80	0.57
36			0.3	5.64	5.64	5.64	0.285	160.74	0.00

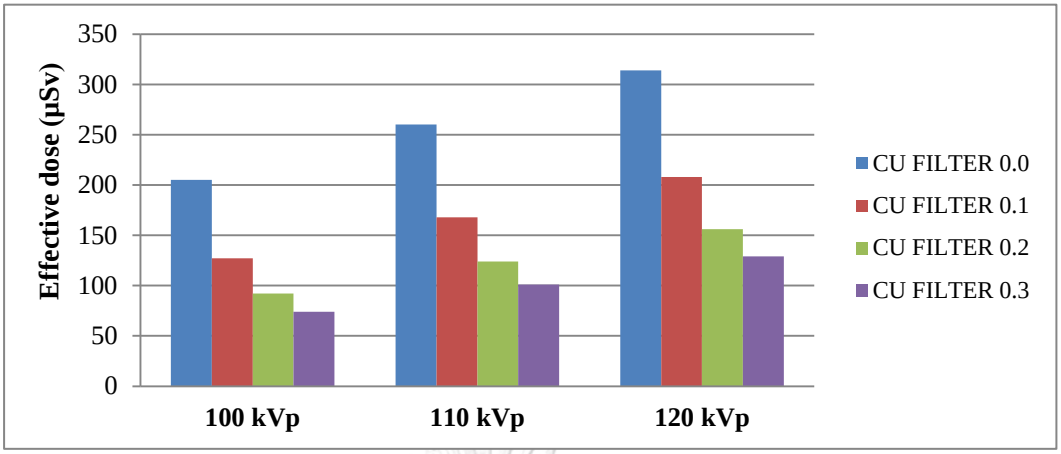

Figure 4.3 Relation between cu-filter, kVp, and ED (µSv) at dose ratio 1:5.

Table 4.5 The result of effective dose (µSv) at dose ratio 1:5.

Dose ratio 1:5	Cu-filter 0.0 mm	Cu-filter 0.1 mm	Cu-filter 0.2 mm	Cu-filter 0.3 mm
100 kVp	205±0.83	127±0.39	92±0.26	74±0.30
110 kVp	260±0.42	168±0.70	124±0.42	101±0.28
120 kVp	314±0.59	208±0.44	156±0.44	129±0.28

According to the results in Table 4.5, the lowest effective dose (ED) was found at parameter of 100 kVp, dose ratio 1:5 and additional copper filter 0.3 mm. This parameter was similar to the previous study reported by Hwang HS et al [18], with the ED of 74.36±0.30 µSv. The results indicated that the average±SD of ESD obtained from vendor's default protocol at 120 kVp, dose ratio 1:10 and no copper filter was 1.68±0.15 mGy. The optimal parameter for DTS was obtained at 110 kVp, dose ratio 1:5, and copper filter at 0.3 mm with the ESD of 0.47±0.02 mGy. The effective doses for the default protocol and optimal protocol were 313.98±0.72 µSv and 100.55±0.28 µSv, respectively.

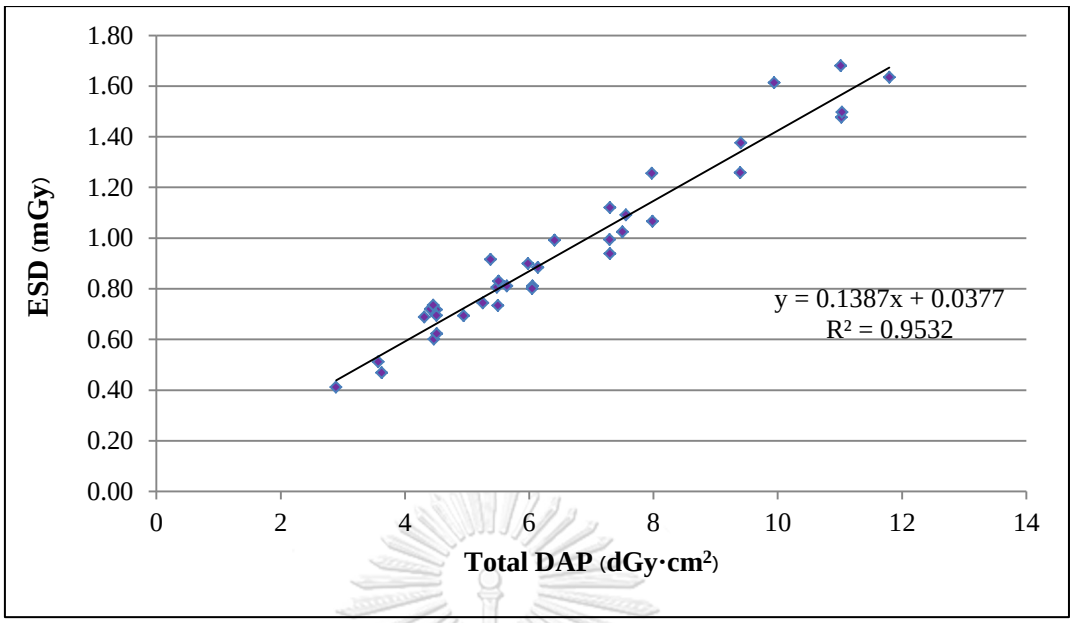

Figure 4.4 The relation between the ESD (mGy) and DAP values with $R^2 = 0.9532$.

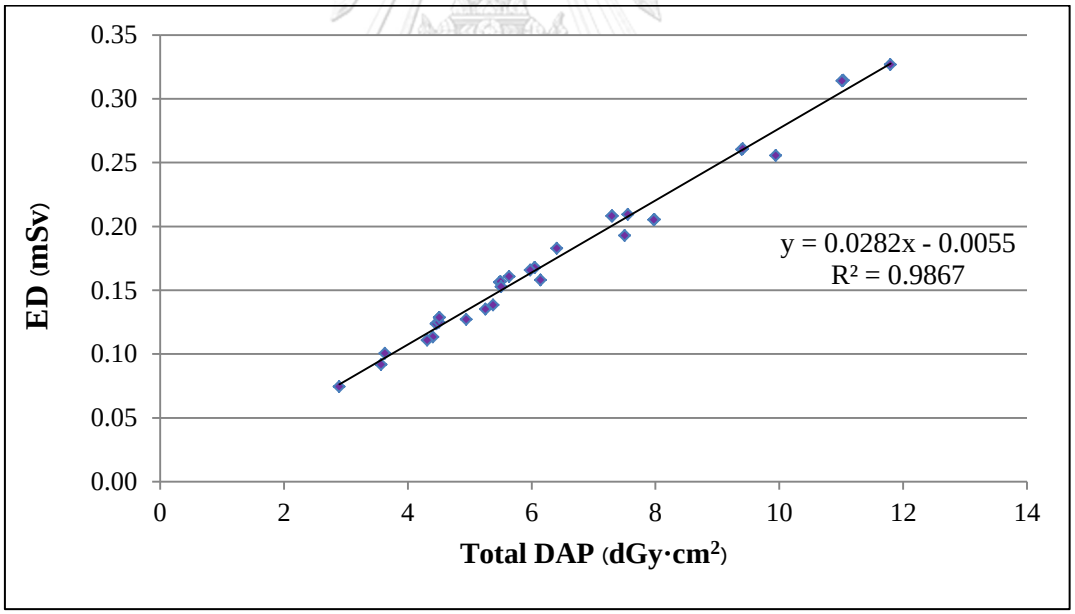

Figure 4.5 The relation between the ED (mSv) and DAP values with $R^2 = 0.9867$.

Figure 4.4 and Figure 4.5 depict the relationship of ESD (mGy) and ED (mSv) to DAP value (dGy.cm^2), respectively. As can be seen from both figures, ESD and ED yielded a linear proportion to DAP value. Both ESD and ED values increased with increasing DAP value. The regression values from ESD and ED were 0.9532 and 0.9867, respectively.

4.3.2 Image Quality

4.3.2.1 Quantitative image quality

The signal-to-noise ratio (SNR) was measured by placing the circular regions of interests (ROIs) within the nodule size 12 mm to determine objective image quality.

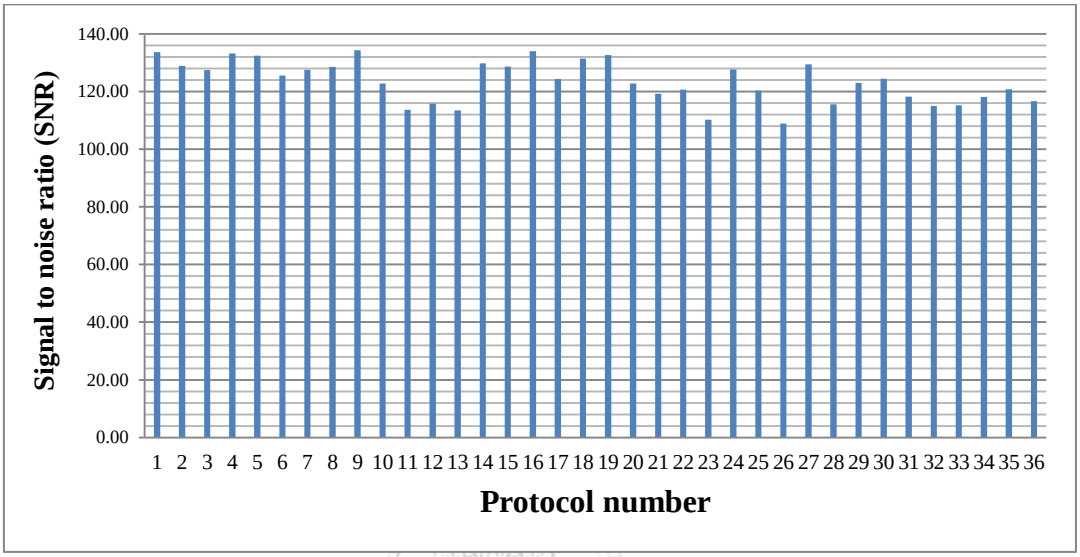

Figure 4.6 Signal to noise ratio (SNR) of 36 protocols in phantom.

Table 4.6 Signal to noise ratio of DTS at dose ratio 1:5.

No.	Dose Ratio	kV	Cu filter	Average SNR	S.D.
1	1:5	100	0	133.68	1.26
2			0.1	128.90	1.47
3			0.2	127.42	0.69
4			0.3	133.19	1.20
5		110	0	132.38	1.78
6			0.1	125.54	1.72
7			0.2	127.53	1.71
8			0.3	128.58	3.48
9		120	0	134.31	1.30
10			0.1	122.75	2.43
11			0.2	113.69	3.30
12			0.3	115.75	1.61

Table 4.7 Signal to noise ratio of DTS at dose ratio 1:8.

No.	Dose Ratio	kV	Cu filter	Average SNR	S.D.
13	1:8	100	0	113.39	0.50
14			0.1	129.79	0.90
15			0.2	128.60	1.39
16			0.3	133.93	1.70
17		110	0	124.28	1.99
18			0.1	131.37	2.86
19			0.2	132.63	0.70
20			0.3	122.74	2.42
21		120	0	119.20	1.05
22			0.1	120.61	2.38
23			0.2	110.22	1.98
24			0.3	127.60	1.49

Table 4.8 Signal to noise ratio of DTS at dose ratio 1:10.

No.	Dose Ratio	kV	Cu filter	Average SNR	S.D.
25	1:10	100	0	120.35	1.19
26			0.1	108.90	1.96
27			0.2	129.47	0.09
28			0.3	115.53	0.86
29		110	0	122.99	0.36
30			0.1	124.43	1.89
31			0.2	118.20	3.95
32			0.3	114.98	1.38
33		120	0	115.24	2.03
34			0.1	118.07	3.50
35			0.2	120.74	1.93
36			0.3	116.62	2.62

4.3.2.2 Qualitative image quality

The image criteria and nodule detection capability were scored by two experienced radiologists who have same experience (10 years) in DTS interpretation in order to evaluate the image quality in each protocol. The results of image scoring by two radiologists for 36 setting protocols are shown as in Table 4.9.

Table 4.9 Image quality scored by two radiologists.

Dose Ratio	kV	Cu-filter (mm)	Radiologist 1		Radiologist 2		Total score
			Nodule detection	Image criteria	Nodule detection	Image criteria	
1:5	100	0	4	6	5	6	21
		0.1	4	6	4	5.5	19.5
		0.2	4	6	4	5.5	19.5
		0.3	4	5.5	5	5.5	20
	110	0	4	6	4	6	20
		0.1	4	6	4	5.5	19.5
		0.2	5	6	4	6	21
		0.3	5	6	5	6	22
	120	0	5	6	5	6	22
		0.1	5	6	5	6	22
		0.2	5	6	5	6	22
		0.3	5	6	4	6	21
1:8	100	0	5	6	4	6	21
		0.1	4	6	4	6	20
		0.2	4	5.5	4	5.5	19
		0.3	5	6	4	6	21
	110	0	5	6	4	6	21
		0.1	4	6	4	6	20
		0.2	4	6	4	6	20
		0.3	4	6	4	6	20
	120	0	5	6	5	6	22
		0.1	5	6	4	6	21
		0.2	5	6	4	6	21
		0.3	4	6	4	6	20
1:10	100	0	5	6	5	6	22
		0.1	4	6	4	5.5	19.5
		0.2	4	6	4	6	20
		0.3	4	5.5	4	5.5	19
	110	0	5	6	5	6	22
		0.1	4	6	4	6	20
		0.2	4	6	4	6	20
		0.3	4	6	4	6	20
	120	0	4	6	5	6	21
		0.1	4	6	5	6	21
		0.2	5	6	5	6	22
		0.3	4	6	4	6	20

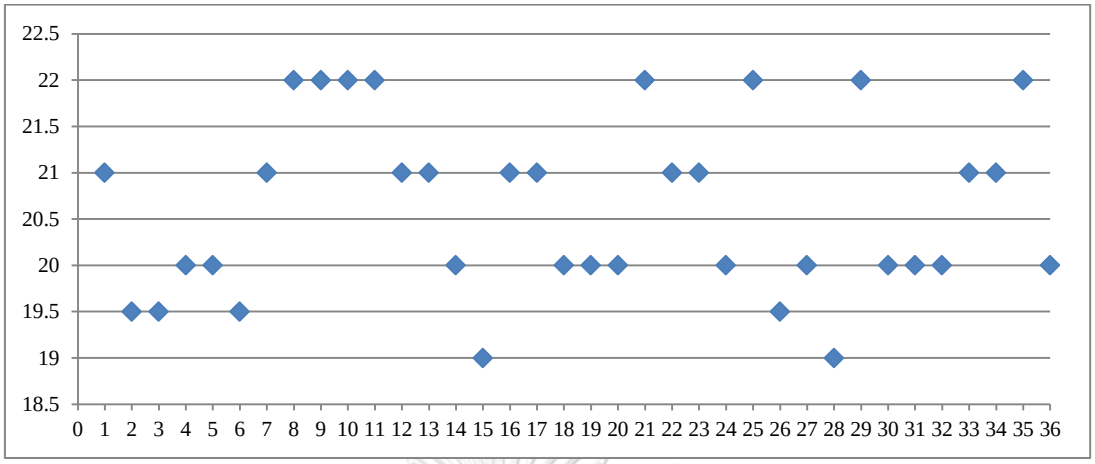

Figure 4.7 Scatter charts of total score in difference protocols.

The agreement results of two radiologists for image quality interpretation are illustrated as below.

Table 4.10 Measurement of agreement between two radiologists.

		Radiologist 1				Total
		9.50	10.00	10.50	11.00	
Radiologist 2	9.50	2	0	1	0	3
	10.00	4	11	0	3	18
	11.00	0	7	0	8	15
Total		6	18	1	11	36

Symmetric Measures

		Value	Asymp. Std. Error[a]	Approx. T[b]	Approx. Sig.
Measure of agreement	Kappa	0.316	0.132	2.585	0.010
N of Valid Cases		36			

The kappa values were calculated using SPSS version 22. The *k*-value from weighted kappa is used to interpret the strength of agreement between two observers. In this study, *k*-value of 0.316 was obtained, which means the strength of agreement is fair.

4.3.3 Optimal protocol

Ranking of the ESD and total image quality in phantom study sorted by lowest to highest ESD is shown as in Table 4.11. The lowest entrance surface dose was found at parameter of 100 kVp, dose ratio 1:5 and additional copper filter 0.3 mm with the entrance surface dose of 0.41±0.01 mGy and the optimal protocol for this study, 110 kVp, dose ratio 1:5 and 0.3 mm copper filter. Image quality score of 22 was found. The effective dose for the optimal protocol and default protocol were 101 µSv (0.10 mSv) and 314 µSv (0.31 mSv) respectively. The ESD for these two protocols were 0.47 mGy and 1.68 mGy respectively. There were slightly different of the image criteria score and nodule detection between optimal and default protocols using visual assessment interpreted by two radiologists.

Table 4.11 Ranking of the ESD and total image quality score.

Dose ratio	kV	cu filter	ESD (mGy)	Image quality score		Total score
				Nodule detection	Image criteria	
5	100	0.3	0.41	9.5	10.5	20
5*	**110**	**0.3**	**0.47**	**11**	**11**	**22**
5	100	0.2	0.51	10	9.5	19.5
5	110	0.2	0.60	11	10	21
8	120	0.3	0.62	10	10	20
8	100	0.3	0.69	11	10	21
5	100	0.1	0.69	10	9.5	19.5
8	110	0.3	0.70	10	10	20
5	120	0.3	0.72	11	10	21
8	100	0.2	0.72	9.5	9.5	19
8	120	0.2	0.73	11	10	21
8	110	0.2	0.73	10	10	20
10	100	0.3	0.74	9.5	9.5	19
8	110	0.1	0.80	10	10	20
5	120	0.2	0.81	11	11	22
5	110	0.1	0.81	10	9.5	19.5
10	120	0.3	0.81	10	10	20
10	110	0.3	0.83	10	10	20
8	100	0.1	0.88	10	10	20
10	110	0.2	0.90	10	10	20
10	100	0.2	0.92	10	10	20
5	120	0.1	0.94	11	11	22
10	120	0.2	0.99	11	11	22
10	120	0.1	0.99	10	11	21
10	100	0.1	1.02	10	9.5	19.5
5	100	0	1.07	10	11	21
10	110	0.1	1.09	10	10	20

8	120	0.1	1.12	11	10	21
8	100	0	1.25	11	10	21
5	110	0	1.26	10	10	20
8	110	0	1.38	11	10	21
5	120	0	1.48	11	11	22
8	120	0	1.50	11	11	22
10	100	0	1.61	11	11	22
10	110	0	1.63	11	11	22
10	120	0	1.68	10	11	21

*Optimal protocol

The comparisons of the image quality between default protocol and optimal protocol in anthropomorphic phantom with various sizes of artificial nodules are shown as in Figure 4.8 – 4.12.

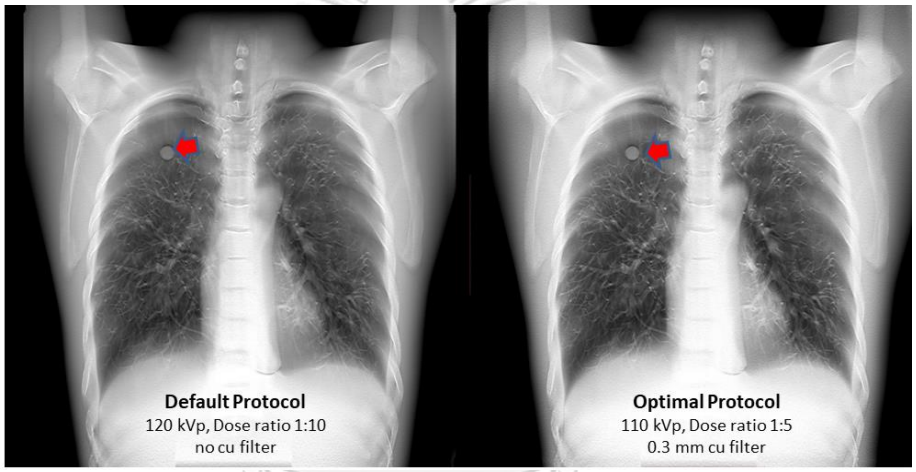

Figure 4.8 Comparison of nodule detection for artificial nodules diameters 12 mm between default and optimal protocols.

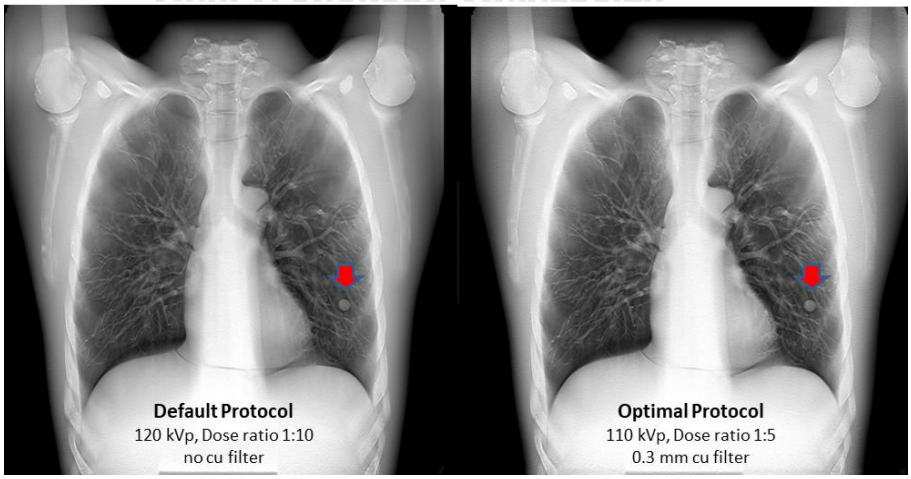

Figure 4.9 Comparison of nodule detection for artificial nodules diameters 10 mm between default and optimal protocols.

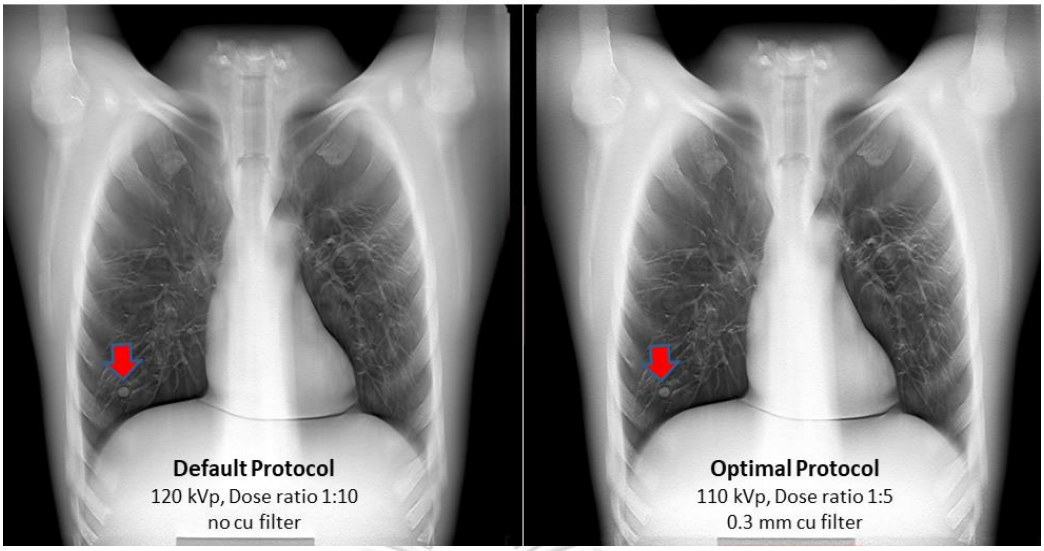

Figure 4.10 Comparison of nodule detection for artificial nodules diameters 8 mm between default and optimal protocols.

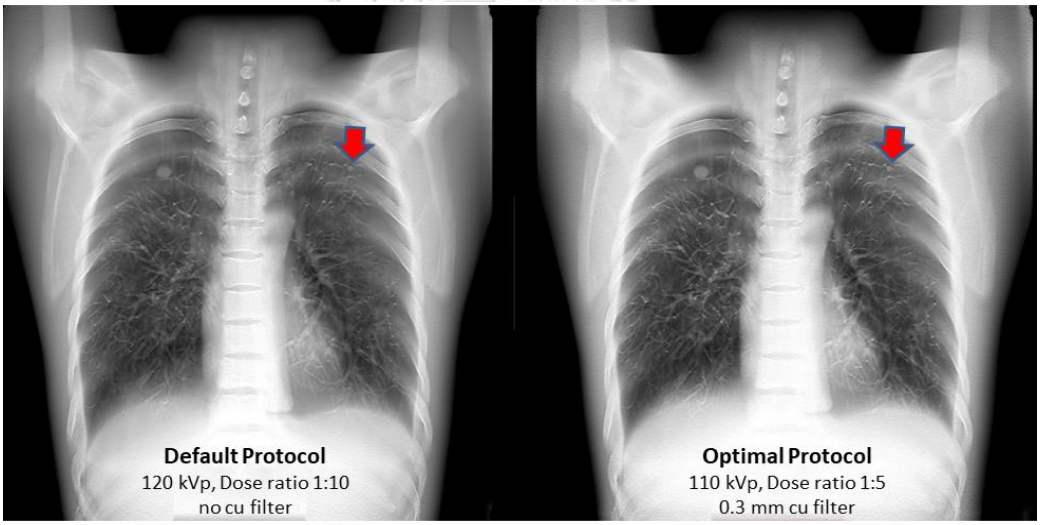

Figure 4.11 Comparison of nodule detection for artificial nodules diameters 5 mm between default and optimal protocols.

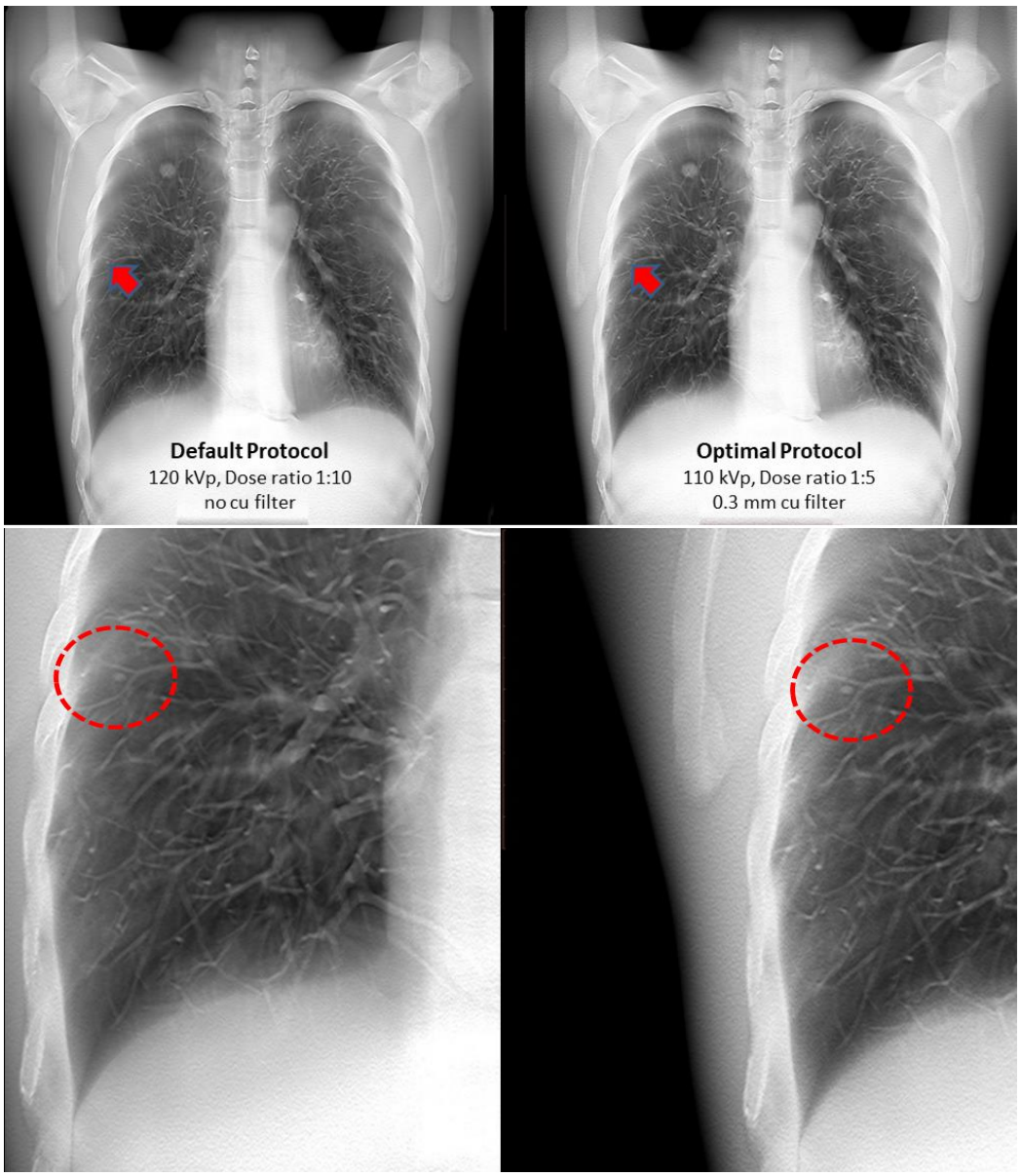

Figure 4.12 Comparison of nodule detection for artificial nodules diameters 3 mm between default and optimal protocols.

4.4 Patients study

Thirty patients; 15 males (50%) and 15 females (50%), were collected and exposed on digital chest tomosynthesis using the optimal protocol derived from the phantom study. The optimal parameters for this study were 110 kVp, dose ratio 1:5 and 0.3 mm copper filter. The inclusion and exclusion criteria were described previously in Chapter III.

Table 4.12 Patient characteristics and the effective dose of 30 patients.

No.	Gender M/F	Age (Y)	Thickness (cm)	Weight (kg)	Total DAP $dGy.cm^2$	ED (mSv)
1	M	57	24.00	79.00	3.58	0.099
2	M	73	24.00	68.00	3.57	0.099
3	F	75	25.80	68.00	3.61	0.100
4	M	75	23.00	73.00	3.70	0.102
5	F	74	19.30	35.70	3.42	0.095
6	F	63	22.00	54.00	3.54	0.098
7	F	58	24.50	63.00	3.59	0.099
8	F	59	24.00	58.30	3.63	0.101
9	M	60	22.00	70.00	3.72	0.103
10	M	70	21.10	60.00	3.66	0.101
11	F	36	20.10	55.00	3.47	0.096
12	M	63	24.30	75.00	3.63	0.101
13	M	73	20.50	74.00	3.56	0.099
14	M	67	21.60	57.40	3.52	0.098
15	M	63	22.30	69.00	3.55	0.098
16	M	54	23.80	87.00	3.72	0.103
17	M	66	23.00	64.00	3.58	0.099
18	M	68	22.00	61.00	3.54	0.098
19	F	48	23.50	74.00	3.60	0.100
20	F	65	24.00	58.00	3.60	0.100
21	F	54	21.50	54.20	3.50	0.097
22	F	62	24.50	62.80	3.59	0.099

23	F	60	20.50	56.00	3.48	0.096
24	M	37	21.20	75.00	3.55	0.098
25	F	69	23.50	62.00	3.58	0.099
26	M	74	24.00	68.00	3.59	0.099
27	M	56	23.50	61.00	3.45	0.096
28	F	41	19.50	43.00	3.44	0.095
29	F	45	22.00	60.00	3.51	0.097
30	F	49	20.20	63.00	3.60	0.100

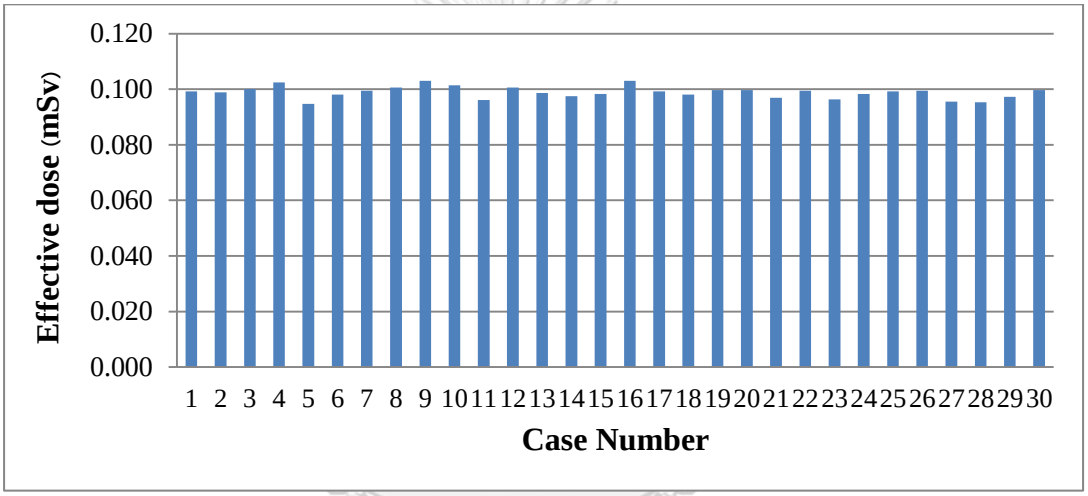

Figure 4.13 Bar charts of the effective dose (mSv) in 30 patients.

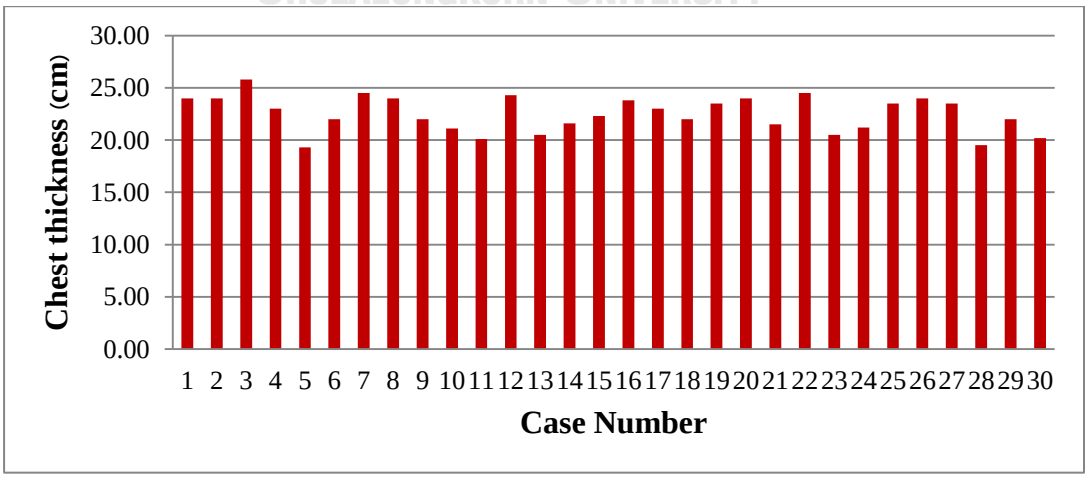

Figure 4.14 Bar charts of chest thickness (cm) in 30 patients.

Table 4.13 The summary of patient data who underwent DTS optimal protocol.

	Average	**S.D.**	**Maximum**	**Minimum**
Age (Y)	60.4	11.17	75	36
Chest thickness (cm)	22.50	1.69	25.80	19.30
Body weight (kg)	63.60	10.39	87.00	35.70
Total DAP ($dGy.cm^2$)	3.57	0.08	3.72	3.42
Effective dose (μSv)	98.87	0.08	103.04	94.73

4.5 Image quality in patient study

The image quality of digital chest tomosynthesis was evaluated by two experienced radiologists using the optimal protocol. The optimal parameters for this study were 110 kVp, dose ratio 1:5 and 0.3 mm copper filter. Thirty patients were collected and exposed on the optimal protocol for digital chest tomosynthesis. The result of image quality interpreted by two radiologists after applying optimal protocol is illustrated as in Table 4.14. We used the European guidelines on quality criteria of chest radiography instead for DTS diagnostic radiographic images [22].

Table 4.14 Image quality of DTS in patient study.

No.	**Radiologist 1**		**Radiologist 2**	
	Image criteria score	Acceptable image quality (Yes / No)	Image criteria score	Acceptable image quality (Yes / No)
1	4.5	Yes	6.0	Yes
2	4.5	Yes	5.5	Yes
3	6.0	Yes	6.0	Yes
4	4.0	Yes	4.5	Yes
5	5.5	Yes	6.0	Yes
6	4.0	Yes	6.0	Yes
7	6.0	Yes	6.0	Yes
8	6.0	Yes	6.0	Yes
9	6.0	Yes	6.0	Yes
10	6.0	Yes	6.0	Yes
11	4.5	Yes	4.5	Yes
12	5.5	Yes	6.0	Yes
13	6.0	Yes	6.0	Yes
14	5.5	Yes	6.0	Yes
15	5.5	Yes	5.5	Yes

No.	Radiologist 1		Radiologist 2	
	Image criteria score	Acceptable image quality (Yes / No)	Image criteria score	Acceptable image quality (Yes / No)
16	5.0	Yes	6.0	Yes
17	4.5	Yes	6.0	Yes
18	6.0	Yes	6.0	Yes
19	6.0	Yes	6.0	Yes
22	6.0	Yes	6.0	Yes
23	6.0	Yes	6.0	Yes
24	6.0	Yes	5.5	Yes
25	6.0	Yes	6.0	Yes
26	6.0	Yes	6.0	Yes
27	6.0	Yes	6.0	Yes
28	6.0	Yes	6.0	Yes
29	6.0	Yes	6.0	Yes
30	6.0	Yes	6.0	Yes

Table 4.15 Overall image quality of patient study.

Image criteria score	Radiologist 1	Radiologist 2
Score		
0	-	-
0.5	-	-
1.0	-	-
1.5	-	-
2.0	-	-
2.5	-	-
3.0	-	-
3.5	-	-
4.0	2 (7%)	-
4.5	4 (13%)	2 (7%)
5.0	1 (3%)	1 (3%)
5.5	4 (13%)	3 (10%)
6.0	19 (63%)	24 (80%)
Total	**30 (100%)**	**30 (100%)**

Table 4.16 The summary of image criteria score interpreted by two radiologists in patient study.

	Average	S.D.	Maximum	Minimum
Radiologist 1	5.57	0.68	6.0	4.0
Radiologist 2	5.82	0.43	6.0	4.5

4.6 Clinical used in optimal protocol

The examples of comparison of the image quality between default protocol and after applying the optimal protocol (110 kVp, dose ratio 1:5, copper filter 0.3 mm) in clinical study with follow-up lung nodules patients are shown as in Figure 4.15.

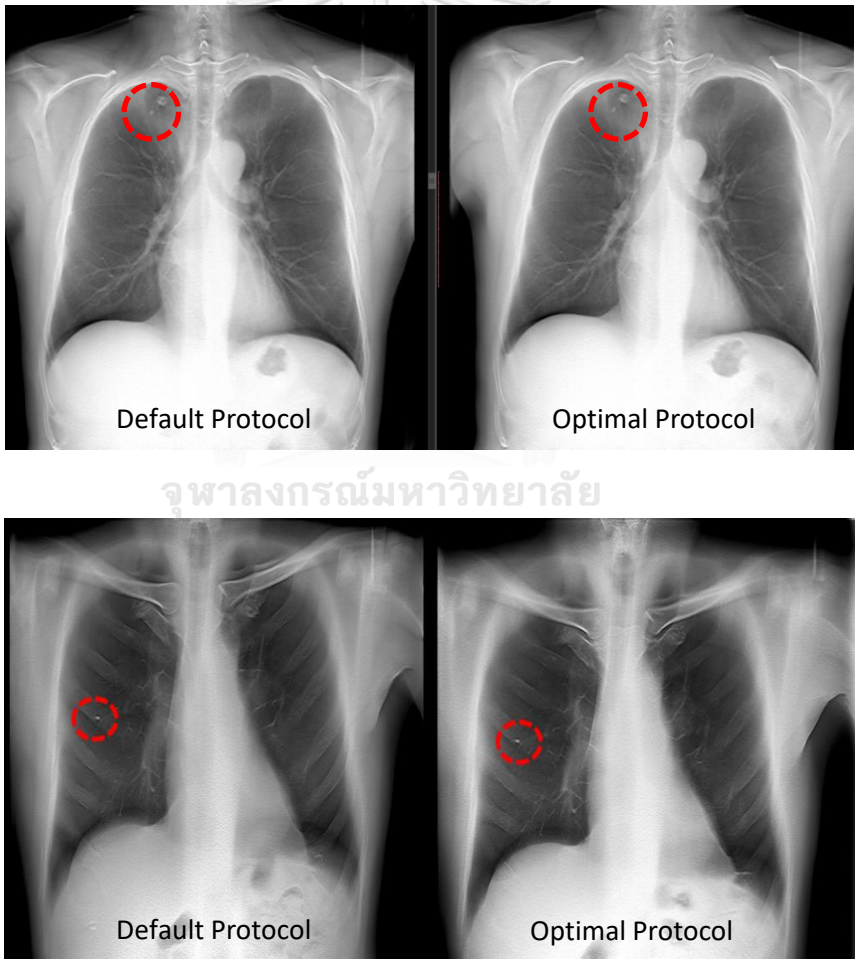

Figure 4.15 The DTS images of patients who were follow-up for lung nodule using optimal protocol.

CHAPTER V
DISCUSSION AND CONCLUSION

5.1 Discussion

Chest radiography remains the mainstay for diagnosis of many lung diseases, despite advances in cross-sectional imaging techniques such as CT. It is frequently the first and may be the only imaging test performed in patients with known or suspected lung disease. Advances in electronics and computer technology have led to the development of digital image receptors and displays. New image processing techniques, advanced applications such as digital subtraction radiography, digital tomosynthesis and computer-assisted detection and diagnosis promise to substantially improve on the performance of conventional chest radiography.

DTS is a newly available imaging modality that offers the potentially substantial improvements over conventional chest radiography for the detection of subtle lung disease. The major advantages of DTS over conventional chest radiography are the removal of overlying structures, the enhancement of local tissue separation, and the availability of depth information for the structure of interest. Despite these advantages, the problem of high radiation dose remains.

In this study, we have determined the optimal parameters for DTS in order to reduce the radiation dose to patients while maintaining the image quality. This was likely the first report of radiation dose investigation using DTS in Thai patients as well. The anthropomorphic phantom was scanned by digital radiographic systems model Definium 8000 manufactured by GE Healthcare. We have scanned a phantom using chest VolumeRAD protocol and adjusted parameters by varying tube voltage range from 100, 110, 120 kVp (high kVp technique**)**, copper filter of 0.0, 0.1, 0.2, 0.3 mm and dose ratio of 1:5, 1:8, 1:10 for evaluating the optimal protocol. The DTS acquired data were then reconstructed with filter back-projection (FBP) algorithm, slice interval of 4 mm, resulting in approximately 60 coronal section images, covering the entire chest of the patient.

Currently, there are three commercially systems for digital chest tomosynthesis. The manufacturers of these three systems are GE Healthcare, Shimadzu, and Fujifilm. The GE and Fujifilm flat-panel detectors are based on indirect conversion, whereas the Shimadzu detector is based on direct conversion. All systems employ a linear movement of the x-ray tube for acquiring projection radiographs at different angles. In the GE and Fujifilm systems, the detector is

stationary whereas the Shimadzu detector performs a linear movement in the opposite direction of the x-ray tube. With the current technology of GE system, 60 low-dose projection images are acquired in 12 seconds, whereas the Shimadzu system acquires 74 projections in 6 seconds. On the Fujifilm system, the acquisition time ranges from 4 to 12 seconds, depending on the number of projections acquired (20–60). The sweep angle varies from 8 to 60 degrees, although the typical sweep angle used is 30 or 40 degrees. In principle, a larger sweep angle results in decreased slice thickness and improved depth resolution.

In our study, the DTS based on GE system was used. As the system has configured by the vendor, the sweep angle was set at 30 degrees. Sixty low-dose projection images of tube angle from -15° to +15° were used to reconstruct 60 coronal sectional images without overlap. The digital chest tomosynthesis was performed in full inspiration breath hold with an imaging time of 12 seconds.

The effective doses from a digital chest tomosynthesis examination have been previously reported in the range from 0.1 to 0.2 mSv [25, 26]. These are values close to the 0.1 mSv typically reported for general chest radiography. Since chest tomosynthesis is a new technique, there has been limited work attempting to further reduce the radiation dose associated with the examination. Nevertheless, a recent study showed that by optimizing the acquisition parameters, an effective dose as low as 0.04 mSv could be reached without a significant decrease in image quality [18]. Regarding the determination of radiation doses in chest tomosynthesis, conversion factors that can be used to estimate the effective dose from the registered dose-area product have been published [21, 25]. However, the radiation dose given to the patient should be optimized in order to achieve the “As low as reasonably achievable” or ALARA principle. According to this rule of thumb, the necessary level of image quality for correct diagnosis in medical imaging should be obtained at the lowest possible radiation dose to the patient.

According to the results in CHAPTER IV, we have found that, the lowest effective dose and ESD were obtained at 100 kVp, dose ratio 1:5, and additional copper filter 0.3 mm which were similar to the previous study reported by Hwang HS et al [18] where they discovered the similar parameters to obtain the lowest effective dose and ESD. In addition, they found the estimated effective dose was 62 µSv and our outcome was 74 µSv.

In phantom study, the results indicated that the average±SD of ESD obtained from vendor’s default protocol at 120 kVp, dose ratio 1:10 using no copper filter was 1.68±0.15 mGy. The optimal parameter for DTS was obtained at 110 kVp, dose ratio 1:5, and copper filter at 0.3 mm with the ESD of 0.47±0.02 mGy. The effective doses for the default protocol and optimal protocol were 313.98±0.72 and 100.55±0.28 µSv,

respectively. Dose ratio and tube voltage were slightly correlated with the total DAP because the AEC technique has been applied. As the purpose of AEC is to achieve adequate image quality by maintaining the constant optical density, the changing exposure parameters is slightly affected the SNR measurement. There were slightly different of the image criteria score and nodule detection between optimal and default protocols using visual assessment interpreted by two radiologists according to the European guidelines on quality criteria for diagnostic radiographic images and Fleischner Society guidelines [22-24].

In patient study, the average±SD effective dose of 98.87±0.08 μSv was obtained after applied the optimal protocol in 30 patients who were follow-up for the lung cancer at Chulabhorn Hospital. We have found that all of the DTS images were acceptable of images quality after acquiring with the optimal protocol in these patients. The majority of image score of 6.0 with 19 cases (63%) were obtained from radiologist 1, and 24 cases (80%) from radiologist 2. It would be implied that the optimal protocol investigated in this study is primarily acceptable for using in clinical study. However, the image quality score depends on patient setup stability causes the motion artifact, as well as full-inspiration breath hold capability of patients.

The dose ratio and tube voltage were in slightly correlated with ESD due to the AEC technique was applied. The ESD of default parameter was decreased by 52% when adding cu-filter to 0.3 mm. The use a copper filter has a potential for reducing the radiation dose to the patients [27]. Therefore, our results have agreed with the previous study reported by Hamer OW et al [28]. The subjectively equivalent chest radiographic image quality was found with an estimated 30% dose reduction after the addition of 0.3 mm copper filter with flat-panel technology. However, the result of ESD in dose ratio 1:5 was not one half of the ESD in dose ratio 1:10.

Hwang HS et al [18] described a low-dose setting for the optimization tomosynthesis, resulting in a radiation dose reduced by 67%. The reduction in dose produces an effective dose similar to that of a two-view chest radiograph (PA and lateral) by reducing tube voltage with additional filtration. As a result, this can reduce the radiation risk of patients accordingly. In theoretical, the radiation dose from DTS can be also reduced using other imaging techniques such as reducing number of projections, reducing tube angle for tomosynthesis even using the iterative reconstruction. It is comparable with our study for the optimization tomosynthesis resulting in the dose reduction of 72%.

We found that, the nodule detection capability depends on nodule size and the slice thickness interval for image reconstruction which is agreed with Dobbins JT et al [10]. They reported that 53% and 71% detection sensitivity were found for 3-5 mm and 5-10 mm nodule sizes, respectively. Vikgren J et al [29] also reported that the sensitivity of 86% was detected for nodules less than 4 mm and nearly 100% visibility

for nodules above 5 mm. These both results show a relatively low detection rate for nodules of less than 4 mm. However, in a clinical setting, detection of nodules larger than 4 mm is more important than detection of smaller nodules, which would not be considered actionable suggested by criteria of the Fleischner Society [23, 24].

According to the previous results described by Dobbins JT et al [10], they proposed the potential implementation for chest tomosynthesis would be a better option for high-risk patients, such as current or former smokers at risk for lung cancer and metastasis work-up patients. This will maximize the chances for improved patient outcomes and minimize cost, radiation dose and workflow issues. As a result, we also suggested that the optimal parameters setting in this study is suitable for work-up patients. The comparison of image quality obtained from default protocol and optimal protocol is illustrated as in Figure 5.1.

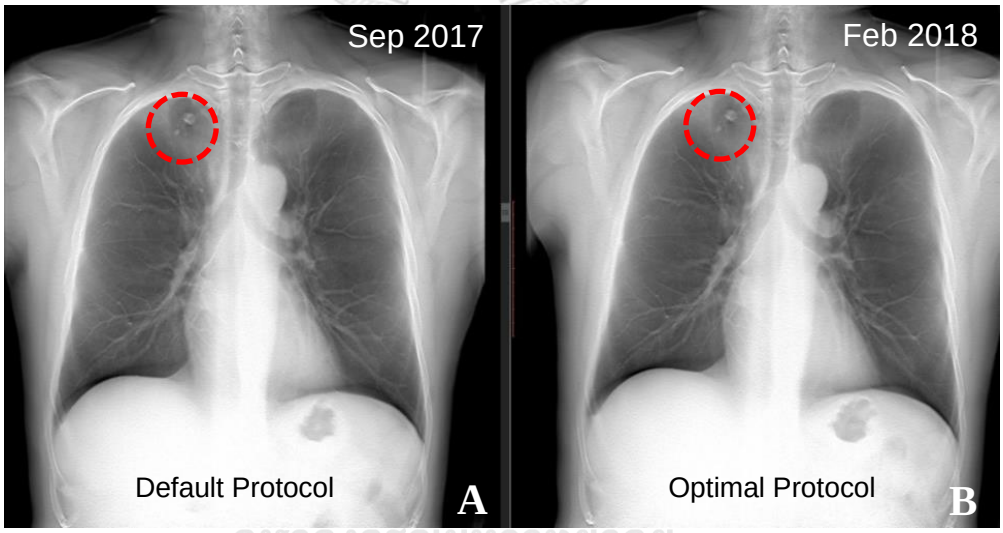

Figure 5.1 The follow-up lung nodule lesion patient images
(A) default protocol, (B) optimal protocol.

For the ESD measured by glass dosimeter, the tin filter in the capsule for GD-352M has been used in order to reduce the energy dependence effect purpose. Consequently, the GD-352M as we used in this study was suitable for measuring the radiation dose for low energy photons such as in the diagnostic radiology, whereas the GD-301 and GD-302M without filters in capsule are suitable to measure the dose of high energy photons as in radiotherapy. However, in the process of dose readout, based on the dose values, the dose ranges are divided into two categories, i.e. low dose range from 10 μGy – 10 Gy, and high dose range between 1 Gy and 500 Gy [14]. Therefore, the ESDs obtained in this study were comparable to ESDs reported by other previous studies [18].

There were some limitations in this study. Firstly, only one thickness of the phantom was used for investigating the optimal protocol. Secondary, as anthropomorphic chest phantom was used instead of human, the detection of nodules in the phantom might have been easier than those in human. This due to there was no overlying internal structures such as pulmonary vessels in the phantom. Finally, there were no officially published criteria of image quality scoring for digital chest tomosynthesis. In this study, therefore, the image criteria based on European guidelines on quality criteria for diagnostic radiographic images were used instead for DTS interpretation.

5.2 Conclusion

This study successfully determines the optimal protocol for chest x-ray using DTS at Department of Diagnostic Radiology, Chulabhorn Hospital. The optimal parameters for DTS obtained in this work were 110 kVp, dose ratio 1:5, copper filter 0.3 mm, and operated with AEC technique. This protocol can substantially reduce radiation dose while preserving the image quality compared to the vendor's default protocol in both of phantom and clinical studies. As a result, the DTS is an effective modality for enhancing pulmonary abnormalities and pulmonary nodule detections with lower dose compared to CT.

5.3 Recommendation

The optimal protocol setting in this study would be more suitable for low risk patients such as non-smokers, young and pediatric patients, as well as the follow-up lung nodule patients with the chest thickness less than or equal to 23 cm for avoiding unnecessary radiation.

REFERENCES

1. World Health Organization (WHO). Cancer February 1, 2018 [Available from: http://www.who.int/en/news-room/fact-sheets/detail/cancer.
2. Kim JH, Lee KH, Kim KT, Kim HJ, Ahn HS, Kim YJ, et al. Comparison of digital tomosynthesis and chest radiography for the detection of pulmonary nodules: systematic review and meta-analysis. Br J Radiol 2016;89-99.
3. Lança L, Silva A. Technical Considerations Concerning Digital Technologies2013. 37-47 p.
4. Bertolaccini L, Viti A, Terzi A. Digital tomosynthesis in lung cancer: state of the art. Ann Transl Med 2015;3:139.
5. Bansal GJ. Digital radiography. A comparison with modern conventional imaging. Postgrad Med J 2006;82:425-8.
6. Lança L, Silva A. Digital radiography detectors–A technical overview: Part 2. Radiography 2009;15:134-8.
7. Lança L, Silva A. Image Enhancement for Digital Radiography. Digital Imaging Systems for Plain Radiography2013. p. 109-36.
8. Jerrold T. Bushberg JAS, Edwin M. Leidholdt, Jr, and John M. Boone The Essential Physics of the Medical Imaging, 3rd ed. Radiology 2012:144-5.
9. Körner M, Weber CH, Wirth S, Pfeifer K-J, Reiser MF, Treitl M. Advances in Digital Radiography: Physical Principles and System Overview. RadioGraphics 2007;27:675-86.
10. Dobbins JT 3rd, McAdams HP. Chest tomosynthesis: technical principles and clinical update. Eur J Radiol 2009;72:244-51.
11. Gomi T, Hirano H, Nakajima M, Umeda T. X-ray digital linear tomosynthesis imaging. Journal of Biomedical Science and Engineering 2011;04:443-53.
12. Lança L, Silva A. Assessment of Patient Dose in Digital Systems. Digital Imaging Systems for Plain Radiography2013. p. 49-62.
13. PP Dendy BH. Physics for Diagnostic Radiology, Third Edition.
14. Y.C. Huang D, Hsu S-M. Radio-Photoluminescence Glass Dosimeter (RPLGD)2011.
15. Williams M, Krupinski E, Strauss K, K Breeden W, Rzeszotarski M, Applegate K, et al. Digital Radiography Image Quality: Image Acquisition2007. 371-88 p.

16. Kumar SG, Garg MK, Khandelwal N, Gupta P, Gupta D, Aggarwal AN, et al. Role of digital tomosynthesis and dual energy subtraction digital radiography in detecting pulmonary nodules. Eur J Radiol 2015;84:1383-91.
17. Quaia E, Baratella E, Poillucci G, Gennari AG, Cova MA. Diagnostic impact of digital tomosynthesis in oncologic patients with suspected pulmonary lesions on chest radiography. Eur Radiol. 2016;26(8):2837-44.
18. Hwang HS, Chung MJ, Lee KS. Digital tomosynthesis of the chest: comparison of patient exposure dose and image quality between standard default setting and low dose setting. Korean J Radiol 2013;14:525-31.
19. AAPM. Report No.74 quality control in diagnostic radiology. The American Association of Physicist in Medicine 2002.
20. KCARE protocol for the QA of Direct Digital Radiography System Commissioning and Annual QA Test. King's Center for the Assessment of Radiological Equipment, King's College Hospital. 2004.
21. Svalkvist A, Mansson LG, Bath M. Monte Carlo simulations of the dosimetry of chest tomosynthesis. Radiat Prot Dosimetry 2010;139:144-52.
22. European Commision. European Guidelines on quality criteria for diagnostic radiographic images, EUR 16260. 1996.
23. MacMahon H, Austin JHM, Gamsu G, Herold CJ, Jett JR, Naidich DP, et al. Guidelines for Management of Small Pulmonary Nodules Detected on CT Scans: A Statement from the Fleischner Society. Radiology 2005;237:395-400.
24. MacMahon H, Naidich DP, Goo JM, Lee KS, Leung ANC, Mayo JR, et al. Guidelines for Management of Incidental Pulmonary Nodules Detected on CT Images: From the Fleischner Society 2017. Radiology 2017;284:228-43.
25. Bath M, Svalkvist A, von Wrangel A, Rismyhr-Olsson H, Cederblad A. Effective dose to patients from chest examinations with tomosynthesis. Radiat Prot Dosimetry 2010;139:153-8.
26. Soderman C, Johnsson AA, Vikgren J, Norrlund RR, Molnar D, Svalkvist A, et al. Evaluation of accuracy and precision of manual size measurements in chest tomosynthesis using simulated pulmonary nodules. Acad Radiol 2015;22:496-504.

27. James T. Dobbins I, Samei E, Chotas HG, Warp RJ, Baydush AH, Carey E. Floyd J, et al. Chest Radiography: Optimization of X-ray Spectrum for Cesium Iodide–Amorphous Silicon Flat-Panel Detector. Radiology 2003;226:221-30.
28. Hamer OW, Sirlin CB, Strotzer M, Borisch I, Zorger N, Feuerbach S, et al. Chest Radiography with a Flat-Panel Detector: Image Quality with Dose Reduction after Copper Filtration. Radiology 2005;237:691-700.
29. Vikgren J, Zachrisson S, Svalkvist A, Johnsson AA, Boijsen M, Flinck A, et al. Comparison of chest tomosynthesis and chest radiography for detection of pulmonary nodules: human observer study of clinical cases. Radiology 2008;249:1034-41.

APPENDIX

Appendix A

Report of digital x-ray system performance

General Information

Location: Diagnostic Radiology Department, Chulabhorn Hospital
Date: 11/06/2017
Room number: Room 1
Manufacturer: GE Healthcare
Model number: Definium 8000
Serial number: 8763M35

Checklist

P	General mechanical and electrical condition
P	Tube angle indicator, tube motion and locks
P	Focus to film distance indicator (SID)
P	Field size indicator
P	Congruency of light and radiation fields
P	Crosshair centering
P	Focal spot size
P	Photo cell consistency
P	Auto exposure control (AEC)
P	Automatic Collimation (PBL)
P	Beam Quality (Half Value Layer)
P	Consistency of exposure (mR/mAs)
P	kVp Accuracy
P	Timer accuracy
P	mA Linearity
N/P	ESE calculations
N/P	Relative radiation wave form
P	Exposure repeatability
N/P	Reciprocity

General Comment

P = Performed
N/P = Not Performed
N/A = Not Applicable

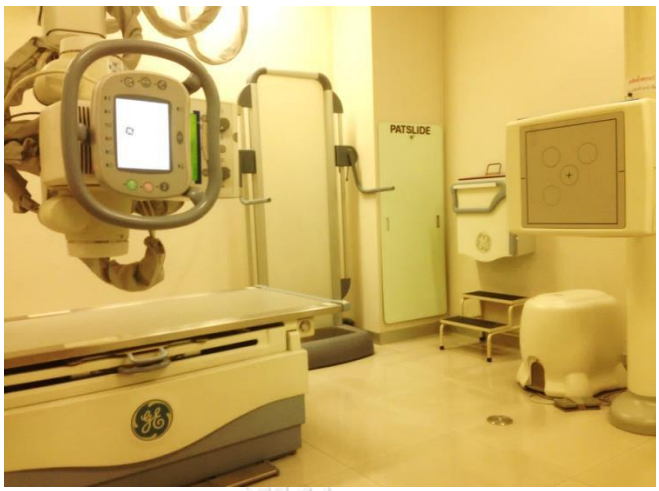

Figure 1 Definium 8000 (GE Healthcare)

General Condition of Mechanical and Electrical Components

NO Is there play in the couch when it is locked?

NO Are there any frayed or exposed electrical wires?

NO Could electrical wires interfere with the use of the unit?

NO Is there play in the couch when it is locked?

YES Does it have the freedom of movement it was designed for?

YES Is the couch level in tube and perpendicular directions?

NO Is there play in the tube when it is locked?

YES Does it have the freedom of movement it was designed to have?

YES Does the visual, and/or, audible beam-on indicator function?

YES Is the dead man switch installed correctly?

1. Target to Film Distance Indicator Check

SID: 180 cm. **Allowable limit = ± 2%**

Measured distance: 179 cm
Indicated distance: 180 cm

% Difference: 0.44 %
Pass/Fail: PASS

2. Tube Angle Indicator Check **Allowable limit = ± 5°**

CW: Clockwise	Measure	CCW: Counterclockwise	Measure
0°	0.00°	**45°**	45.00°
45°	44.00°	**90°**	90.00°
90°	91.00°		

Pass/Fail: PASS

3. Motion and Lock Check

Motion and Lock Check	Motion	Lock
Tube Longitudinal	Y	N
Tube Rotate	Y	N
Tube Transverse	Y	N
Tube Vertical	Y	N
Tube Angulate	Y	N
Collimator Jaws	Y	N
Collimator Rotation	Y	N

4. Field Size Indication

Purpose: To insure that the radiographer can set a desired field size using the light field collimator.
Requirement: ± 2% SID.
SID: 100 cm.

Indicator Setting (cm)	**Measured** Longitudinal (cm)	**Measured** Transverse (cm)	**% Variation**	**Pass / Fail**
25×25	24.4	24.10	0.01	PASS
35×35	34.2	34.6	0.01	PASS

5. Automatic Collimation (PBL)

YES Does the PBL system collimate in less than 5 sec?

YES Does the PBL system collimate smaller than the set field size?

YES Does the PBL system collimate larger than the set field size?

N/A Is there an override key?

N/A With the key removed, is PBL system activated?

6. Automatic Collimation (PBL)

When collimation is performed automatically, the field size measured at the SID and that indicated on the collimator should be within ± 2% of the SID.
SID: 100 cm.

Indicator Setting (cm)	**Measured** Longitudinal (cm)	**Measured** Transverse (cm)	**% Variation**	**Pass / Fail**
43.00×35.00	44.20	36.20	0.01	PASS
35.00×43.00	36.00	45.00	0.02	PASS
30.00×24.00	31.20	25.50	0.02	PASS
24.00×30.00	25.00	31.50	0.02	PASS

7. Congruence of Light and Radiation Fields

Purpose: To determine the alignment of the light and radiation fields.

Requirement: Alignment to within +/- 2% of indicated SID.

Method: Mark corners of light field and compare to radiation field

SID: 100 cm.

Field Size (cm)	Light Field Size		Radiation Field Size		% CV	Pass/ Fail
	Measure Longitudinal (cm)	Measure Transverse (cm)	Measure Longitudinal (cm)	Measure Transverse (cm)		
25 × 25	24.40	24.10	25.09	24.57	0.01	PASS
35 × 35	34.20	34.60	33.30	33.90	0.01	PASS

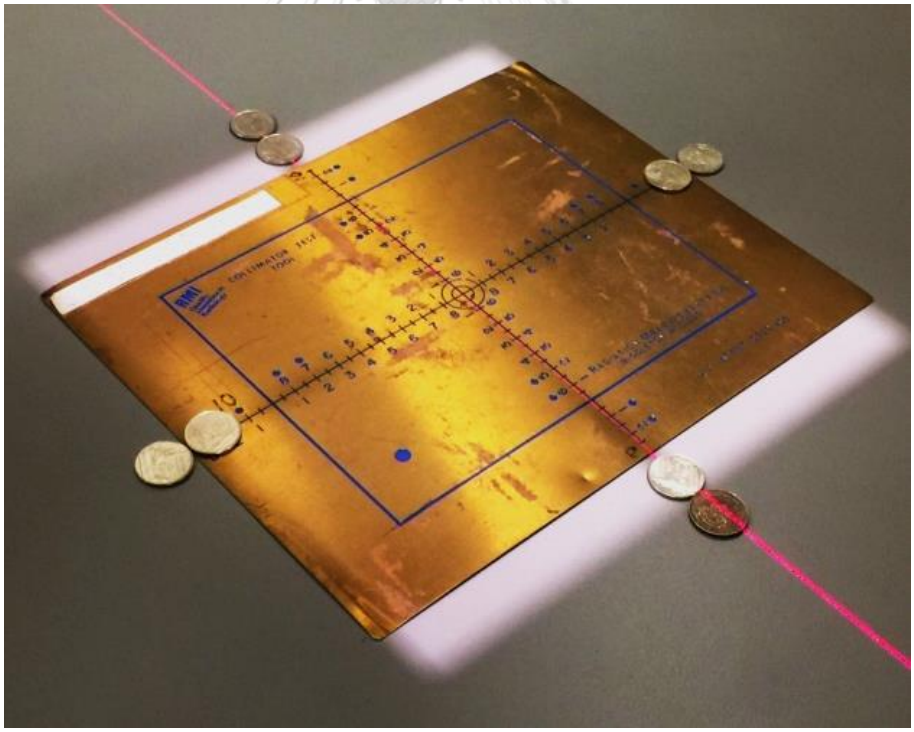

Figure 2 Light and Radiation Fields

8. Cross Hair Centering

Purpose: To determine if the light field cross hair indicates the central axis of beam.

Requirement: Within +/- 2% of indicated SID.
SID: 100 cm.

Deviation between radiation and optical field centers: 1.50 cm.
Pass/Fail: PASS

9. Focal Spot Size

Purpose: To determine the size of the focal spot at a known technique with a view to detect degradation of the focal spot.

Method: Star test pattern

Large Focal Spot

Set kVp: 55 Set mA: 400 Set time: 4

Degree of Star: 2

Star dimension:

Actual: 55.00 Radiographic: 104.58

Blur: 43.53 Manufacturer specifications: 1.25

Computed Focal Spot Size: 1.68

Meets NEMA: YES

Small Focal Spot

Set kVp: 55 Set mA: 100 Set time: 16

Degree of Star: 2

Star dimension:

Actual: 55.00 Radiographic: 104.58

Blur: 23.18 Manufacturer specifications: 0.60

Computed Focal Spot Size: 0.89

Meets NEMA: YES

10. Beam Quality (Half Value Layer)

Figure 3 Test beam quality of digital radiography system.

Method: Set 80 kVp.

Requirement: NCRP #33 *recommends* not less than 2.3 mmAl at 81 kVp.

Set kVp: 80.00 **Measured kVp:** 78.93

Filter (mmAl)	Instrument Reading
OPEN	1.374
1	1.073
2	0.862
3	0.707
3.5	0.647

Calculated HVL: 3.10 mmAl

Pass/Fail: PASS

11. Photo Cell Consistency
Purpose: To insure consistent densities between exposures.
Method: Compare the pixel value using the center cell with constant kVp.

Set kVp: 90

mAs:	**pixel value**
4.74/14.3	3156.98
4.71/14.3	3155.29
4.71/14.5	3155.27
4.72/14.6	3152.17

Mean: 3154.928
Std.Dev.: 2.005
C.V.: 0.001

Pass/Fail: PASS

12. Exposure Consistency

Purpose: To determine if the exposre is remaining consistent.
Requirement: Coefficient of variation should be </= 0.05.
Method: Use Radcal Accu-Gold

Set SCD: 40 inches **Set kVp:** 80

Set mA: 320 **Set time:** 1/10 **Set mAs:** 25

	kVp	Time	mGy
	80.90	78.6400	1.372
	81.00	78.6400	1.371
	80.90	78.5400	1.372
	80.90	78.5400	1.354
Mean:	80.925	78.6067	1.37
Std. Dev.	0.0433	0.0471	0.0077
C.V.	0.0005	0.0006	0.0056

Pass/Fail: PASS

13. Timer Accuracy

Requirement: within 10% of set time.
Method: At about 80 kVp, mid-current mA station, record measured time for each time setting (use Radcal Accu-Gold).

SCD: 40 inches **KVp:** 80 mA: 320 Large FS

Seconds (set)	Measured (milliseconds)	% Variation
0.025	0.0254	1.60%
0.50	0.0504	0.76%
0.10	0.1006	0.60%
156.00	156.80	0.51%
250.00	250.60	0.24%
500.00	500.7000	0.14%

Pass/Fail: PASS

14. kVp Linearity

Method: At a mid-current station, vary the kVp from minimum to maximum in steps of 10 kVp. Record the measured kVp.
(Use the Radcal Accu-Gold).

Requirement: The deviation should not exceed 5 kVp or 10% of set kVp, whichever is larger.

Set SID: 40 inches **Phase:** 3

mA: 250 **mAs:** 25

Set kVp	Avg.	% Dev.	mGy	mGy/mAs	HVL
50	49.70	0.60%	0.48	0.02	1.966
60	60.50	0.83%	0.75	0.03	2.338
70	69.70	0.43%	1.04	0.04	2.727
80	81.00	1.25%	1.36	0.06	3.105
90	91.90	2.11%	1.70	0.07	3.476
100	102.40	2.40%	2.07	0.09	3.848
110	112.50	2.27%	2.47	0.10	4.214
120	123.30	2.75%	2.87	0.11	4.584
130	134.20	3.23%	3.31	0.13	4.965
140	144.90	3.50%	3.76	0.15	5.344
150	156.00	4.00%	4.06	0.16	5.647

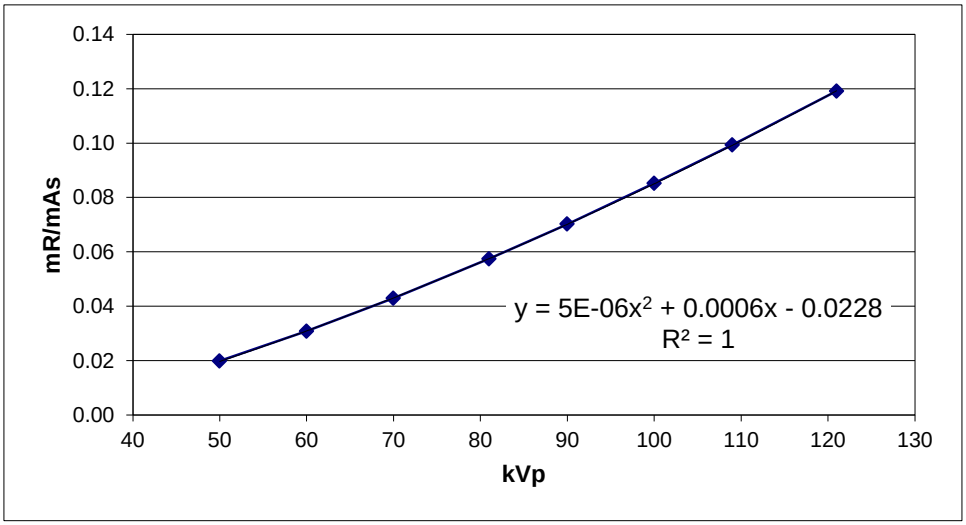

15. mA or mAs Linearity

Method: Select 80 kVp and time close to 0.100 ms (1/10 sec) and cycle through all mA stations and record the exposure in mR (use Radcal Accu-Gold).
Requirement: coefficient of variation should not exceed 0.1.

S/L	Ave. kVp	mA	Time	mAs	mGy	mGY/ mAs	C.V.
L	80.90	160	100.6	16.0	0.8773	0.055	0.002
L	81.00	200	100.6	20.0	1.092	0.055	0.000
L	80.90	250	100.5	25.0	1.365	0.055	0.004
L	80.90	320	100.5	32.0	1.735	0.054	-0.002
L	80.90	400	100.5	40.0	2.178	0.054	0.000
S	80.80	500	100.5	50.0	2.725	0.055	0.001
S	80.90	630	100.5	63.0	3.426	0.054	0.003
S	80.90	800	100.6	80.0	4.321	0.054	-0.004
S	81.00	1000	100.5	100.0	5.444	0.054	

Global Mean: 0.05445
Global Std. Dev.: 0.00024
Global C.V.: 0.00432

Pass/Fail: PASS

16. Automatic Exposure Control

Method:

1. Select the center cell and choose the Normal density setting.
2. Use 1.5 mm Cu filter.
3. Make one exposure each at 70, 80, and 90 kVp on an image receptor.
4. Record the pixel value.

kVp	Post Exposure mAs/Time	pixel value
70	22.33/69.7	3408.82
80	8.75/26.7	3273.06
90	4.73/14.8	3153.96

Method:

1. Select the center cell and the Normal density setting on the AEC control.
2. Use two sheets of 1.5 mm Cu (3.0 totals) filter.
3. Expose at 90 kVp and record the pixel value.

Filter Thickness	Post Exposure mAs/Time	pixel value
3	49.2/154	3266.42

Method:

1. Place 1.5 mm of Cu to intercept the beam and expose.
2. Select the center cell, choose 80 kVp, and Normal density.
3. Repeat four times and record the pixel value. (consistency)

Trial Number	Post Exposure mAs/Time	pixel value
1	8.75/26.7	3273.06
2	8.76/27.7	3269.33
3	8.75/28.3	3270.46
4	8.79/27.0	3271.06

17. Automatic Exposure Control

Method:

1. Using the same setup as the previous procedure, using 81 kVp
2. Vary the density two steps below and two steps above the Normal density on the AEC.
3. Expose and record the pixel value.

Density Selected	Post Exposure mAs/Time	Pixel value
-2	N/A	N/A
-1	N/A	N/A
Normal	8.75/26.7	3273.06
1	N/A	N/A
2	N/A	N/A

Method:

1. Select the Normal density setting, 1.5 mmCu filter, and choose 81 kVp.
2. Select one phototimer cell at a time and expose.
3. Record the pixel value..

Cell Selected	Post Exposure mAs/Time	pixel value
Left	8.92/28.3	3245.72
Center	8.75/26.7	3273.06
Right	8.55/26.4	3307.20
All	8.40/25.9	3229.63

Average Optical Density: 3269.566

Standard Deviation: 55.060

Appendix B

Quality control of image receptor

General Information

Location:	Diagnostic Radiology Department, Chulabhorn Hospital
Date:	11/06/2017
Room number:	Room 1
Manufacturer:	GE Healthcare (Definium 8000)
Detector type:	Wall stand detector (size 41× 41 cm)
Detector ID:	TA42975-1

Commission Tests

Objective: To assess digital image receptor performance Materials

1. Tape measurement
2. Adhesive tape
3. 1.0 mm Cu filtration
4. Dosimeter Radcal model: *Radcal Accu-Gold with* AGMS-D+)
5. TO20 threshold contrast test object
6. Resolution test object (Hunttner 18)
7. M1 TO geometry test object
8. MS1, MS3, and MS4 test object
9. Lead glass phantom (10x10)

The tests should be performed x-ray unit and workstation that machines passed QC tests. These tests require the use of the higher quality reporting workstation like a clinical workstation.

Quality assurance of digital detector (Wall stand)

1. Dosimetry

Purpose: To measure entrance receptor doses required for later test.

Method:

1. Set SID at 180 cm.
2. Set SCD at 180 cm. (AGMS-D+: Solid State detector)
3. Collimate to the dosimeter.
4. Exposed the chamber such that the inverse square law corrected dose to the chamber is approximately 10 µGy, using 70 kVp, and 1 mmCu filtration.
5. Record the measured.
6. Under the same beam conditions determine the mAs required to deliver 1 µGy, 4 µGy, 12 µGy, and 50 µGy.

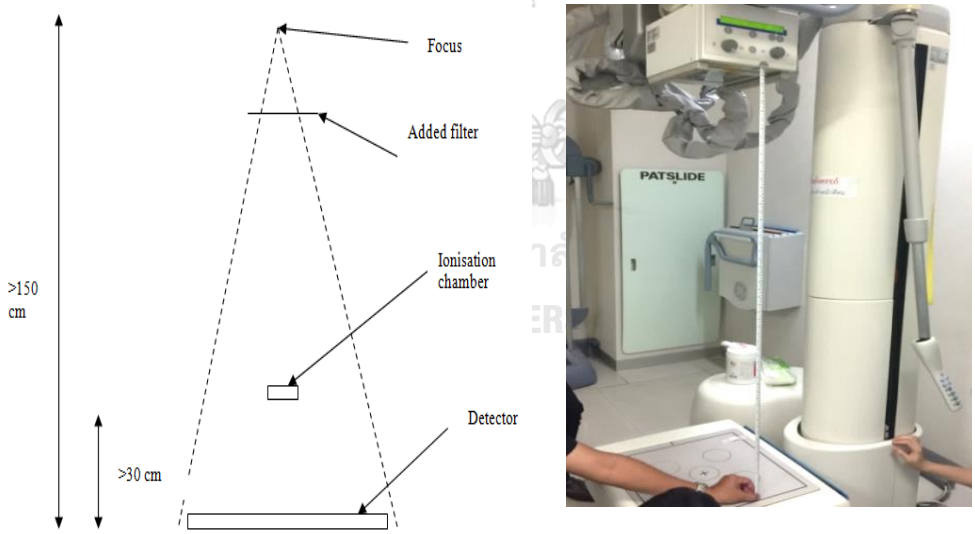

Figure 1 Set up detector for dosimetry.

Result:

Table 1 The mAs was create receptor dose at 4 µGy,10 µGy, 12 µGy, 50 µGy.

Radiation dose (µGy)	SCD (cm)	kV	Time (msec.)	mAs	Measured dose at dosimeter (SCD)	Calculated dose at detector (SID)
1	180	70	7.81	2.5	0.9737	0.974
4	180	70	31	16	4.178	4.178
10	180	70	78.1	40	10.73	10.730
12	180	70	100	50	13.49	13.490
50	180	70	391	200	52.09	52.090

2. Dark Noise

Purpose: To assess the level of noise inherent in the system.

Methods:

1. Remove the grid from the system.
2. Close the collimators and cover the image receptor with a lead apron.
3. Set a low exposure at 50 kVp and 0.5 mAs.
4. Record the image receptor dose indicator value, and pixel value.

Table 2 Show pixel value, maximum pixel value and percentage different of pixel value.

kV	mAs	Exposure index	Pixel Value	Max. Pixel Value	% different of pixel value	Artifact free? Y / N
50	0.5	0	7750.1	7750.21	0.06	Y

Tolerance: This test is used to set a baseline for future QA tests.

3. Linearity and system transfer properties

Purpose: To establish the relationship between receptor dose and pixel value so that this relationship can be corrected for in image retention and uniformity tests. Also,to establish that the indicated exposure (calculated from the image receptor dose indicator responds linearly to increases in dose).

Method:

1. Remove grid from system.
2. Expose the entire area of the image receptor at 70 kVp with 1 mmCu at the tube head. Set a mAs and SID to deliver a dose of 1 μGy.
3. Record the image receptor dose indicator value.
4. Repeat for doses of order 4 μGy, 10 μGy, 12 μGy, and 50 μGy.
5. Record a pixel value from the 5 points of each image.

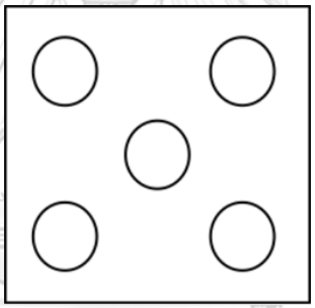

Figure 2 Five position for pixel value measurement.

Figure 3 Set up detector for linearity and system transfer properties.

6. Plot a graph of pixel value versus receptor dose using a graph plotting. Obtain the equation of the trend-line for this graph (the pixel value as a function of receptor dose).

Table 3 Mean pixel value and exposer index of each receptor dose.

kVp	Receptor dose (µGy)	mAs	EI	Mean pixel value
70	1	2.5	0.64	5826.62
70	4	10	3	4177.65
70	10	25	7	3000.38
70	12	32	9	2664.71
70	50	125	34	681.00

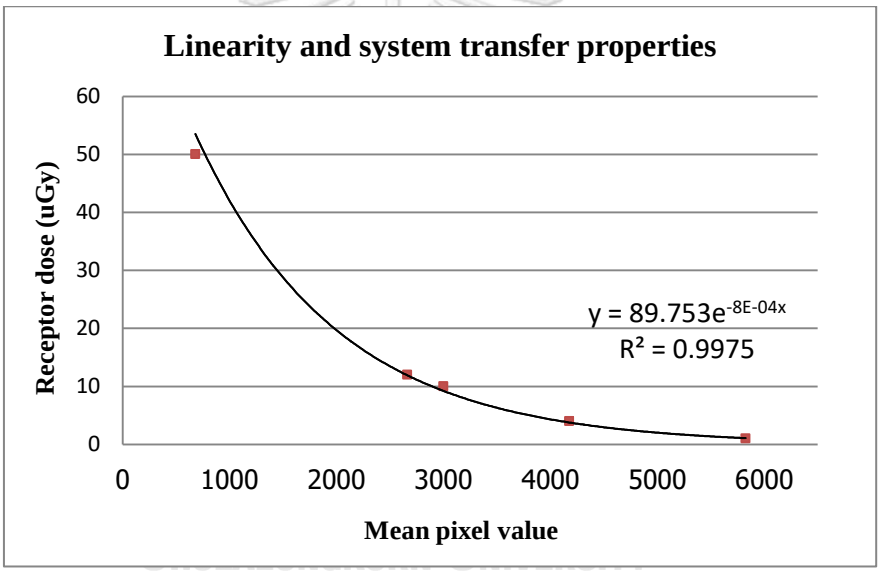

Figure 4 Relation graph between pixel value and receptor dose.

Tolerance:

The trend-line plotted in excel should have an R^2 fit value > 0.95. (R = 0.9975) There is no tolerance for the STP equation. However, the pixel value to dose relationship should be a simple relationship.

Pass/Fail: Pass

4. Image retention

Purpose: To test that any detectable residual signal (ghosting) that remains in subsequent images is minimal.

Method:

1. Remove grid from system and ensured that there is no attenuation in the beam.
2. Set the focus to detector distance (SID) to be 180 cm.
3. Close the collimators and cover the detector with a lead apron. Set a low exposure 50 kVp and 0.5 mAs.

Figure 5 Close detectors with a lead apron and image after exposure.

4. Open the collimators and place the attenuating material-Lead glass 10 x10 cm^2 on the detector. Make an exposure at 70 kVp and 16 mAs to deliver a receptor dose of 4 μGy.

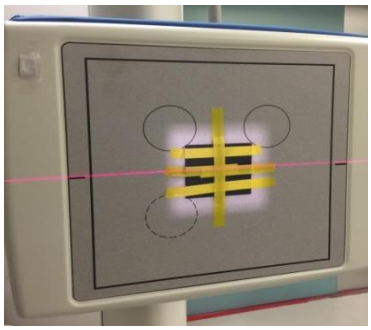

Figure 6 Place the attenuating material-Lead glass 10x10 cm^2 on the detector.

5. Obtain another blank image as described in step 3.

6. Set a very narrow window and adjust the level. Visually inspect the image for any remnant of the previous image. If a remnant is visible, use region of interest analysis to quantify the difference in pixel value between the ghosted and unghosted areas.

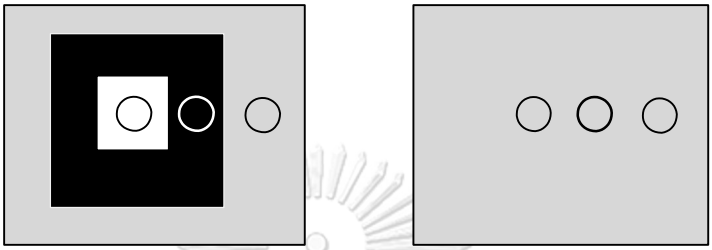

Figure 7 Region of interest for image retention.

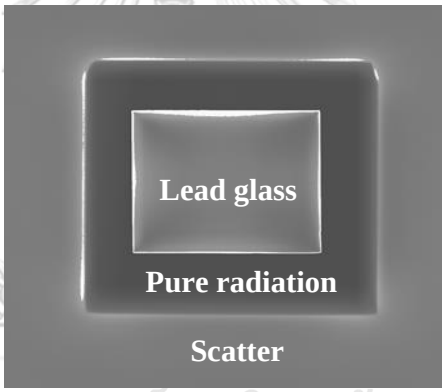

Figure 8 Region of three areas for measurement pixel value.

Table 4 Evaluation of ghosting artifact in each exposure technique

kV	mAs	EI	PV center	Pb area	Area of pure radiation	Area of scatter	Ghosting Artifact? (Y/N)
50	0.5	0	7750.06	7750.23	7750.13	7750.19	
70	10	0.54	5004.98	5057.32	1078.23	4781.1	N
50	0.5	0	7750.08	7750.2	7750.14	7750.24	

% diff = 0.0008

Tolerance:

If no evidence of ghosting is found from visual inspection of the images then the test is passed and there is no need to perform ROI analysis. There should be <5% (remedial) difference between the STP corrected pixel values in the ghosted region and the surrounding areas.

Pass/Fail: Pass

5. Detector dose indicator consistency

Purpose: To assess the variation of EI between exposures, and set a baseline for monitoring system sensitivity for future QA testing.

Methods:

1. Remove the grid from the system.
2. Set a field size to cover the entire image receptor and SID 180 cm.
3. Expose the image receptor to a known dose of 10 μGy at 70 kVp with 1.0 mmCu at the tube head.
4. Record the organ program, LUT name and image receptor dose indicator, without changing the window and levelling.
5. Repeat steps 3 times
6. Also repeat for 1 μGy and 12 μGy (1 image for each).

Result:

Table 5 Detector dose indicator consistency of image receptor.

kVp	Dose (μGy)	mAs	EI	Average EI	% different of sensitivity indices
70	10	25	6.63		0 %
70	10	25	6.63	6.63	0 %
70	10	25	6.63		0 %
70	1	2.5	0.65		
70	12	32	8.9		

*LUT: Chest PA Upright

- The percentage different of EI were less than 1%.

Tolerance:

The indicated sensitivity indices should not differ by greater than 20 of equivalent exposure, between exposures. The measurement should be used to set a baseline for future QA tests.

Pass/Fail: Pass

6. Uniformity

Purpose: To assess the uniformity of the recorded signal from a uniformly exposed image receptor. A non-uniform response could affect clinical image quality.

Method:

1. Remove grid from system.
2. Expose the entire area of the image receptor at 70 kVp with 1 mmCu to deliver a dose of 1μGy.
3. Also repeat for 10 μGy and 12 μGy
4. The five values obtained from ROI analysis should be used to calculate five indicated receptor dose values.

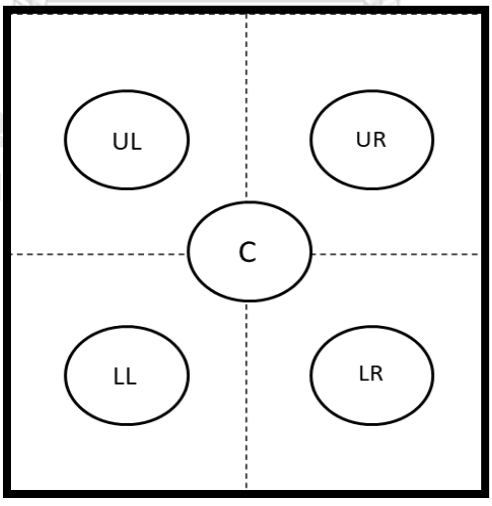

Figure 9 Position of ROI for uniformity test.

Result:

Table 6 The value obtained from ROI analysis and coefficient of variation (CV).

10 µGy	**Center**	**UL**	**UR**	**LL**	**LR**	**Avg.**	**S.D.**	**C.V.**
Mean	3068.11	3073.43	3073.37	3051.83	3046.88	3062.72	12.51	0.004
10 µGy	**Center**	**UL**	**UR**	**LL**	**LR**	**Avg.**	**S.D.**	**C.V.**
Mean	3068.35	3073.69	3073.50	3052.04	3046.94	3062.90	12.56	0.004
10 µGy	**Center**	**UL**	**UR**	**LL**	**LR**	**Avg.**	**S.D.**	**C.V.**
Mean	3068.15	3073.72	3073.54	3052.05	3047.26	3062.94	12.45	0.004
1 µGy	**Center**	**UL**	**UR**	**LL**	**LR**	**Avg.**	**S.D.**	**C.V.**
Mean	5834.46	5833.78	5837.13	5816.7	5811.38	5826.69	11.76	0.002
12 µGy	**Center**	**UL**	**UR**	**LL**	**LR**	**Avg.**	**S.D.**	**C.V.**
Mean	2680.46	2672.93	2676.04	2649.56	2644.46	2664.69	16.45	0.006

- The artifact was not found and the coefficients of variation of 5 System Transfer Properties (STP) were less than 1%.

Tolerance:

The images should not have obvious artefacts. The ratio of the standard deviation of the 5 STP corrected ROI values to their mean (the coefficient of variation) should be less than 10%.

Pass/Fail: Pass

7. Scaling errors

Purpose: To assess the accuracy of software distance indicators and check for distortion.

Method:

1. Remove grid from system.
2. Position the M1 TO test object direct onto the detector with an SID of 180 cm.
3. Exposure the detector at 50 kVp 10 mAs with no attenuation in the beam.
4. Using the distance measuring software tools measure the dimensions (x and y) in both the horizontal and vertical directions.

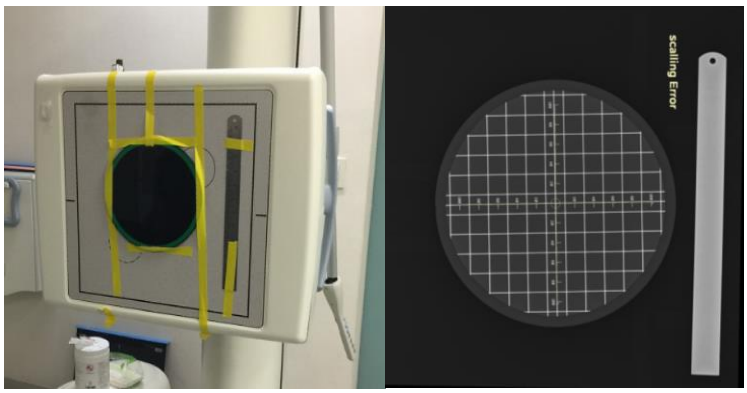

Figure 10 Place the M1 TO test object and stainless steel ruler direct onto the detector.

Table 7 The results of measurement distance (mm) using software compare with set distance (mm).

Axis	Set Distance (mm)	Measurement Distance (mm)	% Diff
x	200	200.44	0.0022
y	200	199.74	-0.0013
x/y	1	1.00	
S.D.	0	0.49	

Tolerance:

The measured distances x and y should agree within 3% of the actual distances at the center or 5% at the corners. All calculated aspect ratios should be within 1.00 ± 0.03 at the center or 5% at the corners.

Pass/Fail: Pass

8. Blurring and stitching artifacts

Purpose: To test for any localized distortion or blurring and to highlight any stitching artifact if the system is formed from more than one detector element.

Method:

1. The test should be made with the grid both in and out of the detector. (this test remove grid reduce affect from grid)
2. There is no attenuation in the beam and that the SID is set as 180 cm.
3. With a contact mesh on the detector, exposure 50 kVp 10 mAs using fine focus.
4. Visually inspect the image for blurring and stitching artifacts.
5. Repeat with a finer mesh.

Figure 11 Place mesh and stainless steel ruler on the detector for any localized distortion, blurring and stitching artifacts.

Tolerance:

No blurring should be present. If stitching artifacts are present there should be no loss of information.

Pass/Fail: Pass

9. Limiting Spatial Resolution

Purpose: To test the high contrast limit of the system ability to resolve details.

Method:

1. Remove grid from system, there is no attenuation in the beam and that the SID is set as 180 cm.
2. Place the resolution test object Huttner test object onto the detector aligned as 45^{o} to its edges.
3. Exposure the detector at 70 kVp 16 mAs on fine focus.
4. Repeat the measurement with the resolution test object placed at longitudinal axis and 45^{o} to longitudinal axis.
5. Adjust the window level and magnification to optimize the resolution.

Result:

Table 9: Number of object in threshold contrast detail detectability

Alignment	kVp	mAs	Line pair Tech monitor (group no.)
0^{o}	70	16	6
45^{o}	70	16	6
90^{o}	70	16	7

Tolerance:

These measurements should be used to set a baseline for future QA tests.

10. Threshold Contrast Detail Detectability

Purpose: To monitor image quality by assessing the visibility of low contrast details.

Method:

1. Remove grid from system.
2. Position the TO20 test object direct onto the detector with an SID of 180 cm.
3. Exposure the detector at 70 kVp and 2.5 mAs, 1.5 mmCu (Dose 1 μGy).
4. Repeat this test for exposures of 4 μGy, 10 μGy, 12 μGy .

Result:

Table 9: Number of object in threshold contrast detail detectability

Circular Detail	Diameter (mm)	Dose (μGy)		
		1	**4**	**12**
A	11.10	5	9	11
B	7.90	7	9	12
C	5.60	6	9	10
D	4.00	4	9	10
E	2.80	4	9	9
F	2.00	4	8	9
G	1.40	7	9	12
H	1.00	6	9	11
J	0.70	7	7	10
K	0.50	7	9	10
L	0.35	5	9	10
M	0.26	6	8	8

Tolerance:

The images should not have obvious artifacts. Using ROI analysis, STP corrected values should be within a range of 10% of the mean.

Pass/Fail: Pass

Tolerance: The results of this test are used to set a baseline for future QA tests. The summary result:

__P__ Dosimetry

__P__ Linearity and system transfer properties

__P__ Image retention

__P__ Sensitivity index consistency

__P__ Uniformity

__P__ Scaling errors

__P__ Blurring and stitching artifacts

__P__ Limiting spatial resolution

__P__ Threshold contrast detail detectability

Appendix C

Data record form

GE Definium 8000

Date……..

Protocol No.……

CASE RECORD FORM - Phantom Study

Digital Chest Tomosynthesis

Phantom Information			
Model : Multipurpose Chest Phantom Kyoto Kagaku **N1** "**LUNGMAN**"		**Thickness:** 23 cm.	
Exposure Parameter			
kVp		Cu-filter	
mAs		Dose ratio	
Radiation dose			
DAP (mGy·cm^2)			
ESD (mGy)			

Image criteria			
Item Image Criteria Score	**Not fulfilled (0)**	**Partly fulfilled (0.5)**	**Fulfilled (1)**
1. Visually sharp reproduction of the vascular pattern in the whole lung, the peripheral vessels			
2. Visually sharp reproduction of the trachea and proximal bronchi			
3. Visually sharp reproduction of the borders of the heart and aorta			
4. Visually sharp reproduction of the diaphragm and lateral costophrenic angles			
5. Visualiszation of the retrocardiac lung and the mediastinum			
6. Visualization of the spine through the heart shadow			
Criteria Score =			

Image criteria

Based on European guidelines on quality criteria for diagnostic radiographic images.

Score ≥ 3: Acceptable

GE Definium 8000 Date…….

Protocol No…….

CASE RECORD FORM - Phantom Study

Phantom Information			
Model : Multipurpose Chest Phantom Kyoto Kagaku **N1** "**LUNGMAN**"		**Thickness:** 23 cm.	
Exposure Parameter			
kVp		Cu-filter	
mAs		Dose ratio	
Radiation dose			
DAP (mGy·cm^2)		Note…….....	
ESD mGy)			

Criteria Score - Nodule Detection	**Detection**
Score 1 : Poor - Visualize 12 mm. in diameter with sharp edge - Partly visualize 10 mm. in diameter	
Score 2 : Fair - Visualize 10 mm. in diameter with sharp edge - Partly visualize 8 mm. in diameter	
Score 3 : Good (Acceptable) - Visualize 8 mm. in diameter with sharp edge - Partly visualize 5 mm. in diameter	
Score 4 : Very Good - Visualize 5 mm. in diameter with sharp edge - Partly visualize 3 mm. in diameter	
Score 5 : Excellent - Visualize all simulated nodules with sharp edge	
Criteria Score =	

Nodule detection Based on Fleischer Society Guidelines
Heber MacMahon H et al. Radiology 2005; 237:395–400

GE Definium 8000 Date……..

Case No.……

CASE RECORD FORM - PATIENT STUDY

Digital Chest Tomosynthesis (Optimal protocol)

Patient Information

Gender (M/F)	
Age (Y)	
Chest Thickness (cm.)	
Weight (kg.)	
Height (cm.)	

Exposure Parameter

kVp	
mAs	
Cu Filter (mm.)	
Dose ratio	

Patient Dose

Total DAP (mGy·cm2)	
Total Dose (mGy)	

GE Definium 8000 Date……..

Case No.……

CASE RECORD FORM - PATIENT STUDY

Digital Chest Tomosynthesis (Optimal protocol)

Image criteria			
Item Image Criteria Score	Not fulfilled (0)	Partly fulfilled (0.5)	Fulfilled (1)
1. Visually sharp reproduction of the vascular pattern in the whole lung, the peripheral vessels			
2. Visually sharp reproduction of the trachea and proximal bronchi			
3. Visually sharp reproduction of the borders of the heart and aorta			
4. Visually sharp reproduction of the diaphragm and lateral costophrenic angles			
5. Visualiszation of the retrocardiac lung and the mediastinum			
6. Visualization of the spine through the heart shadow			
Criteria Score =			

……
……
……
……

Image criteria

Based on European guidelines on quality criteria for diagnostic radiographic images.

☐ Acceptable image quality
☐ Unacceptable image quality

……
Radiologist

Appendix D

The Approval of Institutional Review Board

COA No. 833/2017

IRB No. 359/60

INSTITUTIONAL REVIEW BOARD

Faculty of Medicine, Chulalongkorn University

1873 Rama 4 Road, Patumwan, Bangkok 10330, Thailand, Tel 662-256-4493

Certificate of Approval

The Institutional Review Board of the Faculty of Medicine, Chulalongkorn University, Bangkok, Thailand, has approved the following study in compliance with the International guidelines for human research protection as Declaration of Helsinki, The Belmont Report, CIOMS Guideline and International Conference on Harmonization in Good Clinical Practice (ICH-GCP)

Study Title	: The Determination of Optimal Protocol for Digital Chest Tomosynthesis.
Study Code	: -
Principal Investigator	: Mr. Sarawut Tongkum
Affiliation of PI	: Department of Radiology, Faculty of Medicine, Chulalongkorn University.
Review Method	: Full board
Continuing Report	: Every 6 months.

Document Reviewed :

1. THESIS PROPOSAL Version 2.0, 28 AUG 2017
2. Protocol Synopsis Version 1 Date 5 MAY 2017
3. Information sheet for research participant Version 3.0 Date 21 Sep 2017
4. Informed Consent for the legal representative Version 1 Date 16 JUNE 2017

Approval granted is subject to the following conditions: (see back of this Certificate)

5. CASE RECORD FORM
6. Curriculum Vitae and GCP Training
   - Mr. Sarawut Tongkum
   - Kitiwat Khamwan, Ph.D.
   - Yothin Rakvongthai, Ph.D.

Signature ..... Signature .....

(Emeritus Professor Tada Sueblinvong MD) (Assistant Professor Prapapan Rajatapiti MD, PhD)

Chairperson Member and Secretary

The Institutional Review Board The Institutional Review Board

Date of Approval : September 26, 2017

Approval Expire Date : September 25, 2018

Approval granted is subject to the following conditions: (see back of this Certificate)

Appendix E

Consent form

	คณะกรรมการพิจารณาจริยธรรมการวิจัย คณะแพทยศาสตร์ จุฬาลงกรณ์มหาวิทยาลัย	เอกสารแสดงความยินยอมเข้าร่วม โครงการสำหรับผู้แทนโดยชอบธรรม	AF 09-06/5.0 หน้า 1/2

การวิจัยเรื่อง โปรโตคอลที่เหมาะสมในการถ่ายภาพรังสีทรวงอกโดยใช้เอกซเรย์ระบบดิจิทัลโทโมซินทีซิส

วันให้คำยินยอม วันที่.....เดือน.....พ.ศ.....

ข้าพเจ้า นาย/นาง/นางสาว.....(ผู้ให้ความยินยอมหรือผู้แทน)

ที่อยู่..... ได้อ่านรายละเอียดจากเอกสารข้อมูลคำอธิบายสำหรับผู้เข้าร่วมการวิจัยที่แนบมาฉบับวันที่..... และข้าพเจ้ายินยอมเข้าร่วมในโครงการวิจัยโดยสมัครใจ

ข้าพเจ้าได้รับสำเนาเอกสารแสดงความยินยอมเข้าร่วมในโครงการวิจัยที่ข้าพเจ้าได้ลงนาม และ วันที่ พร้อมด้วยเอกสารข้อมูลคำอธิบายสำหรับผู้เข้าร่วมในโครงการวิจัย ทั้งนี้ก่อนที่จะลงนามในใบยินยอมเข้าร่วมในการวิจัยนี้ ข้าพเจ้าและผู้เข้าร่วมการวิจัยได้รับการอธิบายจากผู้วิจัยถึงวัตถุประสงค์ของการวิจัย ระยะเวลาของการทำวิจัย วิธีการวิจัย อันตราย หรืออาการที่อาจเกิดขึ้นจากการวิจัย หรือจากยาที่ใช้รวมทั้งประโยชน์ที่จะเกิดขึ้นจากการวิจัยและแนวทางรักษาโดยวิธีอื่นอย่างละเอียด ข้าพเจ้าและผู้เข้าร่วมการวิจัยมีเวลาและโอกาสเพียงพอในการซักถามข้อสงสัยทั้งหมดจนมีความเข้าใจอย่างดีแล้ว โดยผู้วิจัยได้ตอบคำถามต่าง ๆ ที่ข้าพเจ้าและผู้เข้าร่วมการวิจัย สงสัยด้วยความเต็มใจไม่ปิดบังซ่อนเร้นจนข้าพเจ้าพอใจ

ข้าพเจ้าได้รับทราบจากผู้วิจัยว่าหากเกิดอันตรายใด ๆ จากการวิจัยดังกล่าว ข้าพเจ้าจะได้รับการรักษาพยาบาล โดยไม่เสียค่าใช้จ่าย (และระบุว่า จะได้รับการชดเชยจากผู้สนับสนุนการวิจัยหรือไม่)

ข้าพเจ้าเข้าใจถึงสิทธิที่จะบอกเลิกการเข้าร่วมการวิจัย เมื่อใดก็ได้โดยไม่จำเป็นต้องแจ้งเหตุผล และการบอกเลิกการเข้าร่วมการวิจัยนี้ จะไม่มีผลต่อการรักษาโรคหรือสิทธิอื่นๆ ที่ผู้เข้าร่วมการวิจัยจะพึงได้รับต่อไป

ผู้วิจัยรับรองว่าจะเก็บข้อมูลเฉพาะเกี่ยวกับตัวของผู้เข้าร่วมการวิจัยเป็นความลับ และจะเปิดเผยได้เฉพาะเมื่อได้รับการยินยอมจากข้าพเจ้าเท่านั้น บุคคลอื่น ในนามของบริษัทผู้สนับสนุนการวิจัย คณะกรรมการพิจารณาจริยธรรมการวิจัยในคน และสำนักงานคณะกรรมการอาหารและยา อาจจะได้รับอนุญาตให้เข้ามาตรวจและประมวลข้อมูลส่วนตัวของผู้เข้าร่วมการวิจัย ทั้งนี้จะต้องกระทำไปเพื่อวัตถุประสงค์เพื่อตรวจสอบความถูกต้องของข้อมูลเท่านั้น โดยการตกลงที่จะเข้าร่วมการศึกษาวิจัยนี้ข้าพเจ้าได้ให้ความยินยอมที่จะให้มีการตรวจสอบข้อมูลประวัติทางการแพทย์ของผู้เข้าร่วมการวิจัยได้

ผู้วิจัยรับรองว่าจะไม่มีการเก็บข้อมูลใด ๆ ของผู้เข้าร่วมการวิจัย เพิ่มเติม หลังจากที่ข้าพเจ้าขอยกเลิกการเข้าร่วมโครงการวิจัยและต้องการให้ทำลายเอกสารและ/หรือตัวอย่างที่ใช้ตรวจสอบทั้งหมดที่สามารถสืบค้นถึงตัวผู้เข้าร่วมการวิจัย

ข้าพเจ้าเข้าใจว่า ข้าพเจ้าและ ผู้เข้าร่วมการวิจัยมีสิทธิ์ที่จะตรวจสอบหรือแก้ไขข้อมูลส่วนตัวของผู้เข้าร่วมการวิจัย และสามารถยกเลิกการให้สิทธิในการใช้ข้อมูลส่วนตัวของผู้เข้าร่วมการวิจัยได้ โดยต้องแจ้งให้ผู้วิจัยรับทราบ

ข้าพเจ้าได้ตระหนักว่าข้อมูลในการวิจัยรวมถึงข้อมูลทางการแพทย์ที่ไม่มีการเปิดเผยชื่อของผู้เข้าร่วมการวิจัย จะผ่านกระบวนการต่าง ๆ เช่น การเก็บข้อมูล การบันทึกข้อมูลในแบบบันทึกและในคอมพิวเตอร์ การตรวจสอบ การวิเคราะห์ และการรายงานข้อมูลเพื่อวัตถุประสงค์ทางวิชาการ รวมทั้งการใช้ข้อมูลทางการแพทย์ในอนาคตหรือการวิจัยทางด้านเภสัชภัณฑ์เท่านั้น

ข้าพเจ้าได้อ่านข้อความข้างต้น และมีความเข้าใจดีทุกประการแล้ว ยินดีเข้าร่วมในโครงการวิจัยด้วยความเต็มใจ จึงได้ลงนามในเอกสารใบยินยอมนี้

.....ลงนามผู้ให้ความยินยอม

(.....) ชื่อผู้ยินยอมตัวบรรจง

วันที่ .....เดือน.....พ.ศ.....

Version...1... Date...16...JUNE...2017.....

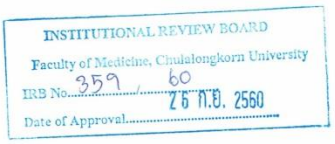

ข้าพเจ้าได้อธิบายถึงวัตถุประสงค์ของการวิจัย วิธีการวิจัย อันตราย อาการไม่พึงประสงค์ หรือความเสี่ยงที่อาจเกิดขึ้นจากการวิจัย หรือจากยาที่ใช้รวมทั้งประโยชน์ที่จะเกิดขึ้นจากการวิจัยอย่างละเอียด ให้ผู้แทนโดยชอบธรรม/ผู้ปกครองของผู้เข้าร่วมการวิจัยตามนามข้างต้นได้ทราบและมีความเข้าใจดีแล้ว พร้อมลงนามลงในเอกสารแสดงความยินยอมด้วยความเต็มใจ

.....ลงนามผู้ทำวิจัย

(.....) ชื่อผู้ทำวิจัย ตัวบรรจง

วันที่ .....เดือน.....พ.ศ.....

.....ลงนามพยาน

(.....) ชื่อพยาน ตัวบรรจง

วันที่ .....เดือน.....พ.ศ.....

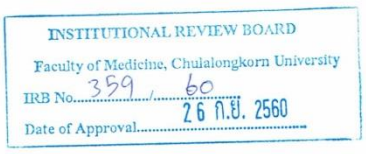

Appendix F

Information sheet

ชื่อโครงการวิจัย โปรโตคอลที่เหมาะสมในการถ่ายภาพรังสีทรวงอกโดยใช้เอกซเรย์ระบบดิจิทัลโทโมซินทีซิส

ผู้วิจัย

ชื่อ	นายศราวุธ ทองคุ้ม
ที่อยู่ที่ทำงานหรือสถานศึกษาของผู้วิจัย	หน่วยรังสีวินิจฉัย โรงพยาบาลจุฬาภรณ์ เขตหลักสี่ กรุงเทพมหานคร
เบอร์โทรศัพท์ติดต่อ 24 ชั่วโมง	086-6063408

ผู้วิจัยร่วม (ทุกท่าน)

ชื่อ	อาจารย์ ดร.กิติวัฒน์ คำวัน
ที่อยู่ที่ทำงานหรือสถานศึกษาของผู้วิจัย	ภาควิชารังสีวิทยา คณะแพทยศาสตร์ จุฬาลงกรณ์มหาวิทยาลัย
เบอร์โทรศัพท์ที่ทำงาน	02-2564000 ต่อ 80370
เบอร์โทรศัพท์ติดต่อ 24 ชั่วโมง	061-9325919

ชื่อ	อาจารย์ ดร.โยธิน รักวงษ์ไทย
ที่อยู่ที่ทำงานหรือสถานศึกษาของผู้วิจัย	ภาควิชารังสีวิทยา คณะแพทยศาสตร์ จุฬาลงกรณ์มหาวิทยาลัย
เบอร์โทรศัพท์ที่ทำงาน	02-2564000 ต่อ 80370
เบอร์โทรศัพท์ติดต่อ 24 ชั่วโมง	095-9024008

เรียน ผู้เข้าร่วมโครงการวิจัยทุกท่าน

ท่านได้รับเชิญให้เข้าร่วมในโครงการวิจัยนี้เนื่องจากท่านเป็นผู้ที่ได้รับการบริการถ่ายภาพรังสีทรวงอกโดยใช้เอกซเรย์ระบบดิจิตอลโทโมซินทีซิส ซึ่งเป็นเทคนิคที่ใช้วิธีการถ่ายภาพเอกซเรย์ในหลายมุม และนำภาพเหล่านั้นมารวบรวมขึ้นเป็นภาพทรวงอกแบบสามมิติ (Digital Chest Tomosynthesis) ก่อนที่ท่านจะตัดสินใจเข้าร่วมในการศึกษาวิจัยดังกล่าว ขอให้ท่านอ่านเอกสารฉบับนี้อย่างถี่ถ้วน เพื่อให้ท่านได้ทราบถึงเหตุผลและรายละเอียดของการศึกษาวิจัยในครั้งนี้ หากท่านมีข้อสงสัยใดๆ เพิ่มเติม กรุณาซักถามจากทีมงานของแพทย์ผู้ทำวิจัย หรือแพทย์ผู้ร่วมทำวิจัยซึ่งจะเป็นผู้สามารถตอบคำถามและให้ความกระจ่างแก่ท่านได้

ท่านสามารถขอคำแนะนำในการเข้าร่วมโครงการวิจัยนี้จากครอบครัว เพื่อน หรือแพทย์ประจำตัวของท่านได้ ท่านมีเวลาอย่างเพียงพอในการตัดสินใจโดยอิสระ ถ้าท่านตัดสินใจแล้วว่าจะเข้าร่วมในโครงการวิจัยนี้ ขอให้ท่านลงนามในเอกสารแสดงความยินยอมของโครงการวิจัยนี้

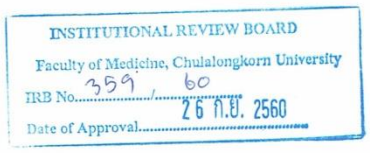

เหตุผลความเป็นมา

การตรวจเอกซเรย์ทรวงอกในปัจจุบันมีหลายเทคนิคเพื่อช่วยให้เห็นรายละเอียดภายในทรวงอกได้ชัดเจนยิ่งขึ้น สามารถนำผลที่ได้จากการตรวจวินิจฉัยไปวางแผนการรักษาได้อย่างถูกต้องแม่นยำ และในปัจจุบันการให้บริการทางรังสีวินิจฉัย หน่วยงานได้ตระหนักถึงคุณภาพของภาพ และปริมาณรังสีที่ผู้ป่วยได้รับหลังการรับบริการการนี้คณะผู้วิจัยจึงมีแนวคิดที่จะหาค่าเทคนิคที่เหมาะสมในการเอกซเรย์ทรวงอกโดยใช้เอกซเรย์ระบบดิจิทัลโทโมซินทีซิส เพื่อให้ผู้ป่วยได้รับประโยชน์สูงสุดจากการรับบริการต่อไป

วัตถุประสงค์ของการศึกษา

วัตถุประสงค์หลังจาการศึกษาในครั้งนี้คือ เพื่อหาค่าปริมาณรังสีที่เหมาะสมในการถ่ายภาพรังสีทรวงอกด้วยเทคนิคดิจิทัลโทโมซินทีซิส (Digital Chest Tomosynthesis) ที่มีคุณภาพที่แพทย์ยอมรับได้ เพื่อใช้เป็นแนวทางในการถ่ายภาพรังสีทรวงอกด้วยเทคนิคดังกล่าว โดยมีจำนวนผู้เข้าร่วมในโครงการทั้งหมด 30 คน

วิธีการที่เกี่ยวข้องกับการวิจัย

หลังจากท่านให้ความยินยอมที่จะเข้าร่วมในโครงการวิจัยนี้ ผู้วิจัยและทีมงานจะทำการถ่ายภาพรังสีทรวงอกโดยใช้เอกซเรย์ระบบดิจิทัลโทโมซินทีซิส โดยจะมีการเอกซเรย์ทรวงอกหลายๆมุม และนำภาพถ่ายมารวบรวมขึ้นเป็นภาพถ่ายทรวงอกแบบสามมิติ (Digital Chest Tomosynthesis) ตามคำสั่งแพทย์โดยวิธีการปกติทั่วไป และจะขอบันทึกข้อมูลของท่านในส่วนที่เป็นปัจจัยสำคัญเกี่ยวข้องกับการตั้งค่าทางเทคนิคอันได้แก่ การตรวจสอบอายุ ชั่งน้ำหนัก ส่วนสูง ความหนาของทรวงอก

หากท่านตกลงที่จะเข้าร่วมในโครงการวิจัยนี้ จะมีข้อปฏิบัติร่วมกันดังนี้

ท่านผู้เข้าร่วมโครงการวิจัยนี้ เป็นผู้ที่ต้องมีคำร้องขอเข้ารับการตรวจวินิจฉัยด้วยภาพถ่ายทางรังสีทรวงอกโดยใช้เอกซเรย์ระบบดิจิทัลโทโมซินทีซิสจากแพทย์ผู้ตรวจเท่านั้น (Digital Chest Tomosynthesis)

- ท่านจะเสียค่าตรวจวินิจฉัยด้วยภาพรังสีเฉพาะในส่วนของภาพรังสีที่แพทย์ผู้ตรวจส่งตรวจเท่านั้น ต้องไม่มีค่าใช้จ่ายใดๆ เพิ่มเติมจากค่าตรวจปกติทั้งสิ้น
- โครงการวิจัยนี้เป็นการเก็บข้อมูลที่จำเป็นในการกำหนดปริมาณรังสีแก่ผู้ป่วยที่เข้ารับวินิจฉัยด้วยภาพรังสีที่พึงปฏิบัติตามปกติวิสัยของการถ่ายภาพรังสีทรวงอกโดยทั่วไป โดยจะทำการเก็บข้อมูลครั้งเดียวสำหรับผู้เข้าร่วมโครงการวิจัยแต่ละท่าน
- โครงการวิจัยนี้เป็นความพยายามเพิ่มคุณภาพของภาพและมาตรฐานของภาพถ่ายรังสีทรวงอก
- ก่อนการถ่ายภาพรังสีทรวงอก ท่านจะได้รับทราบข้อมูลของการถ่ายภาพทางรังสีจากทีมงานของผู้ทำวิจัยที่ทำการเก็บข้อมูลตามความเป็นจริง อันได้แก่ วิธีการปฏิบัติระหว่างการรับการบริการถ่ายภาพรังสีทรวงอก
- ในระหว่างการถ่ายภาพรังสีทรวงอก ท่านต้องปฏิบัติตามคำแนะนำของนักรังสีการแพทย์ที่ปฏิบัติงาน เพื่อป้องกันการถ่ายภาพซ้ำ
- การเข้าร่วมการศึกษานี้ เป็นไปโดยสมัครใจ ท่านอาจปฏิเสธที่จะเข้าร่วมการศึกษานี้ โดยไม่กระทบต่อการให้บริการการตรวจวินิจฉัยที่ท่านจะได้รับจากนักรังสีการแพทย์และรังสีแพทย์ หรือผู้ที่ให้บริการท่านอื่นๆ

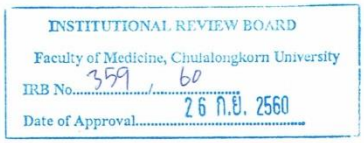

ความรับผิดชอบของอาสาสมัครผู้เข้าร่วมในโครงการวิจัย

เพื่อให้งานวิจัยนี้ประสบความสำเร็จ ผู้ทำวิจัยใคร่ขอความความร่วมมือจากท่าน โดยจะขอให้ท่านปฏิบัติตามคำแนะนำของผู้ทำวิจัยอย่างเคร่งครัด รวมทั้งแจ้งอาการผิดปกติต่าง ๆ ที่เกิดขึ้นกับท่านระหว่างที่ท่านเข้าร่วมในโครงการวิจัยให้ผู้ทำวิจัยได้รับทราบ

ความเสี่ยงที่อาจได้รับ

การถ่ายภาพรังสีโดยทั่วไป จะมีความเสี่ยงที่จะเกิดอันตรายต่อร่างกายอันมาจากการได้รับรังสี ซึ่งจะมีผลมากหรือน้อยแตกต่างกันตามชนิด ปริมาณของรังสีที่ได้รับ และความไวของเซลล์หรือเนื้อเยื่อของผู้ที่ได้รับรังสี

ความเสี่ยงที่ไม่ทราบแน่นอน

หากท่านมีข้อสงสัยใดๆ เกี่ยวกับความเสี่ยงที่อาจได้รับจากการเข้าร่วมในโครงการวิจัย ท่านสามารถสอบถามจากผู้ทำวิจัยได้ตลอดเวลา

หากมีการค้นพบข้อมูลใหม่ ๆ ที่อาจมีผลต่อความปลอดภัยของท่านในระหว่างที่ท่านเข้าร่วมในโครงการวิจัย ผู้ทำวิจัยจะแจ้งให้ท่านทราบทันที เพื่อให้ท่านตัดสินใจว่าจะอยู่ในโครงการวิจัยต่อไปหรือจะขอถอนตัวออกจากการวิจัย

ประโยชน์ที่อาจได้รับ

ท่านจะไม่ได้รับประโยชน์ใด ๆ จากการเข้าร่วมในการวิจัยนี้ แต่ผลของการศึกษาวิจัยในครั้งนี้ จะนำมาเป็นแนวทางในปรับค่าพารามิเตอร์ในการถ่ายภาพรังสีทรวงอกด้วยเทคนิคโทโมซินทีซิสต่อไป

ข้อปฏิบัติของท่านขณะที่ร่วมในโครงการวิจัย

ขอให้ท่านปฏิบัติดังนี้

- ขอให้ท่านให้ข้อมูลทางการแพทย์ของท่านทั้งในอดีต และปัจจุบัน แก่ผู้ทำวิจัยด้วยความสัตย์จริง
- ขอให้ท่านแจ้งให้ผู้ทำวิจัยทราบความผิดปกติที่เกิดขึ้นระหว่างที่ท่านร่วมในโครงการวิจัย

อันตรายที่อาจเกิดขึ้นจากการเข้าร่วมในโครงการวิจัยและความรับผิดชอบของผู้ทำวิจัย/ผู้สนับสนุนการวิจัย

หากพบอันตรายที่เกิดขึ้นจากการเข้าร่วมการวิจัย ท่านจะได้รับการรักษาอย่างเหมาะสมทันที หากท่านปฏิบัติตามคำแนะนำของทีมผู้ทำวิจัยแล้ว ผู้ทำวิจัย/ผู้สนับสนุนการวิจัยยินดีจะรับผิดชอบค่าใช้จ่ายในการรักษาพยาบาลของท่าน และการลงนามในเอกสารให้ความยินยอมไม่ได้หมายความว่าท่านได้สละสิทธิ์ทางกฎหมายตามปกติที่ท่านพึงมี

ในกรณีที่ท่านได้รับอันตรายใด ๆ หรือต้องการข้อมูลเพิ่มเติมที่เกี่ยวข้องกับโครงการวิจัย ท่านสามารถติดต่อกับผู้ทำวิจัยคือนายศราวุธ ทองคุ้ม ได้ตลอด 24 ชั่วโมง

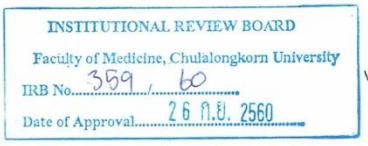

Version...3... Date...21...SEP...2017.....

ค่าใช้จ่ายของท่านในการเข้าร่วมการวิจัย

ท่านจะต้องรับผิดชอบค่าใช้จ่ายในการถ่ายภาพรังสีทรวงอกโดยใช้เอกซเรย์ระบบดิจิทัลโทโมซินทีซิสเฉพาะในส่วนที่แพทย์ผู้ส่งตรวจเท่านั้น โดยไม่มีค่าใช้จ่ายใดๆ เพิ่มเติมจากค่าตรวจปกติทั้งสิ้น

ค่าตอบแทนสำหรับผู้เข้าร่วมวิจัย

ท่านจะไม่ได้รับเงินค่าตอบแทนจากการเข้าร่วมในการวิจัย

การเข้าร่วมและการสิ้นสุดการเข้าร่วมโครงการวิจัย

การเข้าร่วมในโครงการวิจัยครั้งนี้เป็นไปโดยความสมัครใจ หากท่านไม่สมัครใจจะเข้าร่วมการศึกษาแล้ว ท่านสามารถถอนตัวได้ตลอดเวลา โดยระยะเวลาของอาสาสมัครที่เข้าร่วมโครงการวิจัย ประมาณ 20 นาที การขอถอนตัวออกจากโครงการวิจัยจะไม่มีผลต่อการดูแลรักษาโรคของท่านแต่อย่างใด

ผู้ทำวิจัยอาจถอนท่านออกจากการเข้าร่วมการวิจัย เพื่อเหตุผลด้านความปลอดภัยของท่าน หรือเมื่อผู้สนับสนุนการวิจัยยุติการดำเนินงานวิจัย หรือ ในกรณีดังต่อไปนี้

- ท่านไม่สามารถปฏิบัติตามคำแนะนำของผู้ทำวิจัย
- ท่านตั้งครรภ์ระหว่างที่เข้าร่วมโครงการวิจัย
- ท่านต้องการปรับเปลี่ยนการรักษาด้วยยาตัวที่ไม่ได้รับอนุญาตจากการวิจัยครั้งนี้

การปกป้องรักษาข้อมูลความลับของอาสาสมัคร

ข้อมูลที่อาจนำไปสู่การเปิดเผยตัวท่าน จะได้รับการปกปิดและจะไม่เปิดเผยแก่สาธารณชน ในกรณีที่ผลการวิจัยได้รับการตีพิมพ์ ชื่อและที่อยู่ของท่านจะต้องได้รับการปกปิดอยู่เสมอ โดยจะใช้เฉพาะรหัสประจำโครงการวิจัยของท่าน

จากการลงนามยินยอมของท่าน ผู้ทำวิจัย สามารถเข้าไปตรวจสอบบันทึกข้อมูลทางการแพทย์ของท่านได้แม้จะสิ้นสุดโครงการวิจัยแล้วก็ตาม หากท่านต้องการยกเลิกการให้สิทธิ์ดังกล่าว ท่านสามารถแจ้ง หรือเขียนบันทึกขอยกเลิกการให้คำยินยอม โดยส่งไปที่ ภาควิชารังสีวิทยา คณะแพทยศาสตร์ จุฬาลงกรณ์มหาวิทยาลัย 1873 ถนนพระรามที่ 4 แขวงปทุมวัน เขตปทุมวัน กทม. 10330 หากท่านขอยกเลิกการให้คำยินยอมหลังจากที่ท่านได้เข้าร่วมโครงการวิจัยแล้ว ข้อมูลส่วนตัวของท่านจะไม่ถูกบันทึกเพิ่มเติม อย่างไรก็ตามข้อมูลอื่นๆของท่านอาจถูกนำมาใช้เพื่อประเมินผลการวิจัย และท่านจะไม่สามารถกลับเข้าร่วมในโครงการนี้ได้อีก ทั้งนี้เนื่องจากข้อมูลของท่านที่จำเป็นสำหรับใช้เพื่อการวิจัยไม่ได้ถูกบันทึก

จากการลงนามยินยอมของท่าน แพทย์ผู้ทำวิจัยสามารถบอกรายละเอียดที่เกี่ยวกับการเข้าร่วมโครงการวิจัยนี้ของท่านให้แก่แพทย์ผู้รักษาท่านได้

สิทธิ์ของผู้เข้าร่วมในโครงการวิจัย

ในฐานะที่ท่านเป็นผู้เข้าร่วมในโครงการวิจัย ท่านจะมีสิทธิ์ดังต่อไปนี้

1. ท่านจะได้รับทราบถึงลักษณะและวัตถุประสงค์ของการวิจัยในครั้งนี้
2. ท่านจะได้รับการอธิบายเกี่ยวกับระเบียบวิธีการของการวิจัยทางการแพทย์ รวมทั้งยาและอุปกรณ์ที่ใช้ในการวิจัยครั้งนี้

3. ท่านจะได้รับการอธิบายถึงความเสี่ยงและความไม่สบายที่จะได้รับจากการวิจัย
4. ท่านจะได้รับการอธิบายถึงประโยชน์ที่ท่านอาจจะได้รับจากการวิจัย
5. ท่านจะได้รับการเปิดเผยถึงทางเลือกในการรักษาด้วยวิธีอื่น ยา หรืออุปกรณ์ซึ่งมีผลดีต่อท่านรวมทั้งประโยชน์และความเสี่ยงที่ท่านอาจได้รับ
6. ท่านจะได้รับทราบแนวทางในการรักษา ในกรณีที่พบโรคแทรกซ้อนภายหลังการเข้าร่วมในโครงการวิจัย
7. ท่านจะมีโอกาสได้ซักถามเกี่ยวกับงานวิจัยหรือขั้นตอนที่เกี่ยวข้องกับงานวิจัย
8. ท่านจะได้รับทราบว่าการยินยอมเข้าร่วมในโครงการวิจัยนี้ ท่านสามารถขอถอนตัวจากโครงการเมื่อไรก็ได้ โดยผู้เข้าร่วมในโครงการวิจัยสามารถขอถอนตัวจากโครงการโดยไม่ได้รับผลกระทบใด ๆ ทั้งสิ้น
9. ท่านจะได้รับเอกสารข้อมูลคำอธิบายสำหรับผู้เข้าร่วมในโครงการวิจัยและสำเนาเอกสารใบยินยอมที่มีทั้งลายเซ็นและวันที่
10. ท่านมีสิทธิ์ในการตัดสินใจว่าจะเข้าร่วมในโครงการวิจัยหรือไม่ก็ได้ โดยปราศจากการใช้อิทธิพลบังคับข่มขู่ หรือการหลอกลวง

หากท่านไม่ได้รับการชดเชยอันควรต่อการบาดเจ็บหรือเจ็บป่วยที่เกิดขึ้นโดยตรงจากการวิจัย หรือท่านไม่ได้รับการปฏิบัติตามที่ปรากฏในเอกสารข้อมูลคำอธิบายสำหรับผู้เข้าร่วมในการวิจัย ท่านสามารถร้องเรียนได้ที่ สำนักงานคณะกรรมการจริยธรรมการวิจัย คณะแพทยศาสตร์ จุฬาลงกรณ์มหาวิทยาลัย ตึกอานันทมหิดลชั้น 3 โรงพยาบาลจุฬาลงกรณ์ ถนนพระราม 4 ปทุมวัน กรุงเทพฯ 10330 โทรศัพท์/โทรสาร 0-2256-4493 ในเวลาราชการ หรือ e-mail : medchulairb@chula.ac.th

การลงนามในเอกสารให้ความยินยอม ไม่ได้หมายความว่าท่านได้สละสิทธิ์ทางกฎหมายตามปกติที่ท่านพึงมี

ขอขอบคุณในการให้ความร่วมมือของท่านมา ณ ที่นี้

.....

INSTITUTIONAL REVIEW BOARD
Faculty of Medicine, Chulalongkorn University
IRB No. 359 / 60
Date of Approval 26 ก.ย. 2560

Appendix G

Glass dosimeter reading process

1. Appearance check – Cleaning
- Check glass elements for chips, dirt and clean the dirt using ethanol.
- Handle glass element with tweezers.

2. Annealing in oven
- Annealing condition: 400 °C for 20 min (60 min at 1 Gy or more).
- Take out glass element of the oven at 40 °C or less for cool it down to the room temperature.

3. Use (Irradiation / Monitoring)
- Use the suitable holder and check the cap closed before use.

4. Preheating in oven
- Preheating condition: 70 °C for 30 min.
- Cool it down to the room temperature.

5. Reading out of accumulated value
- Use a suitable read out magazine (length, irradiated dose value).
- Check the mode and the read out parameters.
- Handle glass elements with care.
- Mind the direction of glass with ID for setting into the magazine.

6. Saving readout data file
- Save the data sheet to the specified folder or removable media as a new file name.

7. Storage of glass elements
- Keep glass elements in holders and store in desiccator.
- Glass elements should be avoided the high humidity.

The method of the fundamental measurement using FGD-1000

1. Set up read-out parameter (M) and select mode 2 for standard type.

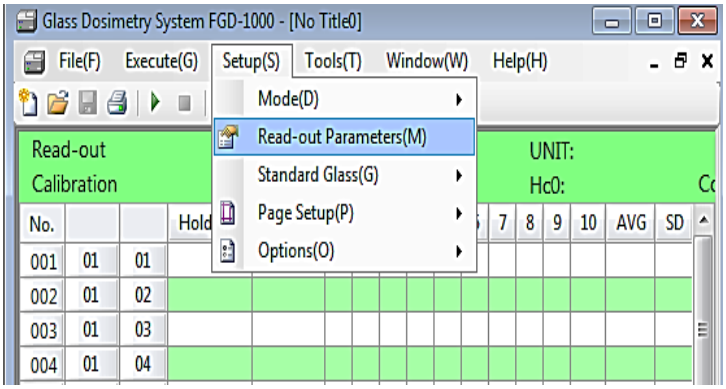

Figure 1 Set up parameter and mode of measurement**.**

2. Click [Apply] button, in order to confirm the specified values.

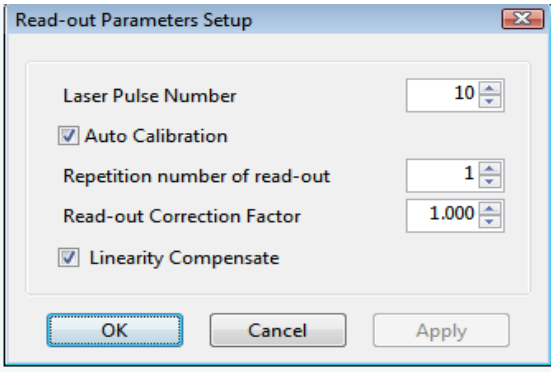

Figure 2 Read out parameter setup.

3. Set the read-out magazine to the reader. The read-out magazine as illustrated in Figure 3 is a magazine for setting glass elements to the reader at the time of read-out. Twenty-glass elements can be set to the read-out magazine, and position No. is printed by each position.

Figure 3 Standard-type magazine for 12 mm.

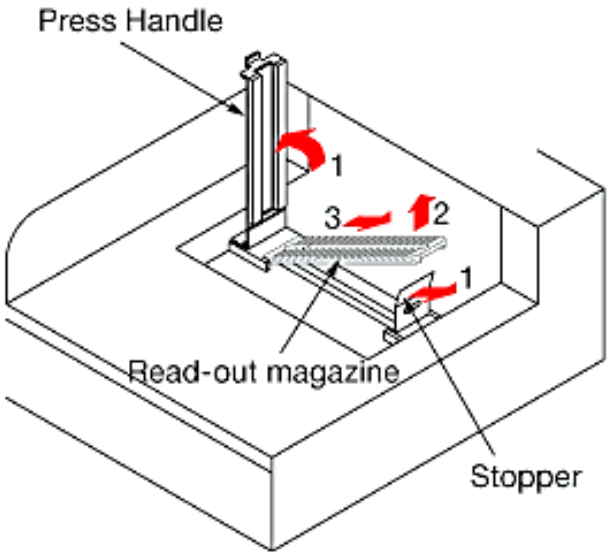

Figure 4 Set the read-out magazine to the reader.

4. Start reading the read-out data as in Figure 5.

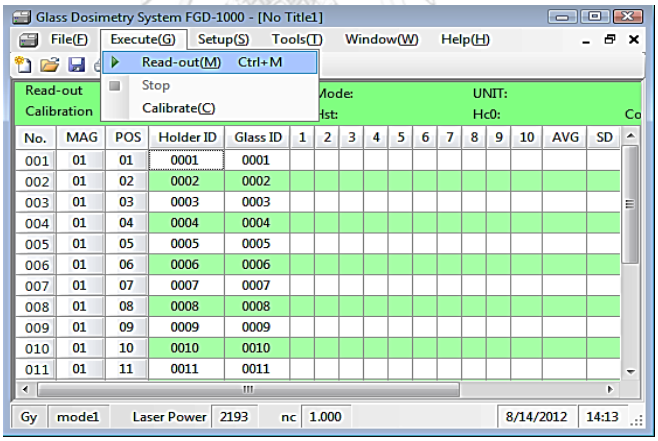

Figure 5 Read-out data.

5. Export the data, and read the data with Microsoft Excel.

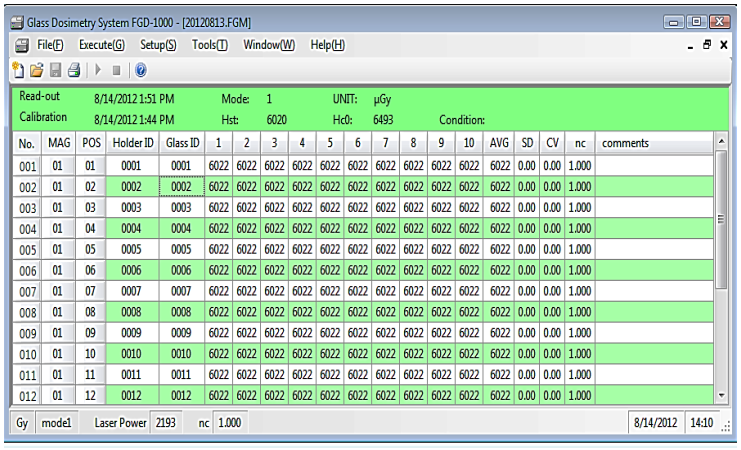

Figure 6 Data of read-out magazine.

Definition of parameters setup

Laser Pulse Number
specifies the laser pulses using a read-out. The default numbers of pulses are 20 pulses.

Auto Calibration
Check [Auto Calibration] check box to calibrate automatically using internal calibration glass.

Repetition number of read-out
specifies the repetition number read-out to one glass element, and the average value is calculated. If the value is 5 times or more, SD and CV are calculated.

Read-out Correction Factor
specifies the factor by which the read-out dose value can always be multiplied. For example, it is convenient if you use it when it calibrates and a correction factor is determined. Usually, set to "1.000".

VITA

Name: Mr. Sarawut Tongkum

Sex: Male

Nationality: Thai

Place of Birth: Prachinburi, Thailand

Date of Birth: June 29, 1981

Education:

- Bachelor of Science Program (Radiological Technology),

Faculty of Allied Health Science, Naresuan University, 2003

- Master of Science Program (Medical Imaging),

Faculty of Medicine, Chulalongkorn University, 2017

Working Experience:

2008-present Radiological Technologist,

Department of Diagnostic Radiology, Chulabhorn Hospital, Bangkok, Thailand.

Address: 9/77 Moo 8 Khlong Nueng, Khlong Luang, Pathum Thani, 12120.

E-mail: sarawut007rt@gmail.com

Publications:

1. Tongkum S, Suwanapradit P, Siripongsakun S, Vidhyarkorn S, Rakvongthai Y, Khamwan K. The determination of optimal protocol for digital chest tomosynthesis. Proceedings of 10th Annual Scientific Meeting of Thai Medical Physicist Society (TMPS). January 17-19, 2018, Bangkok, Thailand.

2. Tongkum S, Suwanapradit P, Siripongsakun S, Vidhyarkorn S, Rakvongthai Y, Khamwan K. The determination of optimal protocol for digital chest tomosynthesis. Proceedings of 15th South East Asian Congress of Medical Physics (SEACOMP). December 1-3, 2017, Ilo-Ilo city, Philippines.

3. Tongkum S, Suksancharoen W, Khamwan K. Evaluation of radiation dose and image quality of dual-energy and single energy CT in cranial non-contrast enhancement: a phantom study. 73rd Annual Meeting of Japan Society of Radiological Technology (JSRT). April 13-16, 2017, Yokohama, Japan. (Abstract)